2009

ASSESSING THE EFFECT OF TREATMENT ON SOLITARY DORMANT METASTATIC CELLS BY MRI AND OPTICAL IMAGING

Jason L. Townson

Follow this and additional works at: https://ir.lib.uwo.ca/digitizedtheses

Recommended Citation

ASSESSING THE EFFECT OF TREATMENT ON SOLITARY DORMANT METASTATIC CELLS BY MRI AND OPTICAL IMAGING

(Spine title: Solitary Dormant Metastatic Cells)

(Thesis format: Integrated-Article)

by

Jason L. <u>Townson</u>

Graduate Program
in
Medical Biophysics

A thesis submitted in partial fulfilment
of the requirements for the degree of
Doctor of Philosophy

School of Graduate and Postdoctoral Studies
The University of Western Ontario
London, Ontario, Canada

ABSTRACT

Metastatic disease is responsible for the majority of cancer related deaths. However, most anti-cancer drugs are not designed or tested for efficacy against this heterogeneous cancer cell population. This is in part due to the technical challenges involved in imaging and quantifying individual cells, or even large metastases, in common non-superficial sites of metastasis including lung, brain, bone marrow and liver. The purpose of the studies presented here was to develop and utilize imaging techniques capable of assessing metastatic cell progression and quantifying the effect of treatment on the majority of metastatic cell population, inclusive of solitary cells.

.   Quantification of the solitary metastatic cells in whole mouse liver was achieved using an MRI technique in which iron labeled cells were visible as areas of signal void. Signal void area was found to be highly correlated with the number of MPIO labeled cell injected into the liver. The MR scanning protocol used here resulted in images in which both signal void (due to iron labeled cells) and hyperintensity due to metastases (>200 μm) were apparent and could be quantified. This technique was subsequently utilized to assess the effect of doxorubicin and the synthetic triterpenoid CDDO-Im on experimental liver metastases in mice. It was found that despite significantly inhibiting the growth of large metastases, neither treatment decreased the number of solitary cells present in the same liver. In order to better understand the effect of treatment on the metastatic cell population at a cellular level, cells that express a cell cycle reporter system that changes colour as cell cycle progresses (fucci) were used in 2D and 3D cell culture. It was found that initial cell density and CDDO-Im treatment altered cell growth, and that cell cycle progression could be monitored longitudinally in individual and groups of cells within the same enclosed culture system.

It is expected that the techniques presented here will enable the screening of therapeutic strategies for their efficacy against not just a subset of the metastatic cell population, but the population as a whole.

CO-AUTHORSHIP

The following thesis contains material from previously published manuscripts in *Cell Cycle*. *Cell Cycle does* not require copyright permission for thesis reproduction.

Chapter 1 and Chapter 5 contain concepts and parts of a previously published review article "Dormancy of solitary metastatic cells" 2006 Aug;5:1744-50.", by J. L. Townson and A. F. Chambers, in: Cell Cycle. 2006 Aug;5:1744-50. I wrote this review with assistance from A. F. Chambers. Both chapters also contain concepts and parts of a book chapter "Tumor dormancy in liver metastasis: clinical and experimental evidence and implications for treatment", by J. L. Townson and A. F. Chambers, in: Liver Metastasis: Biology and Clinical Management. Springer Publishing (in press). I wrote this chapter with assistance from A. F. Chambers.

Chapter 2 has been published as "Three-dimensional imaging and quantification of both solitary cells and metastases in whole mouse liver by magnetic resonance imaging", by J.L Townson, S.S. Ramadan, C. Simedrea, B. K. Rutt, I.C. MacDonald, P.J. Foster and A.F. Chambers. Cancer Res, 2009; 69: 8326-31.

I designed and carried out the experiments described in this publication. S. S. Ramadan operated the MRI, determined the proper system settings, and contributed to the analysis of the images. C. Simedrea provided assistance with histology. B. K. Rutt, I.C. MacDonald, P.J. Foster and A.F. Chambers provided supervision and assistance in editing the manuscript.

Chapter 3 has been prepared for submission as "The synthetic triterpenoid CDDO-Imidazolide suppresses experimental liver metastasis", , by J. L. Townson, K. Liby, L.M. Mackenzie, C. Simedrea, P. J. Foster, I. C. MacDonald, M. B. Sporn and A. F. Chambers.

I designed and carried out the experiments described in this manuscript. L. T. MacKenzie and C. Simedrea provided assistance with animal handling and histology, respectively. K. Liby and M. B Sporn provided the synthetic triterpenoids and assisted in planning experiments. P. J. Foster, I. C. MacDonald, M. B. Sporn and A. F. Chambers provided supervision and assistance in editing the manuscript.

Chapter 4 is being prepared for submission as "Monitoring metastatic cell growth and cell cycle progression in 2D and 3D cell culture"", by J. L. Townson, M. L. Lizardo, M.B Sporn, I. C. MacDonald, and A. F. Chambers.

I designed and carried out the experiments described in this publication. M. L. Lizardo created the stable MDA-MB-231-luc-D3H2LN-fucci cells. M. B. Sporn provided the CDDO-Im used in the experiments. I. C. MacDonald and A. F. Chambers provided supervision and assistance in editing the manuscript.

ACKNOWLEDGMENTS

GRANT SUPPORT

TABLE OF CONTENTS

LIST OF TABLES

TABLE   **Page**

xiv

LIST OF FIGURES

FIGURE   **Page**

CHAPTER 1:

CHAPTER 2:

CHAPTER 3:

LIST OF ABBREVIATIONS

2-D	two-dimensional
3-D	three-dimensional
ANOVA	analysis of variance
CCD	charge-couple device
CDK	cyclin dependent kinase
CDKI	cyclin dependent kinase inhibitor
cFLIP	death-receptor inhibitor cellular caspase-8 (FLICE)-like inhibitory protein
CD24	cluster of differentiation 24
CD44	cluster of differentiation 44
CDDO-Im	1-[2-cyano-3-,12-dioxooleana-1,9(11)-dien-28-oyl]imidazole
CSC	cancer stem cell
CT	computed tomography
DIC	differential interference contrast
DR4	death receptor 4
DR5	death receptor 5
DXR	doxorubicin
fucci	fluorescent ubiquitination cell cycle indicator
FBS	fetal bovine serum
FIESTA	fast imaging employing steady state acquisition
GFP	green fluorescent protein
H&E	haematoxylin and eosin
HER2	human epidermal growth factor Receptor 2
IP	intraperitoneal
I.V.	intravenous
IVVM	*in vivo* videomicroscopy
mm	millimeters
MPIO	micron-sized iron oxide particles
MRI	magnetic resonance imaging

MEM	minimal essential medium
nm	nanometers
nM	nanomolar
PBS	phosphate-buffered saline
PET	positron emission tomography
ROI	region of interest
s.c.	sub-cutaneous
SE	standard error of the mean
SEM	standard error of measurement
SPECT	single photon emission computed tomography
SPIO	super-paramagnetic iron oxide
µL	microlitres
µm	micrometers

1. INTRODUCTION

This chapter contains concepts and parts of a book chapter "Tumor dormancy in liver metastasis: clinical and experimental evidence and implications for treatment", by J. L. Townson and A. F. Chambers, in: Liver Metastasis: Biology and Clinical Management. Springer (In Press), and of a published review "Dormancy of solitary metastatic cells", by J. L. Townson and A. F. Chambers in Cell Cycle. 2006 Aug;5:1744-50.

1.1 METASTASIS AND LIVER METASTASIS

1.1.1 *The problem and the process*

Significant progress has been made in our understanding of cancer risk factors and cancer cell biology, as well as ability to detect, localize and treat specific types of cancer. Indications that these advances are having an impact have recently been observed including a 4.5% increase in five-year relative survival for all cancers between 1992-1994 and 2002-2004 (1, 2). However, despite considerable resources, dedicated research, knowledge generation and technological advancements, cancer remains a leading cause of death, responsible for approximately 1 in 4 deaths (1, 2). The majority of cancer related deaths however are not due to primary tumors, but to metastatic tumors arising from the spread of cancer from one site to another (3, 4). Yet despite the associated lethality, metastasis is a highly inefficient process by which only a small fraction of the cancer cells that leave a primary tumor successfully form a tumor in a secondary site (3-11). This inefficiency is primarily due to cell death at one of the multiple steps a cell must successfully complete in order to form a large metastasis, including: detachment and migration from a primary tumor; intravasation into, and transit through, blood or lymph vessels; arrest in a secondary site; extravasation; and ultimately the initiation of proliferation, sustained growth and angiogenesis (Fig. 1.1). While cell death is often the

primary reason for metastatic inefficiency, experimental metastasis models have revealed that metastatic inefficiency is also due, at least initially, to an often significant population of metastatic cells that remain in the tissue as solitary dormant cells (4-6,8, 9, 12-16). It has been proposed that this population of cells, in conjunction with dormant micrometastases, may be responsible for recurrence that can occur months to decades following apparently successful treatment (17-22). However, the mechanisms regulating metastatic dormancy, and in fact the ultimate clinical significance of dormant metastatic disease, are incompletely understood.

3
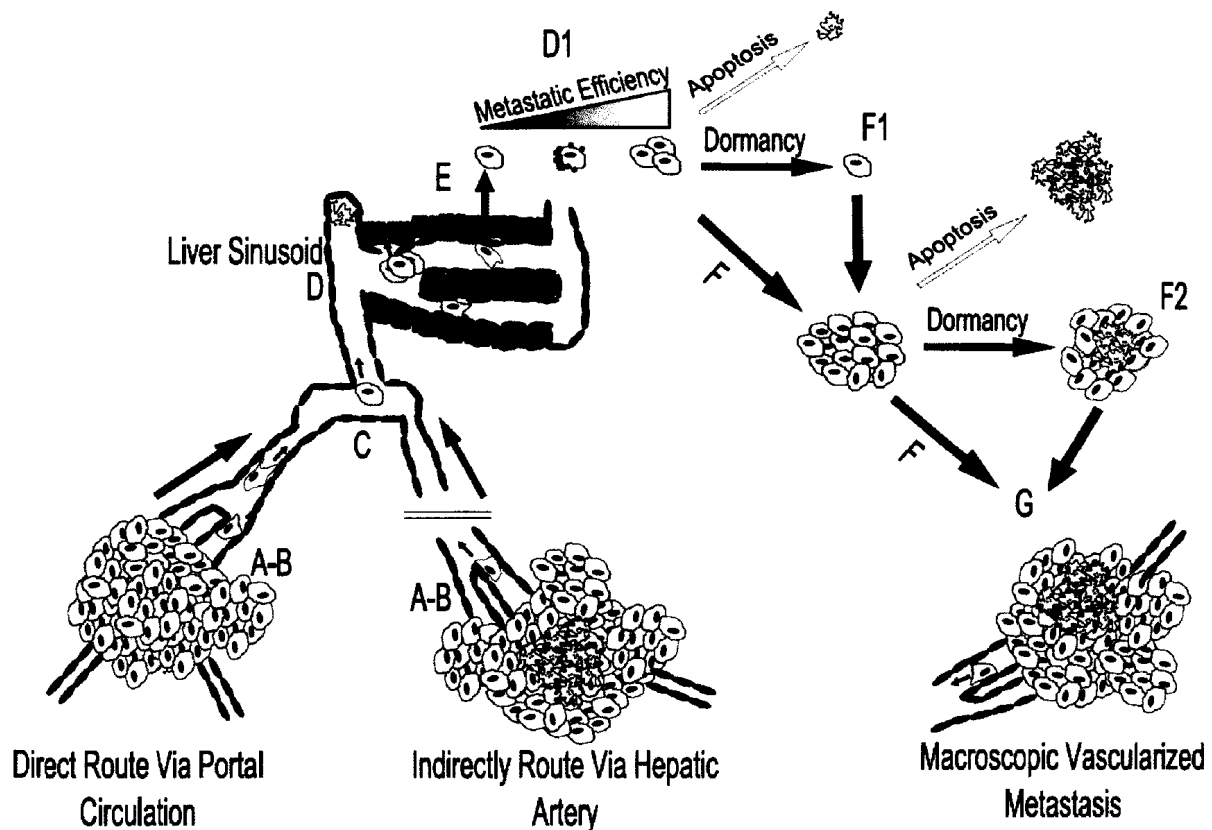
Figure 1.1 – The metastatic process. Metastasis is a multistep process in which all steps must be completed in order for a clinically apparent metastasis to be formed. The process of metastasis leading to a large vascularised secondary tumor starts with escape of a cell or group of cells from a primary tumor (A), intravasation into blood or lymph vasculature (B), transit in the vasculature (C), arrest in a secondary site (D), extravasation (E), proliferation and sustained growth (F) and angiogenesis (G). Metastatic dormancy is observed at two stages in the process, the solitary cell (F1) and micrometastasis (F2) stage. Arrest as a bolus of cells or a cell with platelets coating it has been found to increase metastatic efficiency (D1). Liver metastases can develop from cancer cells that originate from primary tumors that drain directly into the portal system or indirectly after passing through an upstream organ and arriving via the hepatic artery.

1.1.2 *Liver Metastasis*

Liver is the second most common site of metastasis and metastasis to this site has been found to occur in approximately 41% of cancer patients with metastatic disease (23). The frequency of metastasis to the liver is not unexpected given the significant volume of nutrient-rich blood that flows through the liver (portal vein and hepatic artery), the number of organs that drain directly into the portal system and the large number of fenestrated sinusoids within the liver. This large blood volume filtered directly downstream of a number of organs is significant if the number of cells that may be shed into the venous circulation (> 3×10^6 per g of tumor/day) is considered (24). While the majority of metastases observed in the liver originate from primary tumors in organs that drain directly into the portal system circulation, many including from the eye, breast and lymph nodes arrive in the liver via an arterial circulation path and thus do not arrive directly at the liver (3, 23, 25, 26). The frequent incidence of liver metastasis from cells delivered via both the portal vein and hepatic artery indicate that the liver is a common site of metastasis due to both the incidence of cell arrest (first pass arrest from portal system) and suitability of the microenvironment for growth (from previously "filtered" arterial system). Yet despite the high incidence of liver metastasis from multiple primary tumors, the efficiency of metastasis formation from cells that successfully arrive in the liver has been shown to be very low (5, 6, 9, 15, 27). While in experimental models the majority of cells have been shown to survive the process of cell arrest and extravasation in lung and liver, most cells will subsequently either die or remain dormant (6, 8, 9, 16). Liver resection techniques and chemotherapy treatment strategies have appreciably improved 5 year survival rates of patients with liver metastases, yet a large proportion of patients still do not survive that long (28). In order to make substantial increases in survival rates of patients with metastases to liver, as well as other organs, treatment strategies may need to be re-examined with increased consideration given to the entire cancer cell population inclusive of the dormant metastatic cell populations.

1.2 TREATMENT AND RECURRENCE

Cancer recurrence and the large number of deaths resulting from metastasis are due to failure of treatment to completely eradicate all cells responsible for the disease. Several plausible explanations for the often significant failure rates of treatment have been proposed including late stage of detection (i.e. number of metastases and extent of invasion), difficulty in accessing the tumor for treatment (barriers to physical and/or chemical intervention) and cellular drug or radiotherapy resistance. More recently it has been proposed that failure to target distinct subpopulations of cancer cells with stem like properties (cancer stem cells [CSCs]) may in fact be responsible for treatment failure and recurrence (29, 30). In any case, if treatment of all clinically apparent tumors is considered successful (i.e. no longer clinically detectable), recurrent disease is then due to occult or sub-clinical metastases, some of which may be dormant. As the dormant metastatic cell population has been shown to survive treatment that successfully inhibits growth of large vascularised metastases, treatment options will need to take into account the unique properties of this cancer cell population in order to eradicate these cells (5, 31). Developing treatments that target specific subpopulations of cancer cells, and metastatic cells in particular, will require modifications to the way in which most treatments are developed and tested (32, 33). Multiple types of pre-clinical models of primary cancer and metastatic disease exist in which drug efficacy can be assessed (Table 1). Yet superficial orthotopic and ectopic injection sites, which are used to model primary tumor growth, are often chosen due to the relative ease of injection and quantification of treatment effect. However, recent evidence suggests that the focus on "primary tumor" models in drug efficacy studies may lead to the development of drugs that have minimal benefit, or may even be harmful, to patients with metastatic disease (32, 34, 35). Along this same line, it is unlikely that dormant metastases (either pre-angiogenic micrometastases or single cells) will respond the same as primary tumors or large vascularised metastases to treatment. This has in fact been demonstrated

in pre-clinical models and is supported by clinical data presented by Demicheli et al., in which adjuvant systemic chemotherapy following surgery had no effect on a second peak (at around 60 months) of recurrence in breast cancer patients, a peak attributed to pre-existing dormant metastases (5, 36). Given the differences in response of the various cancer cell subpopulations to treatment, it may be advantageous to choose pre-clinical models that better relate to the clinical setting in which the drug will be used, as outlined in Table 1. As such, a better understanding of metastatic dormancy and its therapeutic implications must also be considered in developing novel treatment strategies. In this chapter we will review experimental and clinical data regarding metastatic dormancy and discuss the implications of the dormant metastatic population on cancer treatment.

Clinical Target	Standard Clinical Treatment	Appropriate Animal Model
Primary Tumor	Surgery and/or Neoadjuvant Therapy	Orthotopic primary tumor model
Presumed micrometastatic disease	Adjuvant Therapy	Micrometastasis/ dormancy models
Macroscopic metastatic disease	Metastatic Therapy	Metastasis models

Table 1.1 – Rational animal models for pre-clinical treatment development. Pre-clinical animal models of treatment efficacy should be chosen based on the clinical target. Patients can present with a primary tumor only, lymph node involvement and/or local metastases and/or distant metastases. The stage of disease progression in combination with other tumor properties (HER2, ER, PR receptors etc.) are used to determine the treatment regimen. Models that best mimic these clinical situations are available and treatment development should make use of experimental models that most closely relate to the stage of disease progression being targeted.

1.3 METASTATIC DORMANCY IN EXPERIMENTAL MODELS – SOLITARY CELLS AND MICROMETASTASES

1.3.1 *Metastatic Dormancy*

Dormancy has been used to describe two distinct subpopulations of metastatic cells, both of which have been observed to exist in multiple metastasis models (6, 12, 15, 17-19,27, 37-39). The two stages of metastatic progression at which dormancy has been observed and characterized are at the solitary cell stage and the pre-angiogenic micrometastasis stage (Fig. 1.1). However, despite both being referred to as metastatic dormancy, and both often referred to as micrometastases, these distinct populations of cells differ in several significant ways and will likely need to be dealt with as two separate treatment targets. After arrival in a secondary site, the first stage at which dormant metastatic cells have been observed occurs at the solitary cell stage (Fig. 1.1-D1). These cells are considered to be dormant due to the absence of markers for proliferation or apoptosis, as well as retention of exogenous labels that fall below the threshold of detection following a couple cycles of division (6, 8, 9, 12-14,38). However, the majority of solitary cells observed within a secondary site will not progress to form metastases (micro or macro) but will instead undergo apoptosis, even after initial survival and a variable period of dormancy (6, 8, 9, 16). The small proportion of solitary cells that do initiate proliferation can give rise to a second category of metastatic dormancy at the micrometastasis stage (Fig. 1.1-F1). These micrometastases are believed to be restricted in their ability to continue tumor growth, through balanced apoptosis and proliferation, primarily due to lack of their own vasculature or due to growth suppression by the immune system (17, 18, 39-41). As these two dormant metastatic cell populations appear to be controlled by different mechanisms and will likely need to be treated as separate therapeutic targets, here we will distinguish between the two and refer to these distinct populations of cells as either solitary dormant metastatic cells or dormant micrometastases (or pre-angiogenic metastases). An understanding of the mechanisms controlling micrometastasis dormancy is much further advanced

than those controlling solitary cell dormancy (17-19). Yet while distinct, these two metastatic cell populations do have multiple similarities that complicate both study and treatment of them. Primary among these is the technical challenges involved in imaging these cell populations in their typical metastatic sites, which include non-superficial tissues such as liver, lung and bone. Additionally, metastatic efficiency from both of these metastatic cell populations is low as few solitary cells and/or micrometastases observed within an organ progress to form large vascularised metastases within the typical period of experimental observation (6, 8, 9, 42). This means that even if a particular metastatic cell or micrometastasis is successfully monitored longitudinally, the chances of it commencing and continuing proliferation are likely to be small.

1.3.2 *The liver as a model for metastatic dormancy*

In addition to the frequency with which liver metastases are observed clinically, multiple properties of the liver make it a useful organ for experimental models of metastasis and metastatic dormancy in particular. First, in comparison to other common sites of metastasis including lung, bone and lymph nodes, the liver is relatively large and easy to access and image due to limited movement or obstruction by bone and/or air (9, 43-48). Direct injection of cells to the liver via the portal vein system, along with the efficient entrapment of cells within the liver, allows for a relatively high degree of control over the number of cells that initially arrest in the liver. This is important as the number of cells initially present in an organ must be known in order to quantify the subsequent fate of the entire population (9, 48). As the majority of cells arrest in the liver following portal vein injection, no significant growth in other organs usually occurs which otherwise would force the experiment to end early due to non-specific morbidity (5, 6, 9). The large number of sinusoids in which cells can arrest also provides an opportunity for cells to arrest as solitary cells or as small groups of cells. This is significant as the number of cells that arrest together within a sinusoid are known to alter cell fate, with increased cell bolus size leading to increased metastatic

efficiency (49, 50). By providing organ specific delivery in which the number of cells arresting can be controlled, while at the same time allowing for distribution of solitary cells throughout the entire organ, the liver provides advantages over injections in which cells arrive as a large fluid bolus of cells (i.e. mammary fat pad, subcutaneous, intradermal etc.) and systemic injections (intracardiac, intravenous, etc.) for the study of metastatic dormancy.

1.3.3 Micrometastasis Dormancy

Dormant solitary cells and micrometastases have been observed in multiple organs, including liver, in a number of different metastasis models (6, 8, 9, 12-15,18, 19, 27, 51). Dormant micrometastases have long been recognized as a logical treatment target, with research yielding considerable advances in the understanding of mechanisms controlling pre-angiogenic dormancy (17, 39, 41, 52). In addition, a number of anti-angiogenic therapies have been developed in order to inhibit growth of tumors beyond the stage of dormant micrometastases (17, 39, 41, 53). Several recent reviews have discussed the mechanisms controlling tumor angiogenesis (and thereby maintenance of pre-angiogenic dormancy of micrometastases) and treatment strategies based on tumor angiogenesis (17, 42, 54). Dormant pre-angiogenic micrometastasis will thus only be discussed here in the context of a significant sub-population of metastatic cells that requires consideration when planning a treatment strategy to ensure eradication of all cancer cells. To this end, it should be emphasized that micrometastasis dormancy is achieved by a state of balanced apoptosis and proliferation such that the tumor does not continue to expand beyond approximately 1 mm (41). Thus while "dormant" in terms of metastatic progression and growth, cells in pre-angiogenic micrometastases may not be dormant from a cell cycle perspective.

1.3.4 Models of solitary metastatic cell dormancy

Solitary dormant metastatic cells differ from dormant micrometastases in that solitary cell dormancy is defined by lack of proliferation and apoptosis (not balanced rates), and the cells are believed be arrested in the G0-G1 phase of the cell cycle (6, 8, 9, 18, 19). These cells have been observed to exist in tissue alone or in the presence of actively proliferating and growing metastases (6, 8, 9, 12-15,18, 19, 27, 51). Despite their common presence few of the solitary metastatic cells observed, at least within typical experimental observation periods, will ever begin proliferating or sustain growth to form the large vascularised metastases that are of primary clinical concern. Most solitary metastatic cells will undergo apoptosis, or remain dormant for the duration of observation (6, 8, 9). Yet solitary dormant metastatic cells have been shown to maintain their ability to proliferate and form tumors in vivo or continue to grow upon isolation in 2D cell culture even following treatment with cytotoxic chemotherapy (6, 14, 15). Relatively few models of solitary cell dormancy, in which cells persist as solitary cells within an organ (without proliferating) for a prolonged period of time, have been identified due to the natural focus of research on cell lines which form metastases during a reasonably short experimental period. However, even in cell lines that are categorized as highly metastatic, an often significant population of solitary dormant cells is observed in the same organ that also contains actively growing metastases (6, 8, 9). In order to avoid the short experimental time frame often caused by the morbidity and mortality associated with rapidly growing metastatic cells lines, it may be better to choose "non-metastatic" or poorly metastatic cell lines in order to study solitary cell dormancy. Cells that persist within an organ for extended periods of time without commencing proliferation allow for a suitable period in which to modify and observe alterations of growth dynamics and fate in order to elucidate the mechanisms controlling dormancy. One of the better characterized and understood models of solitary metastatic cell dormancy is the D2.0R murine mammary carcinoma cell line in mouse liver (5, 6, 55-59). When injected into

mouse liver via mesenteric vein injection a large proportion of cells initially remain dormant but maintain the capacity to form large macroscopic metastases approximately 11 weeks after injection (5, 6). Additional cell lines have also been shown to preferentially survive in liver or lung for extended periods of time, yet the mechanism controlling site specific survival and dormancy remain to be fully understood (14, 15, 27).

1.4 IMAGING AND MECHANISMS OF SOLITARY CELL DORMANCY

1.4.1 Imaging of metastatic dormancy

Recent advances in imaging and diagnostic technology have increased the ability to both image and detect solitary metastatic cells in vivo. Yet while a number of imaging modalities now possess detailed μm (10s - 100s) scale resolution (magnetic resonance imaging (MRI), computed tomography (CT), ultrasound and intravital microscopy), only MRI and intravital microscopy are currently capable of detecting, and only intravital microscopy capable of resolving, at the scale of a single cell (60). Additionally, optical microscopy continues to be the only imaging modality currently capable of the resolution necessary to visualize sub-cellular events. The ability to detect and image single cells has been enhanced by a number of improvements in fluorescent cell labels and molecular identification of human cells in a mouse (45, 60-66). Both endogenous and exogenous fluorescent cell labels continue to improve producing brighter, more specific (wavelengths and cellular localization) and stable cellular fluorescence options. Cellular MRI can also be used to provide a non-invasive means by which the metastatic cell population can be monitored longitudinally, as solitary cells labelled with iron particles have been observed in brain and liver (12, 13, 38). However, beyond single time point (or short observation times) imaging and detection, longitudinal in vivo cellular imaging remains a significant technical challenge.

1.4.2 *Optical and magnetic resonance imaging of solitary cancer cells in vivo*

Studies of solitary cancer cells in vivo have generally relied on optical imaging of cells labelled with either transient labels that permit identification of cells prior to dilution of the label by cell division, or stably expressed fluorescent markers that identify all cells arising from the original population, whether or not they have undergone cell division. These markers have included transient fluorescent labels such as Calcein AM and nanospheres, and constitutively expressed labels such as green and red fluorescent proteins (5, 9, 14, 15). These fluorescent markers, along with tumor cell specific antibodies and reporter genes such as LacZ, have been used to find solitary cells in tissues. However, the disadvantages of these markers include that some may photobleach, they may be masked by background tissue fluorescence, provide poor definition of cell boundaries, or are only useful during histological examination. Ideally when studying solitary cells one would like to be able to observe what is happening longitudinally to the entire cell population as well as at the individual cell and molecular levels.

While optical imaging is capable of single cell resolution in vivo, it is not as efficient as other modalities at imaging whole populations of cells in a large organ or entire animal due to its often-limited depth of penetration and field of view. Although whole body optical imaging is capable of detecting small tumors and of imaging populations of cells longitudinally and noninvasively, it is not yet capable of doing this reliably at the single cell level (60). However, the feasibility of imaging a population of metastatic cells longitudinally and noninvasively over time has improved recently due to advances in MRI. Using iron oxide nanoparticle labelled cells (which increase relaxivity leading to signal voids in T2 weighted images) researchers have been able to image different cell types at the single cell level in vivo (12, 13). Identification of cells is limited to a few cell divisions due to dilution of the iron label. The ability of MRI to longitudinally monitor single cell populations in entire organs combined with the high resolution

of optical imaging greatly facilitates study of cell progression, fate and response to treatment and molecular manipulation of metastatic cells.

1.4.3 Mechanisms of metastatic dormancy

Barkan et al., recently showed that while no significant period of dormancy is observed in metastatic cells lines in 2D in vitro culture, variable periods of solitary cell dormancy are observed in multiple cells lines in 3D cell culture conditions (56). This included the D2.0R cell line, which remained dormant in the 3D cell culture model for the entire 14 day period of observation. In addition, a number of other cell lines were found to remain dormant in 3D cell culture in a manner that correlated with their proliferative behavior in vivo (56). It was reported that integrin-β1 binding and myosin light chain kinase (MLCK) signalling were responsible for controlling solitary dormancy in this 3D cell culture model, and inhibition of MLCK led to enhanced solitary cell dormancy in a lung metastasis model. These results were subsequently confirmed in a similar 3D cell culture and lung metastasis models in which integrin-β1 signalling through focal adhesion kinase (FAK) was found to control solitary cell dormancy (55). The results of these 3D cell culture models are in agreement with a number of in vivo experiments indicating that solitary metastatic cell dormancy is controlled by cell surface receptor binding (e.g. fibronectin, integrin-β1 or uPAR etc.), subsequent signal transduction (via MLCK, FAK, p38, ERK) and cell cycle control via cyclin dependent kinases (CDK) and cyclin dependent kinase inhibitors (CDKI) (55, 56, 67-76).

1.5 CLINICAL DORMANCY AND RECURRENCE

1.5.1 *Clinical evidence of cancer dormancy*

Improved screening techniques made possible by advances in medical imaging and diagnostic technology have allowed for detection and diagnosis of cancer while tumors are still relatively small. Detection of single or small numbers of cancer cells in bone marrow (disseminated tumor cells – DTCs) and blood (circulating tumor cells – CTSs) is possible using a variety of cytometric, immunological or molecular methods (77). However, while it is possible to detect the presence of individual cancer cells in bone marrow, blood and other fluids, localization and longitudinal observation of individual solitary cells or pre-angiogenic micrometastases in patients over time is not yet feasible. As such, the majority of clinical data regarding metastatic dormancy has been obtained primarily from studies of recurrence and/or death patterns following initial treatment or detailed examination of tissue at autopsy (7, 21-23,36, 78-85). However, despite comprising much of the clinical data regarding dormancy, several limitations exist regarding interpretation of these data with respect to metastatic dormancy. While analysis of recurrence patterns following initial treatment provides evidence for the existence of clinically undetectable disease, it does not yield any information regarding mechanisms and does not prove that recurrence is due to metastatic dormancy. In addition, much like in experimental models, only amplified by relative size and lack of cell labelling, the chance of "false negative" results during autopsy of liver are high and autopsies only provide information about the cells at a single point in time (79). Regardless, these two sources of clinical data combined yield significant information regarding a subpopulation of cells that are likely responsible for recurrence and ultimate treatment failure. Much of the data regarding recurrence and mortality following primary treatment has originated from patients with primary breast cancer, a tumor type that often metastasizes to the liver (3, 86, 87). Interestingly, with respect to the findings regarding recurrence and mortality rates, many may

be generalized to multiple sites of metastasis including liver, as Demicheli et al., have recently found that breast cancer recurrence dynamics did not depend on the site of recurrence (88).

1.5.2 *Patterns of recurrence*

While no definitive criteria for clinical classification of cancer as dormant have been established, it has been demonstrated that many cases of recurrence are better explained by a kinetic growth model consisting of a period of dormancy followed by rapid growth than by a model of constant tumor growth (21, 22, 78, 89). Retrospective analysis of breast cancer patients treated by mastectomy with or without adjuvant therapy has provided significant insight into the dynamics of recurrence and dormancy, revealing recurrence up to two decades following initial treatment (22, 36, 81, 84). In 1173 patients treated by mastectomy alone between 1964-1980, two distinct peaks in recurrence (at any site) were observed at 18 and 60 months following surgery (21). These peaks of recurrence following treatment have further been shown to be influenced by other factors including menopausal status, lymph node involvement, primary tumor size and adjuvant treatment (21, 36, 84, 90). Interestingly, adjuvant treatment with CMF was shown to reduce early recurrences (first 4 years) with little benefit for late recurrence or the overall recurrence rate (36, 82, 90, 91). This has been speculated to be due to effective treatment of pre-existing micrometastases that would be sensitive to adjuvant therapy (and recur first) and inability to kill solitary dormant cells that may recur later (36, 82, 91). Analysis of more recent data from patients treated with current standard therapy (combinations of surgery, radiation, chemotherapy and hormone and molecular targeted therapy depending on tumor markers) have not consistently revealed the same dual peak recurrence pattern, however delayed recurrence is still observed and suggestive of the presence of metastatic dormancy (92-94).

1.5.3 *Circulating and disseminated tumor cells*

A number of recent studies have shown CTCs and DTCs are present in many cancer patients (77). While the significance of the presence of CTCs is still being evaluated, the presence of DTCs at the time of resection in a variety of primary cancers has been reported to correlate with poor prognosis (77). Although able to show the presence of individual or small groups of cells, technologies for DTC and CTC detection are still subject to the limitation that they show the presence of cells but not if the cells are dormant metastases. Taken together the clinical evidence discussed above strongly supports the clinical presence of dormant metastases. The detection of individual or small groups of cells (autopsy, CTCs and DTCs) that are associated with recurrence is better explained by kinetic models in which a period of dormancy exists. At a minimum, these finding support the idea that a heterogeneous population of cancer cells is present in most patients and will thus likely require multiple treatment strategies in order to eradicate all cells.

1.6 THERAPEUTIC IMPLICATIONS

1.6.1 *Differential response to treatment*

The presence of dormant metastases presents a number of therapeutic challenges ranging from detection and localization of such inherently small events to treatment resistance of cells which have been shown to exhibit multiple passive and active defence mechanisms against traditional cancer treatments (5, 18, 19, 30, 95-97). There is growing evidence that treatment that effectively inhibits growth of primary tumors may have little effect on metastases and may in some cases enhance metastasis (32, 34, 35, 83). This concept may be applied further to the different metastatic cell populations (i.e. solitary cells, micrometastases and large vascularised metastases) where treatment that effectively inhibits growing metastases has been shown to have no effect on

viability or growth potential of solitary dormant cells (5, 97). Making the situation more complex, it is likely that not all occult metastases are dormant and not all dormant cells share the same fate or even metastatic potential. It is not currently feasible to determine if any given solitary dormant cell will eventually undergo apoptosis, continue to remain dormant or commence and continue proliferation and growth to form a clinically apparent large vascularised metastasis. Regardless of the fate of an individual cell, it is unlikely that these distinct populations of cells which differ in their vascularisation, proliferation status, drug resistance mechanisms and size will respond uniformly to treatment (Fig. 2). As such, the unique properties of the heterogeneous metastatic cell population, inclusive of dormant metastatic cell populations, should be considered in order to achieve the treatment goal of eradicating all cancer cells.

Available Imaging, Localization and Treatment Options

Large Vascularized Tumor	Pre-angiogenic Tumor	Solitary Cell	Dormant cell	Cancer Stem Cell
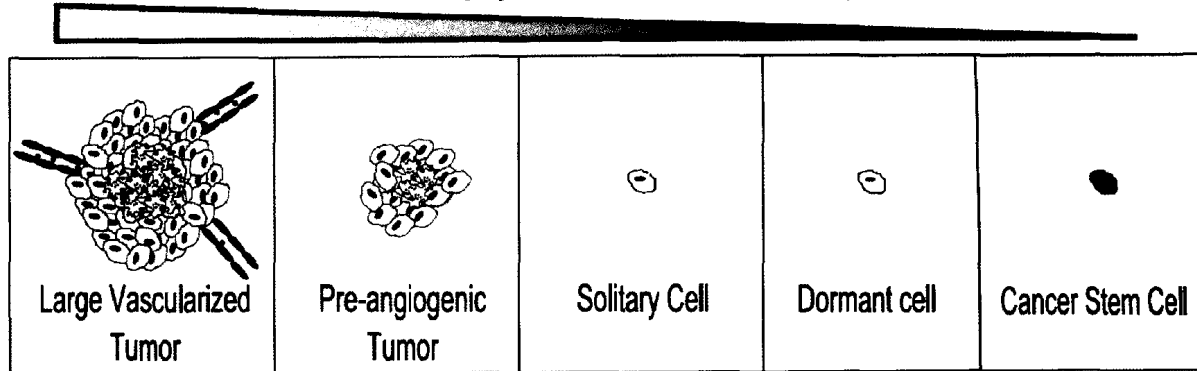
Figure 1.2 – The heterogeneous cancer cell population differs in their response to treatment as well as their ability to be detected and localized clinically. Large, vascularized and localized tumors can often be successfully treated by local treatment (surgery, radiotherapy). However, the number of treatment options and ability to image the cancer cell population decreases with the size of the tumor to the individual cell level and disseminated nature of metastatic disease. The gain of passive (dormancy) and active (drug resistance) defence mechanisms likely makes dormant cells and cells with stem like properties a more difficult cell population to eradicate by treatment.

1.6.2 *Direct treatment limitations imposed by size*

At the most basic level, the first challenge associated with treatment of dormant metastatic cells is detection and localization of individual or small groups of cancer cells that can be as small as 10-20 micrometers. Advances in imaging technologies have successfully lowered the threshold of tumor detection to the millimetre range, however this is insufficient to detect dormant solitary cells and in most cases micrometastases. As such, these cancers are often referred to as "occult" or "clinically undetectable" metastases. And while it is possible to detect the presence of small numbers of cells in bone marrow and body fluids, this does not assist in localization of cells for direct treatment methods including surgery and radiation. Surgical resection of all visible liver metastases significantly improves survival, yet a considerable number of patients die from recurrence of metastases not originally apparent (occult or sub-clinical) at the time of initial resection even with the addition of adjuvant chemotherapy (98-100). And while the addition of repeat resections, staged resections and portal vein embolization to treatments regimens have appreciably improved outcome, a significant proportion of patients with metastatic liver cancer do not survive to 5 years (28, 101). Surgical removal of tumors provides obvious and immediate clinical benefit, however it has also been proposed that surgery may also have a growth promoting effect on residual metastases by removing angiogenesis inhibition (102). In addition, wound healing and immune suppression have both been shown (clinically and experimentally) to promote metastasis growth and recurrence, raising a danger of unintended consequences of treatment (40, 103-105). In any case, inability to localize occult metastases seems to require the use of adjuvant systemic therapy capable of targeting all occult cancer cells, including dormant metastatic cells, regardless of the ability to observe or localize them.

1.6.3 Systemic Therapy

Ideal systemic therapy would be delivered to and be effective against all target cells with limited effect and toxicity on non-target cells. This has long been a goal of cancer treatments. However, it may be that design of treatments that specifically target an individual cell will work better scaled up to target larger metastases than most treatments scaled down from larger tumor treatment tend to be. A number of therapeutic strategies are now emerging that have the potential to treat all cells in the metastatic cell population regardless of state of proliferation or ability to clinically localize them. Targeting of individual metastatic cell populations may be achievable by increasing cell specific delivery and/or specific activity of the treatment on a particular cell type. These include a number of molecular targeting agents that exploit functional differences in cell surface receptor expression, kinase activity and signalling pathways between cancer and non-cancer cells (106-108). In addition, targeted therapy that has the potential to deliver much higher doses of drug to specific cells types has significant promise (109-111). These types of therapies may be most advantageous as they would increase therapeutic ratio by increasing the amount and specificity of treatment delivered to cancer cells. A number of therapies that increase specific delivery and/or activity are now used in the clinic or being evaluated in pre-clinical models and clinical trials. Cancer vaccines have a number of obvious advantages, however notable challenges related to identification of cancer specific antigens and the associated danger of inducing an autoimmune reaction remain to been fully overcome (40, 112-114). It is easier to cease an administered treatment to limit toxicity than to stop the activity of the immune system once it has be activated. A natural systemic approach that is showing promise is that of oncolytic viruses (115-119). Their ability to preferentially infect and kill cancer cells (dependent on aberrant pathway expression) as well as self-propagate and spread systemically to secondary tumors after inoculation is a major advantage. Indeed, treatment with an oncolytic reovirus in patients (phase 1 clinical trial) with refractory primary or metastatic liver cancer resulted in stable disease or partial

regression in nine of ten patients who had large tumors and were heavily pre-treated (116). In addition, recent experimental evidence has demonstrated the ability of an oncolytic reovirus to target CSCs (CD44+/CD24- and Aldefluor +) as well as non-CSCs in an experimental mouse model of breast cancer (115). This ability to target a number of specific cancer cell subpopulations regardless of their differences will be essential for ultimately successful treatment and will likely require combination therapy.

1.6.4 *Treatment delivery and combinations*

Synthetic drug delivery systems have been developed which are now capable of delivering much higher drug concentrations with adjustable drug loading and release properties (109, 111, 120, 121). Combining advanced drug delivery technology with cell membrane ligand identification techniques will allow for much more specific and concentrated drug delivery. A recent study of the membrane proteome of metastatic cells found that a number of unique surface markers exist, including many that were previously believed to be expressed only internally (122). Targeting specific cell pathways, as well as rational drug combinations, have also shown promise to target solitary cells. Interestingly, in an experimental model of multiple myeloma, treatment with bortezomib induced dormancy in subpopulation of cells, however addition of salubrinal was able to eradicate this dormant cell fraction (123). Given the heterogeneous nature of the cancer cell population, it is likely that a number of treatment approaches in which ability to target specific cells with high drug concentrations of molecular targeting agents will be necessary in order to eradicate all cancer cells within the body.

1.6.5 *1-[2-cyano-3-,12-dioxooleana-1,9(11)-dien-28-oyl]imidazole (CDDO-Im)*

CDDO-Im is one of a number of synthetic oleanane triterpenoids that have multifunctional effects that are dependent on both cell type and drug concentration (124). This includes induction of differentiation, growth arrest and

apoptosis in a number of cell lines, including cancer cell lines (125-128). In vivo, synthetic triterpenoids inhibit carcinogen induced cancers, primary tumor growth and subsequent spontaneous metastasis to the lungs via effect on a number of different molecular targets (124-128). Due to multifunction effect that the synethetic triterpenoid family has on a number of cancer cell lines, as well as its ability to be dosed orally and accumulate in the liver (129), CDDO-Im was used in Chapter 3 to determine its effect on experimental liver metastases.

1.7 CONCLUSION

Treatments that target primary tumors often do not effectively treat metastases and in some cases may actually enhance metastatic growth (32, 34, 35, 83). Experimental evidence also suggests that treatment that successfully inhibits actively growing metastases does not target dormant metastatic cells (5). As such, treatment failure and recurrence may therefore be the result of failure to target all cells in the heterogeneous metastasis cell population. Recent advancements in cellular imaging and targeted therapies may assist in development of treatments capable of targeting the entire population of metastatic cells. However, appropriate experimental models that better mimic clinical disease progression should be used to develop effective treatments (Table 1.1). In order to target all cells within the cancer cell population much remains to be learned about the mechanisms controlling this heterogeneous cell population. This includes further elucidation of the intracellular and extracellular control mechanisms that regulate both solitary cell and micrometastatic dormancy. Indeed, the true clinical importance of these metastatic cell populations still remains to be determined. Does presence of these cell populations indeed cause poor outcome, or are they cancer that patients will die with, not from? Do different subpopulations exist within the dormant cell populations? Are surface receptors used to identify specific types of cancer expressed equally on all populations of cells such that they can be used for targeted therapy? Can treatment be used to maintain dormancy indefinitely? Is it

possible to determine successful treatment against a population of individual cells distributed throughout the body? Regardless, until we have a better understanding of the significance and mechanisms controlling the heterogeneous metastatic cell populations, emphasis should be placed on treatment and eradication of all metastatic cells, inclusive of the clinically unobservable dormant cell populations.

1.8 THESIS OBJECTIVE

To develop methods by which to better assess differential effects of treatment on the entire population of metastatic cells, inclusive of solitary cells, micrometastases and macroscopic metastases.

1.8.1 Specific Aims

1. To develop and validate an MRI method for quantification of the entire metastatic cell population, inclusive of the solitary cell population, in whole mouse liver.

2. To determine the effect of the synthetic triterpenoid CDDO-Im on a pair of metastatic cell lines in vitro and on metastasis growth in an in vivo (mouse) liver metastasis model.

3. To modify and use a 3D cell culture model of metastatic growth and a fluorescent cell cycle reporter (fucci) to longitudinally monitor metastatic cell cycle progression and evaluation of treatment effect on the entire population of metastatic cells.

1.9 THESIS OUTLINE

The accomplishment of the preceding specific aims is described in detail in Chapters 2 through 4. A summary of these chapters follows.

1.9.1 *Chapter 2: 3D imaging and quantification of both solitary cells and metastases in whole mouse liver by magnetic resonance imaging*

This study describes development and application of a novel MRI technique capable of quantifying nearly the entire population of metastatic cells in the liver. Using the technique described in this chapter, solitary cells and metastases larger than 200 μm could be quantified. It was found that signal void area from MPIO labeled cells highly correlated with the number of MPIO labeled cells in the liver. The number of cells was found to decrease in a manner anticipated based on data from previous optical imaging studies with the same cell line. The technique was used in a subsequent study, also presented in this chapter, which showed that doxorubicin is capable of inhibiting liver metastasis growth but has no effect on the number of solitary cells in the same livers.

1.9.2 *Chapter 3: The synthetic triterpenoid CDDO-Imidazolide suppresses experimental liver metastasis*

This study describes the effect of CDDO-Im on a human colon cancer (HT29) and a mouse melanoma (B16F1) cells in 2D culture and in an in vivo liver metastasis model. It was found that treatment with CDDO-Im inhibited proliferation and induced apoptosis at nanomolar concentrations in vitro. CDDO-Im treatment was also capable of inhibiting growth of large metastases in vivo, however no reduction in the number of solitary cells (as quantified by the MRI method developed in Chapter 2) was observed.

1.9.3 *Chapter 4: Monitoring metastatic cell growth and cell cycle progression in 2D and 3D cell culture*

Longitudinal imaging of cellular events in the entire metastatic cell population, particularly the solitary dormant metastatic cell population, in vivo is complicated by a number of technical challenges. This study describes use of a 3D cell culture system (basement membrane matrix – Matrigel) in order to longitudinally observe and assess the effect of CDDO-Im treatment on the metastatic cell population. It was found that a heterogeneous metastatic cell population, ranging from solitary cells to large metastases as often observed in vivo, was present in 231LN-fucci and D2.0R 3D culture. Normal and CDDO-Im manipulated cell cycle progression were directly monitored using a novel fluorescent cell cycle reporter (fucci) that leads to changes in nuclear fluorescence as cells progress throughout the cell cycle. CDDO-Im treatment of 231LN-fucci cells in 2D and 3D culture led to the arrest of proliferation as determined by nuclear fluorescence.

1.10 REFERENCES

1. Canadian Cancer Society. Canadian Cancer Statistics 2009.

2. American Cancer Society. Cancer Facts & Figures 2009. Atlanta: American Cancer Society 2009.

3. Chambers AF, Groom AC, MacDonald IC. Dissemination and growth of cancer cells in metastatic sites. Nat. Rev. Cancer 2002;2:563-72.

4. Ambrus JL, Ambrus CM, Mink IB, Pickren JW. Causes of death in cancer patients. J Med 1975;6:61-4.

5. Naumov GN, Townson JL, MacDonald IC, Wilson SM, Bramwell VHC, Groom AC et al.. Ineffectiveness of doxorubicin treatment on solitary dormant mammary carcinoma cells or late-developing metastases. Breast Cancer Res. Treat. 2003;82:199-206.

6. Naumov GN, MacDonald IC, Weinmeister PM, Kerkvliet N, Nadkarni KV, Wilson SM et al.. Persistence of solitary mammary carcinoma cells in a secondary site: a possible contributor to dormancy. Cancer Res. 2002;62:2162-8.

7. Weiss L. Metastasis of cancer: a conceptual history from antiquity to the 1990s. Cancer Metastasis Rev. 2000;19:I-XI, 193-383.

8. Cameron MD, Schmidt EE, Kerkvliet N, Nadkarni KV, Morris VL, Groom AC et al.. Temporal progression of metastasis in lung: cell survival, dormancy, and location dependence of metastatic inefficiency. Cancer Res. 2000;60:2541-6.

9. Luzzi KJ, MacDonald IC, Schmidt EE, Kerkvliet N, Morris VL, Chambers AF et al.. Multistep nature of metastatic inefficiency: dormancy of solitary cells after successful extravasation and limited survival of early micrometastases. Am. J. Pathol. 1998;153:865-73.

10. Weiss L. Metastatic inefficiency: intravascular and intraperitoneal implantation of cancer cells. Cancer Treat. Res. 1996;82:1-11.

11. Tarin D, Price JE, Kettlewell MG, Souter RG, Vass AC, Crossley B. Mechanisms of human tumor metastasis studied in patients with peritoneovenous shunts. Cancer Res. 1984;44:3584-92.

12. Shapiro EM, Sharer K, Skrtic S, Koretsky AP. In vivo detection of single cells by MRI. Magn Reson Med 2006;55:242-9.

13. Heyn C, Ronald JA, Ramadan SS, Snir JA, Barry AM, MacKenzie LT et al.. In vivo MRI of cancer cell fate at the single-cell level in a mouse model of breast cancer metastasis to the brain. Magn Reson Med 2006;56:1001-10.

14. Goodison S, Kawai K, Hihara J, Jiang P, Yang M, Urquidi V et al.. Prolonged dormancy and site-specific growth potential of cancer cells spontaneously disseminated from nonmetastatic breast tumors as revealed by labeling with green fluorescent protein. Clin. Cancer Res. 2003;9:3808-14.

15. Guba M, Cernaianu G, Koehl G, Geissler EK, Jauch KW, Anthuber M et al.. A primary tumor promotes dormancy of solitary tumor cells before inhibiting angiogenesis. Cancer Res. 2001;61:5575-9.

16. Koop S, MacDonald IC, Luzzi K, Schmidt EE, Morris VL, Grattan M et al.. Fate of melanoma cells entering the microcirculation: over 80% survive and extravasate. Cancer Res. 1995;55:2520-3.

17. Naumov GN, Folkman J, Straume O, Akslen LA. Tumor-vascular interactions and tumor dormancy. APMIS 2008;116:569-85.

18. Aguirre-Ghiso JA. Models, mechanisms and clinical evidence for cancer dormancy. Nat. Rev. Cancer 2007;7:834-46.

19. Townson JL, Chambers AF. Dormancy of solitary metastatic cells. Cell Cycle 2006;5:1744-50.

20. Naumov GN, MacDonald IC, Chambers AF, Groom AC. Solitary cancer cells as a possible source of tumour dormancy?. Semin. Cancer Biol. 2001;11:271-6.

21. Demicheli R, Abbattista A, Miceli R, Valagussa P, Bonadonna G. Time distribution of the recurrence risk for breast cancer patients undergoing mastectomy: further support about the concept of tumor dormancy. Breast Cancer Res. Treat. 1996;41:177-85.

22. Demicheli R, Terenziani M, Valagussa P, Moliterni A, Zambetti M, Bonadonna G. Local recurrences following mastectomy: support for the concept of tumor dormancy. J. Natl. Cancer Inst. 1994;86:45-8.

23. Pickren J, Tsukada Y, Lane W. Liver Metastasis (ed. eds. Weiss, L. & Gilbert, L.) (G.K. Hall Medical Publishers, 1982).

24. Butler TP, Gullino PM. Quantitation of cell shedding into efferent blood of mammary adenocarcinoma. Cancer Res. 1975;35:512-6.

25. Diamond JR, Finlayson CA, Borges VF. Hepatic complications of breast cancer. Lancet Oncol. 2009;10:615-21.

26. Bakalian S, Marshall J, Logan P, Faingold D, Maloney S, Di Cesare S et al.. Molecular pathways mediating liver metastasis in patients with uveal melanoma. Clin. Cancer Res. 2008;14:951-6.

27. Logan PT, Fernandes BF, Di Cesare S, Marshall JA, Maloney SC, Burnier MNJ. Single-cell tumor dormancy model of uveal melanoma. Clin. Exp. Metastasis 2008;25:509-16.

28. Sharma S, Camci C, Jabbour N. Management of hepatic metastasis from colorectal cancers: an update. J Hepatobiliary Pancreat Surg 2008;15:570-80.

29. Goss P, Allan AL, Rodenhiser DI, Foster PJ, Chambers AF. New clinical and experimental approaches for studying tumor dormancy: does tumor dormancy offer a therapeutic target?. APMIS 2008;116:552-68.

30. Croker A, Townson J, Allan A, Chambers A. Tumor Dormancy, Metastasis, and Cancer Stem Cells (ed. eds. Teicher, B. & Bagley, R.) (Humana Press, 2009).

31. Eccles SA, Welch DR. Metastasis: recent discoveries and novel treatment strategies. Lancet 2007;369:1742-57.

32. Steeg PS, Anderson RL, Bar-Eli M, Chambers AF, Eccles SA, Hunter K et al.. Preclinical Drug Development Must Consider the Impact on Metastasis. Clin. Cancer Res. 2009; 15: 4529-453.

33. Welch DR. Do we need to redefine a cancer metastasis and staging definitions?. Breast Dis 2006-2007;26:3-12.

34. Pàez-Ribes M, Allen E, Hudock J, Takeda T, Okuyama H, Viñals F et al.. Antiangiogenic therapy elicits malignant progression of tumors to increased local invasion and distant metastasis. Cancer Cell 2009;15:220-31.

35. Ebos JML, Lee CR, Cruz-Munoz W, Bjarnason GA, Christensen JG, Kerbel RS. Accelerated metastasis after short-term treatment with a potent inhibitor of tumor angiogenesis. Cancer Cell 2009;15:232-9.

36. Demicheli R, Miceli R, Moliterni A, Zambetti M, Hrushesky WJM, Retsky MW et al.. Breast cancer recurrence dynamics following adjuvant CMF is consistent with tumor dormancy and mastectomy-driven acceleration of the metastatic process. Ann. Oncol. 2005;16:1449-57.

37. Naumov GN, Bender E, Zurakowski D, Kang S, Sampson D, Flynn E et al.. A model of human tumor dormancy: an angiogenic switch from the nonangiogenic phenotype. J. Natl. Cancer Inst. 2006;98:316-25.

38. Heyn C, Ronald JA, Mackenzie LT, MacDonald IC, Chambers AF, Rutt BK et al.. In vivo magnetic resonance imaging of single cells in mouse brain with optical validation. Magn Reson Med 2006;55:23-9.

39. O'Reilly MS, Holmgren L, Shing Y, Chen C, Rosenthal RA, Moses M et al.. Angiostatin: a novel angiogenesis inhibitor that mediates the suppression of metastases by a Lewis lung carcinoma. Cell 1994;79:315-28.

40. Finn OJ. Human tumor antigens, immunosurveillance, and cancer vaccines. Immunol. Res. 2006;36:73-82.

41. Holmgren L, O'Reilly MS, Folkman J. Dormancy of micrometastases: balanced proliferation and apoptosis in the presence of angiogenesis suppression. Nat. Med. 1995;1:149-53.

42. Naumov GN, Akslen LA, Folkman J. Role of angiogenesis in human tumor dormancy: animal models of the angiogenic switch. Cell Cycle 2006;5:1779-87.

43. Graham KC, Ford NL, MacKenzie LT, Postenka CO, Groom AC, MacDonald IC et al.. Noninvasive quantification of tumor volume in preclinical liver metastasis models using contrast-enhanced x-ray computed tomography. Invest Radiol 2008;43:92-9.

44. Amoh Y, Nagakura C, Maitra A, Moossa AR, Katsuoka K, Hoffman RM et al.. Dual-color imaging of nascent angiogenesis and its inhibition in liver metastases of pancreatic cancer. Anticancer Res. 2006;26:3237-42.

45. Bouvet M, Tsuji K, Yang M, Jiang P, Moossa AR, Hoffman RM. In vivo color-coded imaging of the interaction of colon cancer cells and splenocytes in the formation of liver metastases. Cancer Res. 2006;66:11293-7.

46. Wirtzfeld LA, Graham KC, Groom AC, Macdonald IC, Chambers AF, Fenster A et al.. Volume measurement variability in three-dimensional high-frequency ultrasound images of murine liver metastases. Phys Med Biol 2006;51:2367-81.

47. Graham KC, Wirtzfeld LA, MacKenzie LT, Postenka CO, Groom AC, MacDonald IC et al.. Three-dimensional high-frequency ultrasound imaging for longitudinal evaluation of liver metastases in preclinical models. Cancer Res. 2005;65:5231-7.

48. MacDonald IC, Groom AC, Chambers AF. Cancer spread and micrometastasis development: quantitative approaches for in vivo models. Bioessays 2002;24:885-93.

49. Enomoto T, Oda T, Aoyagi Y, Sugiura S, Nakajima M, Satake M et al.. Consistent liver metastases in a rat model by portal injection of microencapsulated cancer cells. Cancer Res. 2006;66:11131-9.

50. Liotta LA, Saidel MG, Kleinerman J. The significance of hematogenous tumor cell clumps in the metastatic process. Cancer Res. 1976;36:889-94.

51. Suzuki M, Mose ES, Montel V, Tarin D. Dormant cancer cells retrieved from metastasis-free organs regain tumorigenic and metastatic potency. Am. J. Pathol. 2006;169:673-81.

52. Folkman J, Merler E, Abernathy C, Williams G. Isolation of a tumor factor responsible for angiogenesis. J. Exp. Med. 1971;133:275-88.

53. O'Reilly MS, Holmgren L, Chen C, Folkman J. Angiostatin induces and sustains dormancy of human primary tumors in mice. Nat. Med. 1996;2:689-92.

54. Favaro E, Amadori A, Indraccolo S. Cellular interactions in the vascular niche: implications in the regulation of tumor dormancy. APMIS 2008;116:648-59.

55. Shibue T, Weinberg RA. Integrin {beta}1-focal adhesion kinase signaling directs the proliferation of metastatic cancer cells disseminated in the lungs. Proc. Natl. Acad. Sci. U.S.A. 2009; 106:10290-5.

56. Barkan D, Kleinman H, Simmons JL, Asmussen H, Kamaraju AK, Hoenorhoff MJ et al.. Inhibition of metastatic outgrowth from single dormant tumor cells by targeting the cytoskeleton. Cancer Res. 2008;68:6241-50.

57. Morris VL, Koop S, MacDonald IC, Schmidt EE, Grattan M, Percy D et al.. Mammary carcinoma cell lines of high and low metastatic potential differ not in extravasation but in subsequent migration and growth. Clin. Exp. Metastasis 1994;12:357-67.

58. Morris VL, Tuck AB, Wilson SM, Percy D, Chambers AF. Tumor progression and metastasis in murine D2 hyperplastic alveolar nodule mammary tumor cell lines. Clin. Exp. Metastasis 1993;11:103-12.

59. Rak JW, McEachern D, Miller FR. Sequential alteration of peanut agglutinin binding-glycoprotein expression during progression of murine mammary neoplasia. Br. J. Cancer 1992;65:641-8.

60. Weissleder R, Pittet MJ. Imaging in the era of molecular oncology. Nature 2008;452:580-9.

61. Yamamoto N, Jiang P, Yang M, Xu M, Yamauchi K, Tsuchiya H et al.. Cellular dynamics visualized in live cells in vitro and in vivo by differential dual-color nuclear-cytoplasmic fluorescent-protein expression. Cancer Res. 2004;64:4251-6.

62. Kobayashi H, Ogawa M, Kosaka N, Choyke PL, Urano Y. Multicolor imaging of lymphatic function with two nanomaterials: quantum dot-labeled cancer cells and dendrimer-based optical agents. Nanomed 2009;4:411-9.

63. Shaner NC, Campbell RE, Steinbach PA, Giepmans BNG, Palmer AE, Tsien RY. Improved monomeric red, orange and yellow fluorescent proteins derived from Discosoma sp. red fluorescent protein. Nat. Biotechnol. 2004;22:1567-72.

64. Ikawa K, Terashima Y, Sasaki K, Tashiro S. Genetic detection of liver micrometastases that are undetectable histologically. J. Surg. Res. 2002;106:124-30.

65. Sakaue-Sawano A, Ohtawa K, Hama H, Kawano M, Ogawa M, Miyawaki A. Tracing the silhouette of individual cells in S/G2/M phases with fluorescence. Chem. Biol. 2008;15:1243-8.

66. Sakaue-Sawano A, Kurokawa H, Morimura T, Hanyu A, Hama H, Osawa H et al.. Visualizing spatiotemporal dynamics of multicellular cell-cycle progression. Cell 2008;132:487-98.

67. Allgayer H, Aguirre-Ghiso JA. The urokinase receptor (u-PAR)--a link between tumor cell dormancy and minimal residual disease in bone marrow?. APMIS 2008;116:602-14.

68. Schewe DM, Aguirre-Ghiso JA. ATF6alpha-Rheb-mTOR signaling promotes survival of dormant tumor cells in vivo. Proc. Natl. Acad. Sci. U.S.A. 2008;105:10519-24.

69. Aguirre-Ghiso JA, Ossowski L, Rosenbaum SK. Green fluorescent protein tagging of extracellular signal-regulated kinase and p38 pathways reveals novel dynamics of pathway activation during primary and metastatic growth. Cancer Res. 2004;64:7336-45.

70. Aguirre-Ghiso JA, Estrada Y, Liu D, Ossowski L. ERK(MAPK) activity as a determinant of tumor growth and dormancy; regulation by p38(SAPK). Cancer Res. 2003;63:1684-95.

71. Liu D, Aguirre Ghiso J, Estrada Y, Ossowski L. EGFR is a transducer of the urokinase receptor initiated signal that is required for in vivo growth of a human carcinoma. Cancer Cell 2002;1:445-57.

72. Aguirre Ghiso JA. Inhibition of FAK signaling activated by urokinase receptor induces dormancy in human carcinoma cells in vivo. Oncogene 2002;21:2513-24.

73. Aguirre-Ghiso JA, Liu D, Mignatti A, Kovalski K, Ossowski L. Urokinase receptor and fibronectin regulate the ERK(MAPK) to p38(MAPK) activity ratios that determine carcinoma cell proliferation or dormancy in vivo. Mol. Biol. Cell 2001;12:863-79.

74. Ossowski L, Aguirre-Ghiso JA. Urokinase receptor and integrin partnership: coordination of signaling for cell adhesion, migration and growth. Curr. Opin. Cell Biol. 2000;12:613-20.

75. Ossowski L, Aguirre Ghiso J, Liu D, Yu W, Kovalski K. The role of plasminogen activator receptor in cancer invasion and dormancy. Medicina (B Aires) 1999;59:547-52.

76. Aguirre Ghiso JA, Kovalski K, Ossowski L. Tumor dormancy induced by downregulation of urokinase receptor in human carcinoma involves integrin and MAPK signaling. J. Cell Biol. 1999;147:89-104.

77. Pantel K, Alix-Panabières C, Riethdorf S. Cancer micrometastases. Nat Rev Clin Oncol 2009;6:339-51.

78. Demicheli R, Retsky MW, Swartzendruber DE, Bonadonna G. Proposal for a new model of breast cancer metastatic development. Ann. Oncol. 1997;8:1075-80.

79. Weiss L. Comments on hematogenous metastatic patterns in humans as revealed by autopsy. Clin. Exp. Metastasis 1992;10:191-9.

80. Demicheli R, Terenziani M, Bonadonna G. Estimate of tumor growth time for breast cancer local recurrences: rapid growth after wake-up?. Breast Cancer Res. Treat. 1998;51:133-7.

81. Karrison TG, Ferguson DJ, Meier P. Dormancy of mammary carcinoma after mastectomy. J. Natl. Cancer Inst. 1999;91:80-5.

82. Demicheli R, Retsky MW, Hrushesky WJM, Baum M. Tumor dormancy and surgery-driven interruption of dormancy in breast cancer: learning from failures. Nat Clin Pract Oncol 2007;4:699-710.

83. Retsky M, Bonadonna G, Demicheli R, Folkman J, Hrushesky W, Valagussa P. Hypothesis: Induced angiogenesis after surgery in premenopausal node-positive breast cancer patients is a major underlying reason why adjuvant chemotherapy works particularly well for those patients. Breast Cancer Res. 2004;6:R372-4.

84. Demicheli R, Bonadonna G, Hrushesky WJM, Retsky MW, Valagussa P. Menopausal status dependence of the timing of breast cancer recurrence after surgical removal of the primary tumour. Breast Cancer Res. 2004;6:R689-96.

85. Demicheli R. Tumour dormancy: findings and hypotheses from clinical research on breast cancer. Semin. Cancer Biol. 2001;11:297-306.

86. Lee YT. Breast carcinoma: pattern of metastasis at autopsy. J Surg Oncol 1983;23:175-80.

87. Cifuentes N, Pickren JW. Metastases from carcinoma of mammary gland: an autopsy study. J Surg Oncol 1979;11:193-205.

88. Demicheli R, Biganzoli E, Boracchi P, Greco M, Retsky MW. Recurrence dynamics does not depend on the recurrence site. Breast Cancer Res. 2008;10:R83.

89. Norton L. Tumor dormancy: separating observations from experimental science. Nat Clin Pract Oncol 2007;4:671.

90. Demicheli R, Miceli R, Brambilla C, Ferrari L, Moliterni A, Zambetti M et al.. Comparative analysis of breast cancer recurrence risk for patients receiving or not receiving adjuvant cyclophosphamide, methotrexate, fluorouracil (CMF). Data supporting the occurrence of 'cures'. Breast Cancer Res. Treat. 1999;53:209-15.

91. Retsky MW, Demicheli R, Swartzendruber DE, Bame PD, Wardwell RH, Bonadonna G et al.. Computer simulation of a breast cancer metastasis model. Breast Cancer Res. Treat. 1997;45:193-202.

92. Dignam JJ, Dukic VM. Comments on: Yin W, Di G, Zhou L, Lu J, Liu G, Wu J, Shen K, Han Q, Shen Z, Shao Z. Time-varying pattern of recurrence risk for Chinese breast cancer patients. Breast Cancer Res. Treat. 2009;116:209-10.

93. Yin W, Di G, Zhou L, Lu J, Liu G, Wu J et al.. Time-varying pattern of recurrence risk for Chinese breast cancer patients. Breast Cancer Res. Treat. 2009;114:527-35.

94. Brackstone M, Townson JL, Chambers AF. Tumour dormancy in breast cancer: an update. Breast Cancer Res. 2007;9:208.

95. Dave B, Chang J. Treatment resistance in stem cells and breast cancer. J Mammary Gland Biol Neoplasia 2009;14:79-82.

96. Zhou J, Zhang Y. Cancer stem cells: Models, mechanisms and implications for improved treatment. Cell Cycle 2008;7:1360-70.

97. Trumpp A, Wiestler OD. Mechanisms of Disease: cancer stem cells--targeting the evil twin. Nat Clin Pract Oncol 2008;5:337-47.

98. Viganò L, Ferrero A, Lo Tesoriere R, Capussotti L. Liver surgery for colorectal metastases: results after 10 years of follow-up. Long-term survivors,

late recurrences, and prognostic role of morbidity. Ann. Surg. Oncol. 2008;15:2458-64.

99. Small R, Lubezky N, Ben-Haim M. Current controversies in the surgical management of colorectal cancer metastases to the liver. Isr. Med. Assoc. J. 2007;9:742-7.

100. Adam R, Delvart V, Pascal G, Valeanu A, Castaing D, Azoulay D et al.. Rescue surgery for unresectable colorectal liver metastases downstaged by chemotherapy: a model to predict long-term survival. Ann. Surg. 2004;240:644-57; discussion 657-8.

101. Bismuth H, Adam R, Navarro F, Castaing D, Engerran L, Abascal A. Re-resection for colorectal liver metastasis. Surg. Oncol. Clin. N. Am. 1996;5:353-64.

102. Demicheli R, Valagussa P, Bonadonna G. Does surgery modify growth kinetics of breast cancer micrometastases?. Br. J. Cancer 2001;85:490-2.

103. von Breitenbuch P, Köhl G, Guba M, Geissler E, Jauch KW, Steinbauer M. Thermoablation of colorectal liver metastases promotes proliferation of residual intrahepatic neoplastic cells. Surgery 2005;138:882-7.

104. Meredith K, Haemmerich D, Qi C, Mahvi D. Hepatic resection but not radiofrequency ablation results in tumor growth and increased growth factor expression. Ann. Surg. 2007;245:771-6.

105. Ohsawa I, Murakami T, Uemoto S, Kobayashi E. In vivo luminescent imaging of cyclosporin A-mediated cancer progression in rats. Transplantation 2006;81:1558-67.

106. Collins I, Workman P. New approaches to molecular cancer therapeutics. Nat. Chem. Biol. 2006;2:689-700.

107. Petrelli A, Giordano S. From single- to multi-target drugs in cancer therapy: when aspecificity becomes an advantage. Curr Med Chem 2008;15:422-32.

108. Press MF, Lenz H. EGFR, HER2 and VEGF pathways: validated targets for cancer treatment. Drugs 2007;67:2045-75.

109. Sajja HK, East MP, Mao H, Wang YA, Nie S, Yang L. Development of multifunctional nanoparticles for targeted drug delivery and noninvasive imaging of therapeutic effect. Curr Drug Discov Technol 2009;6:43-51.

110. Farokhzad OC, Langer R. Impact of nanotechnology on drug delivery. ACS Nano 2009;3:16-20.

111. Peer D, Karp JM, Hong S, Farokhzad OC, Margalit R, Langer R. Nanocarriers as an emerging platform for cancer therapy. Nat Nanotechnol 2007;2:751-60.

112. Pittet MJ. Behavior of immune players in the tumor microenvironment. Curr Opin Oncol 2009;21:53-9.

113. Aussilhou B, Panis Y, Alves A, Nicco C, Klatzmann D. Tumor recurrence after partial hepatectomy for liver metastases in rats: prevention by in vivo injection of irradiated cancer cells expressing GMCSF and IL-12. J. Surg. Res. 2008;149:184-91.

114. Pejawar-Gaddy S, Finn OJ. Cancer vaccines: accomplishments and challenges. Crit. Rev. Oncol. Hematol. 2008;67:93-102.

115. Marcato P, Dean CA, Giacomantonio CA, Lee PWK. Oncolytic reovirus effectively targets breast cancer stem cells. Mol. Ther. 2009;17:972-9.

116. Park B, Hwang T, Liu T, Sze DY, Kim J, Kwon H et al.. Use of a targeted oncolytic poxvirus, JX-594, in patients with refractory primary or metastatic liver cancer: a phase I trial. Lancet Oncol. 2008;9:533-42.

117. Bell JC. Oncolytic viruses: what's next?. Curr Cancer Drug Targets 2007;7:127-31.

118. Nguyên TL, Abdelbary H, Arguello M, Breitbach C, Leveille S, Diallo J et al.. Chemical targeting of the innate antiviral response by histone deacetylase inhibitors renders refractory cancers sensitive to viral oncolysis. Proc. Natl. Acad. Sci. U.S.A. 2008;105:14981-6.

119. Muster T, Rajtarova J, Sachet M, Unger H, Fleischhacker R, Romirer I et al.. Interferon resistance promotes oncolysis by influenza virus NS1-deletion mutants. Int. J. Cancer 2004;110:15-21.

120. Liu J, Stace-Naughton A, Jiang X, Brinker CJ. Porous nanoparticle supported lipid bilayers (protocells) as delivery vehicles. J. Am. Chem. Soc. 2009;131:1354-5.

121. Liu J, Jiang X, Ashley C, Brinker CJ. Electrostatically mediated liposome fusion and lipid exchange with a nanoparticle-supported bilayer for control of surface charge, drug containment, and delivery. J. Am. Chem. Soc. 2009;131:7567-9.

122. Roesli C, Borgia B, Schliemann C, Gunthert M, Wunderli-Allenspach H, Giavazzi R et al.. Comparative analysis of the membrane proteome of closely related metastatic and nonmetastatic tumor cells. Cancer Res. 2009;69:5406-14.

123. Schewe DM, Aguirre-Ghiso JA. Inhibition of eIF2alpha dephosphorylation maximizes bortezomib efficiency and eliminates quiescent multiple myeloma cells surviving proteasome inhibitor therapy. Cancer Res. 2009;69:1545-52.

124. Liby KT, Yore MM, Sporn MB. Triterpenoids and rexinoids as multifunctional agents for the prevention and treatment of cancer. Nat. Rev. Cancer 2007;7:357-69.

125. Ling X, Konopleva M, Zeng Z, Ruvolo V, Stephens LC, Schober W et al.. The novel triterpenoid C-28 methyl ester of 2-cyano-3, 12-dioxoolen-1, 9-dien-28-oic acid inhibits metastatic murine breast tumor growth through inactivation of STAT3 signaling. Cancer Res. 2007;67:4210-8.

126. Hyer ML, Shi R, Krajewska M, Meyer C, Lebedeva IV, Fisher PB et al.. Apoptotic activity and mechanism of 2-cyano-3,12-dioxoolean-1,9-dien-28-oic-acid and related synthetic triterpenoids in prostate cancer. Cancer Res. 2008;68:2927-33.

127. Deeb D, Gao X, Jiang H, Dulchavsky SA, Gautam SC. Oleanane triterpenoid CDDO-Me inhibits growth and induces apoptosis in prostate cancer cells by independently targeting pro-survival Akt and mTOR. Prostate 2009;69:851-60.

128. Suh N, Wang Y, Honda T, Gribble GW, Dmitrovsky E, Hickey WF et al.. A novel synthetic oleanane triterpenoid, 2-cyano-3,12-dioxoolean-1,9-dien-28-oic acid, with potent differentiating, antiproliferative, and anti-inflammatory activity. Cancer Res. 1999;59:336-41.

129. Yates MS, Tauchi M, Katsuoka F, Flanders KC, Liby KT, Honda T et al.. Pharmacodynamic characterization of chemopreventive triterpenoids as

exceptionally potent inducers of Nrf2-regulated genes. Mol. Cancer Ther.
2007;6:154-62.

2. 3D IMAGING AND QUANTIFICATION OF BOTH SOLITARY CELLS AND METASTASES IN WHOLE MOUSE LIVER BY MAGNETIC RESONANCE IMAGING

The content of this chapter has been adapted from "3D imaging and quantification of both solitary cells and metastases in whole mouse liver by magnetic resonance imaging"., by J.L Townson, S.S. Ramadan, C. Simedrea, B. K. Rutt, I.C. MacDonald, P.J. Foster and A.F. Chambers. Cancer Res, 2009; 69: 8326-31.

2.1 INTRODUCTION

Successful treatment of metastatic disease remains a significant clinical challenge, with treatment failure often attributed to tumor inaccessibility, advanced stage of the disease upon detection, poor drug delivery or drug resistance (1-3). However, experimental metastasis models have revealed that the population of metastatic cells within a secondary organ is heterogeneous and unlikely to respond uniformly to treatment (4-8). This situation was demonstrated by Naumov et al. who showed that doxorubicin was able to inhibit growth of large vascularized metastases but had no effect on the number or viability of solitary dormant cells present in the same organs or their ability to subsequently form metastases (5). Ultimate treatment failure in patients therefore may also be the result of failure to target the entire population of metastatic cells, in particular solitary dormant cells. However, experimental studies of solitary dormant metastatic cells and development of treatments to target them are complicated by the difficulties associated with detecting and quantifying single cells in vivo.

A number of imaging modalities have been used to study metastasis. The advantages and limitations of these modalities, including positron emission tomography (PET), single photon emission computed tomography (SPECT), computed tomography (CT), MR, ultrasound, bioluminescent and fluorescent optical imaging are well documented (9-14). To date, the majority of studies

focusing specifically on solitary metastatic cells have relied on fluorescent optical imaging, due primarily to the high resolution capabilities of this modality. In fact, the dormant metastatic cell population has been defined by optical characteristics including retention of exogenous fluorescent markers that are diluted and no longer visible following a few cycles of replication (5, 7, 8, 15). However, while fluorescent optical imaging has been used most frequently and provides the most detailed resolution for the study of single cells in vivo, the restricted field of view and depth of penetration often limit attempts to quantify solitary metastatic cells as well as growing metastases distributed throughout an entire organ or animal. In addition, this method is destructive to the tissue and samples only a small subset of the organ.

Advances in cellular magnetic resonance imaging (MRI) have provided a powerful imaging modality by which single cells can be detected and quantified non-invasively on a scale ranging from small tissue samples to whole animals (9, 16-19). Heyn et al. showed that solitary cells, including cancer cells, could be detected in mouse brain by MRI when labelled with iron oxide particles (MPIO) (16, 18). Labelling MDA-MB-231BR breast cancer cells with micron-sized iron oxide particles (MPIO) had no effect on the growth of the cells in vitro or their subsequent ability to form brain metastases in mice (18). Comparison of MR images and histological sections confirmed that signal voids in MR images corresponded with sections in the brain where fluorescent MPIO labelled cancer cells were present (16, 18). In addition, Shapiro et al. showed that individual MPIO labelled hepatocytes could be detected in liver following migration from the spleen (17). However, the utility of cellular MRI techniques for quantifying the effect of a cancer treatment on the entire metastatic cell population in whole organs has not yet been shown.

Here we describe an MRI method by which the majority of the metastatic population of B16F1 melanoma cells in mouse liver, including both solitary cells and growing metastases, can be rapidly (<6 min scan/liver) quantified in intact livers while keeping the tissue intact for further analysis. This novel method of quantification was then used to determine the effect of doxorubicin on both

solitary cells and growing metastases. It was found that doxorubicin significantly decreased total metastatic tumor volume but failed to reduce the number of solitary dormant metastatic cells in the same livers.

2.2 MATERIALS AND METHODS

2.2.1 *Cell Culture and MPIO Labelling*

Cell culture and MPIO labelling procedures were similar to those described previously (8, 16). Briefly, B16F1 murine melanoma cells were maintained in alpha-MEM media containing 10% FBS at 37°C and 5% CO_2. For MPIO labelling cells were grown in a T75 tissue culture flask using media with FBS until 80-90% confluent. MPIO beads (312.5 µL supplied stock suspension, 0.9 µm diameter, 63% magnetite, labelled with Dragon Green; Bangs Laboratory, Fishers, IN) were then added to 10 ml of media with FBS/flask and incubated for 24 hrs. The cells were washed thoroughly with serum free alpha-MEM to remove unincorporated MPIO beads. Cells were then centrifuged and resuspended in serum free alpha-MEM at the appropriate concentration for injection.

2.2.2 *Experimental Metastasis Assay and Doxorubicin Treatment*

Female 6-10 weeks old C57BL/6 mice (Harlan, Indianapolis, IN) were cared for in accordance with the Canadian Council on Animal Care, under a protocol approved by the University of Western Ontario Council on Animal Care. For experimental metastasis assays, mice were anesthetised with an i.p. injection of xylazine/ketamine (2.6 mg ketamine and 0.13 mg xylazine per 20 g body mass). Anesthetised mice received mesenteric vein injections of 100 µL of B16F1 cells suspended in alpha-MEM to target cells directly to liver as described previously (8). To quantify how signal void volume varies with the number of cells injected, mice (3-4 per group, total n = 14) were injected with 3.75 x 10^4, 7.5 x 10^4, 1.5 x 10^5 or 3.0 x 10^5 cells per mouse (in 100 µL) and sacrificed 10-15 min following cell injection. For tumor burden and treatment experiments 3 x 10^5

B16F1 cells (in 100 μL) were injected. Livers to be scanned and correlated with MR images were removed at day eleven. Treatment with doxorubicin (Pharmacia, Mississauga, ON, Canada) at 1 mg/kg, or vehicle control (0.9% sodium chloride), commenced 24 hours following cell injection and continued 3x weekly for a total of 4 treatments. Mice (n = 11 control, 11 = treated) were sacrificed 9 days following cell injection and livers were removed and fixed in formalin for at least 48 hours.

2.2.3 Magnetic Resonance Imaging and Image Analysis

Mice were sacrificed and livers removed immediately (10-15 min) or at 9 (doxorubicin experiment) or 11 (histology correlation) days following cell injection. Formalin-fixed livers were scanned using a 3T clinical MRI. All MRI examinations were performed on a 3T GE CV/i whole-body clinical MR scanner as described previously (18). In brief, this included a custom-built gradient coil (inner diameter = 12 cm, maximum gradient strength = 600 mT/m, and peak slew rate = 2000 T/m/s) and solenoidal radiofrequency (RF) coil (inner diameter = 1.5 cm). Images were obtained using the 3D fast imaging employing steady state acquisition (FIESTA) pulse sequence (20). The scanned resolution was $100 \times 100 \times 200$ μm^3 and the total acquisition time was less than 6 min per whole liver. No additional contrast agent (other than MPIO in cells) is used in these studies.

Tumor and liver volume analysis and 3D reconstruction of images was completed using VGStudio Max (Volume Graphics GmbH, Germany) or OsiriX imaging software (open source). This process is semi-automated as hyperintense areas of images were automatically thresholded and subsequent manual correction of misclassified regions (such as vasculature) was performed. Signal void area was measured using ImageJ image analysis software (NIH, USA). For each group of mice a pixel value threshold was established manually and subsequent analysis for all scans within each experiment was automatically calculated using the fixed pixel intensity threshold. At least 125 images per organ were used to calculate signal void area.

2.2.4 *Histology and Statistics*

Digital images of whole formalin-fixed livers were acquired using a 7.1 mega pixel digital camera (Canon) mounted to a tripod. These were used for comparison of visible surface tumors with surface rendered MRI images of hyperintense regions. For histological correlation, livers were paraffin-embedded, sectioned (4 μm) and stained with hematoxylin and eosin.

Statistical analysis of tumor volume and signal void area following doxorubicin treatment was performed using a t-test comparing volume and area (respectively) from at least 125 MR images per liver. Data are presented as the mean +/- SEM. A standard curve and R^2 value were generated by linear regression and used to quantify the correlation between signal void area and the number of solitary cells present in the liver. All statistical analyses were performed using Graphpad Prism software.

2.3 RESULTS

2.3.1 *MRI signal void area strongly correlates with the number of MPIO labelled cells in liver*

To determine if MRI signal void area could be used to quantify the number of cells present in the liver, we assessed the correlation between signal void area and the number of B16F1 cells labelled with MPIO in that organ (Fig. 2.1). Known numbers (3×10^5 or 1.5×10^5 or 7.5×10^4 or 3.75×10^4) of B16F1 cells labelled with MPIO were delivered to mouse liver via mesenteric vein injection. Livers were removed immediately following injections, fixed in formalin and scanned by 3T MRI as described in Materials and Methods. As seen in Fig. 2.1B, it is readily apparent that both the number and area of signal voids (arrows) increases with the number of cells injected into the liver. The coefficient of determination (R^2) value between signal void area and cell number over the entire range of cells injected from zero to 300 000 was 0.83 ($p < 0.001$) (Fig. 2.1A inset). However,

within the range between 3.75 x 10^4 and 1.5 x 10^5 cells R^2 increased to 0.96 (p < 0.001) (Fig. 2.1A). A decrease of 3.75 x 10^4 cells (between 3.75 x 10^4 and 7.5 x 10^4 cells), representing only 12.5% of number of cells initially injected, was found to be significantly different (t-test, p = 0.0019) within a population of only eight mice. The high degree of correlation between the number of MPIO labelled cells and signal void area (cell number explaining up to 96% of the variance in signal void area) indicates that quantification of this MR image parameter is a useful measure of the number of cells and ultimately quantification of the effect of treatment on this population of cells.

A

Number of cells vs signal void area

$R^2 = 0.96$
$p < 0.001$

Signal Void Area (mm^2)

1250
1000
750
500
250
0

$R^2 = 0.83$
$p < 0.001$

1000

0

0   75000   150000   225000   300000

0   25000   50000   75000   100000   125000   150000   175000

Number of Cells Injected

B

5 mm
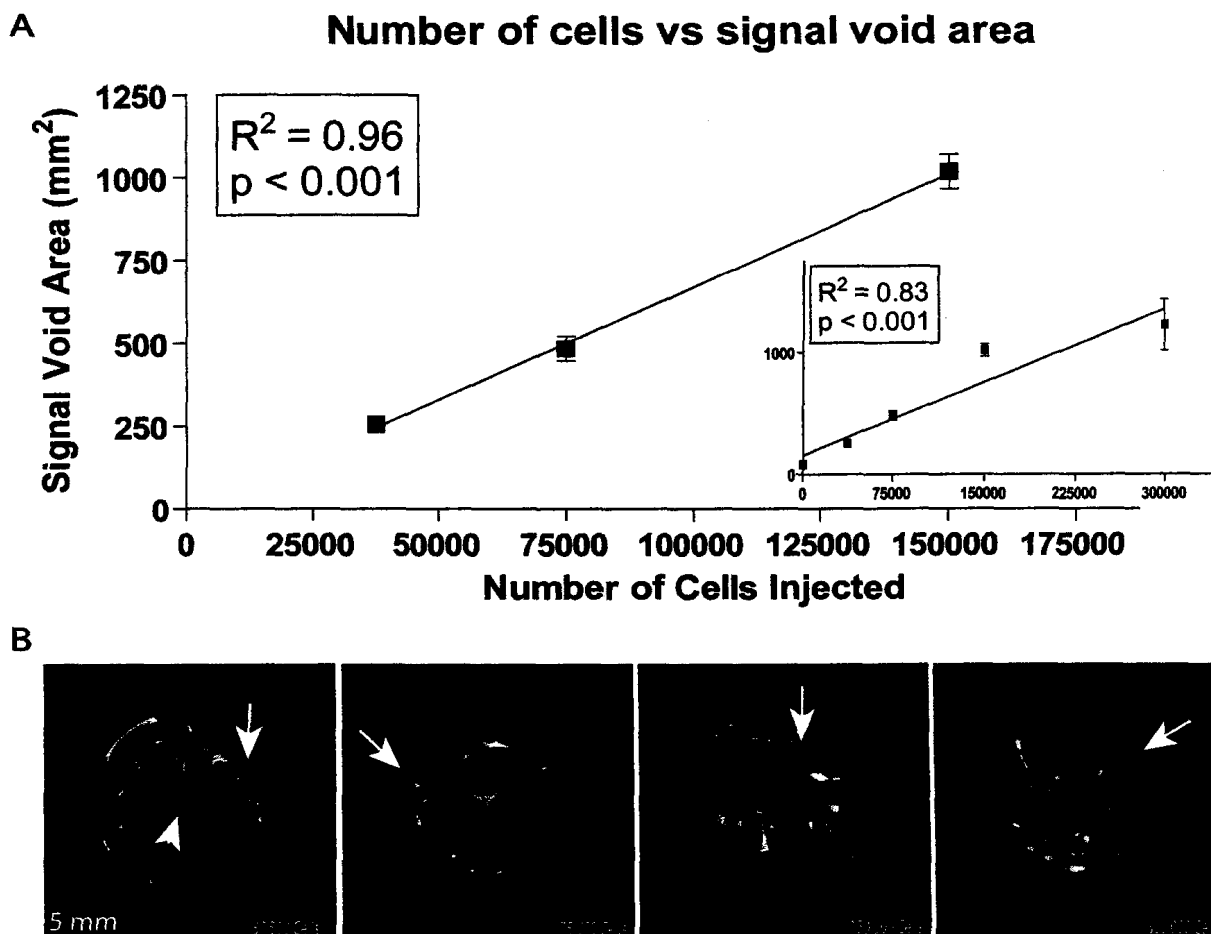
Figure 2.1 - Signal void area strongly correlates with the number of MPIO labelled B16F1 cells in the liver. A strong correlation ($R^2 = 0.96$, $p < 0.001$) exists between the number of cells injected and the total signal void area detected in whole mouse livers (A). This correlation covers the range from 3.75 x 10^4-1.5 x 10^5 cells. For the entire range between 0 to 3 x 10^5 cells the R^2 correlation is 0.83 ($p < 0.001$) (Inset). MPIO labelled B16F1 cells are apparent in MR images as multiple signal voids (dark spots, e.g., arrows) in a background of normal liver tissue that appears grey (e.g., arrow head). An increase in the number and size of signal voids can is apparent in the representative MR images of an increasing number of cells [3.75 x 10^4, 7.5 x 10^4, 1.5 x 10^5 and 3.0 x 10^5 (B)].

2.3.2 Quantification of B16F1 liver metastases (hyperintensity) in MRI images

To assess the utility of the 6 minute whole liver 3T MRI scan for quantification of liver metastasis volume, unlabeled B16F1 cells were injected into liver via mesenteric vein. Livers were removed at day 11 following injection and imaged by MRI as described above. As seen in Fig. 2.2 A-B, tumor tissue in histological images (lower panels), from which tumor burden, area or size have traditionally been quantified, is readily apparent as areas of hyperintensity in corresponding MR images (upper panels). Tumor tissue hyperintensity from metastases as small as 200 μm in diameter, by histology, were also visible in MR images (Fig. 2.1C). The appearance of tumor tissue as hyperintense regions in the liver is consistent with previous publications using T2 weighted images (21-23). Tumor hyperintensity can be used to calculate multiple tumor parameters, including volume, and can also be used to segment the tissue into multiple regions of interest that can be used to render 3D images. 3D images rendered using semi-automated segmentation based on tumor tissue hyperintensity closely resemble whole scanned liver lobes as can be seen by the surface tumor pattern (Fig. 2.2D).
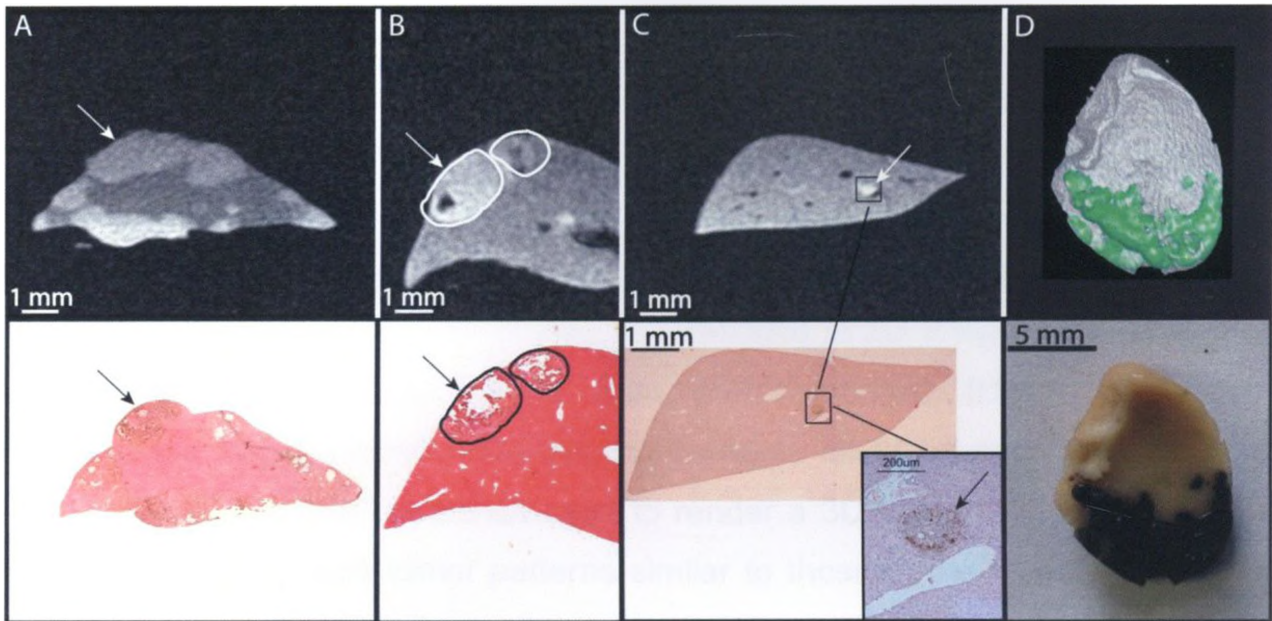
Figure 2.2 - MR image hyperintensity corresponds with metastatic tissue in histological sections. Hyperintense regions (white arrows) in MR images (A-B upper) correlate with regions of B16F1 metastatic tumors (black arrows) in H&E stained histological sections (A-B lower). B16F1 metastases as small as 200 µm were apparent in MR images (C upper) and corresponded with small metastases visible in histological sections (C lower). 2D MR images (top panel A-C), and which sample the entire liver, can be used to render representative 3D images in which tumor is apparent (pseudocolored green). 3D rendering of liver closely resembles the picture of the scanned liver lobe (D lower).

2.3.3 *Metastases and solitary dormant cells are apparent in the same MR image*

To determine the feasibility of quantifying both solitary cells and growing metastases from the same MR images, livers injected with MPIO labelled B16F1 cells were removed and imaged at day 9. Whole intact livers (Fig. 2.3A) were scanned by MRI as described above. This resulted in 2D images (Fig. 2.3B) in which both signal voids (arrow) from MPIO labelled B16F1 cells and hyperintense areas (arrowheads) from metastases could be seen in the same image. The 2D images were then used to render a 3D image (Fig. 2.3C) of the whole liver with surface tumor patterns similar to those of the intact whole liver (Fig. 2.3A). As the entire liver volume is scanned, MRI images can be used to quantify size, number and total tumor and normal tissue volume information from the whole liver (Fig. 2.3 inset table). All metastases in the organ can be assessed, in contrast to the limited number of representative sections that are routinely assessed with histology (Fig. 2.3D). In addition, this rapid MRI scanning procedure is non-destructive so tissue is preserved for further analysis following the scans.
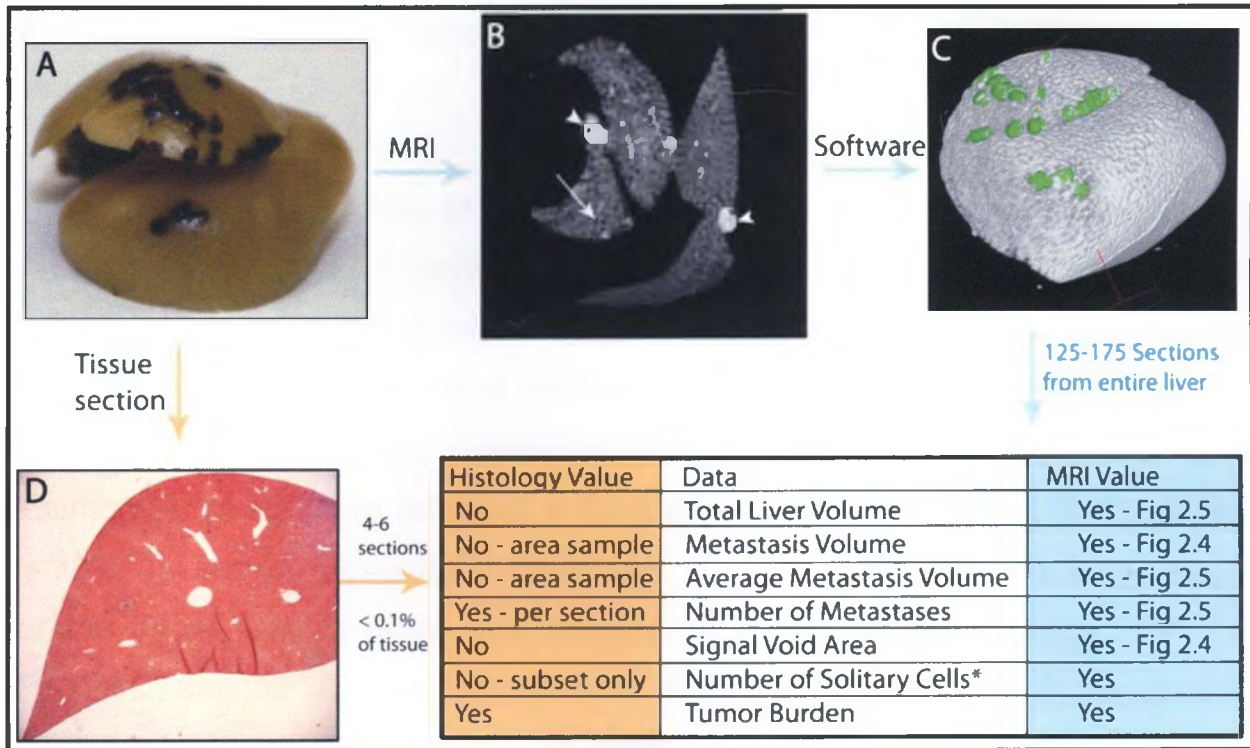
Figure 2.3 - Diagram showing how MR images of entire liver can be used to calculate multiple tumor, solitary cell and liver parameters. Whole livers (A) can be scanned by MR in order to generate 2D images (100 x 100 x 200 μm resolution) from which signal void area is calculated (B). 2D MRI sections (125-175 spanning entire liver) can be used to render 3D images (C) from which volume measurements can be made (See also supplemental video 1). A limited number of random or representative histological sections (D) are generally used to determine tumor and solitary cell data. MRI image data can be used to calculate multiple variables (light blue) that are restricted in analysis of histological sections (orange) (table insert).

2.3.4 *Doxorubicin decreased metastatic tumor volume but not signal void area*

To assess the ability of the MRI technique described here to quantify the effect of doxorubicin on both growing metastases and the solitary dormant metastatic cell population in whole mouse liver, 3×10^5 B16F1 cells labelled with MPIO were injected into the liver via the mesenteric vein. Mice were treated with 1 mg/kg doxorubicin, or vehicle control, three times weekly (four total treatments). Livers were removed 9 days after cell injection, fixed and scanned by MRI as above. Doxorubicin treatment resulted in an obvious decrease in surface tumor area in whole liver images (Fig. 2.4A), 3D MR image rendering (Fig. 2.4C) and 2D MR image tumor area (hyperintensity) (Fig. 2.4B). Analysis of MR images showed that doxorubicin treatment resulted in a significant decrease in metastatic tumor volume (t-test, n = 11 per group, p = 0.02) (Fig. 2.4D – left panel). However, doxorubicin treatment did not decrease the number of solitary cells in the same livers (t-test, p = 0.2), as quantified by MR signal void area at endpoint (Fig. 2.4D – right panel). The mean signal void area from all livers at endpoint ($434 +/- 29$ mm^2) corresponds with $6.5 \times 10^4 +/- 5.8 \times 10^3$ cells (Fig. 2.1A). MR images were also analyzed to determine the total number of metastases, liver volume, total liver and tumor volume and average metastasis volume for all livers (Fig. 2.5). The results of this experiment thus demonstrate the utility of this rapid MRI technique in simultaneously assessing the effect of treatment on solitary tumor cells and metastases, and shows that doxorubicin has a differential effect on metastases and solitary tumor cells, inhibiting metastatic growth but not affecting the number of solitary tumor cells in the same livers.

Figure 2.4 - Doxorubicin inhibited growth of metastases but did not decrease the number of dormant cells as measured by signal void area. Whole livers, showing black melanotic tumors visible at the liver surface (A) were scanned by MRI producing multiple 2D images (representative images, B) sampling the entire liver. 2D images were combined to render 3D volumetric images of the originally scanned livers (C). A decrease in surface tumor is visible as a decrease in black or green false coloring in (A) and (C) respectively. Decreased area of hyperintensity (tumor tissue) was apparent in 2D MRI images (B) of doxorubicin treated mice. Quantification of signal void area from 2D images, and metastatic tumor volume from 3D images, showed that doxorubicin treatment resulted in a significant decrease in tumor volume (t-test, $n = 11$ per treatment group, $p = 0.02$) (D). However, doxorubicin treatment did not decrease the number of dormant cells in the same livers (t-test, $p = 0.2$) as quantified by MR signal void area at endpoint (D).

FIGURE 2.4
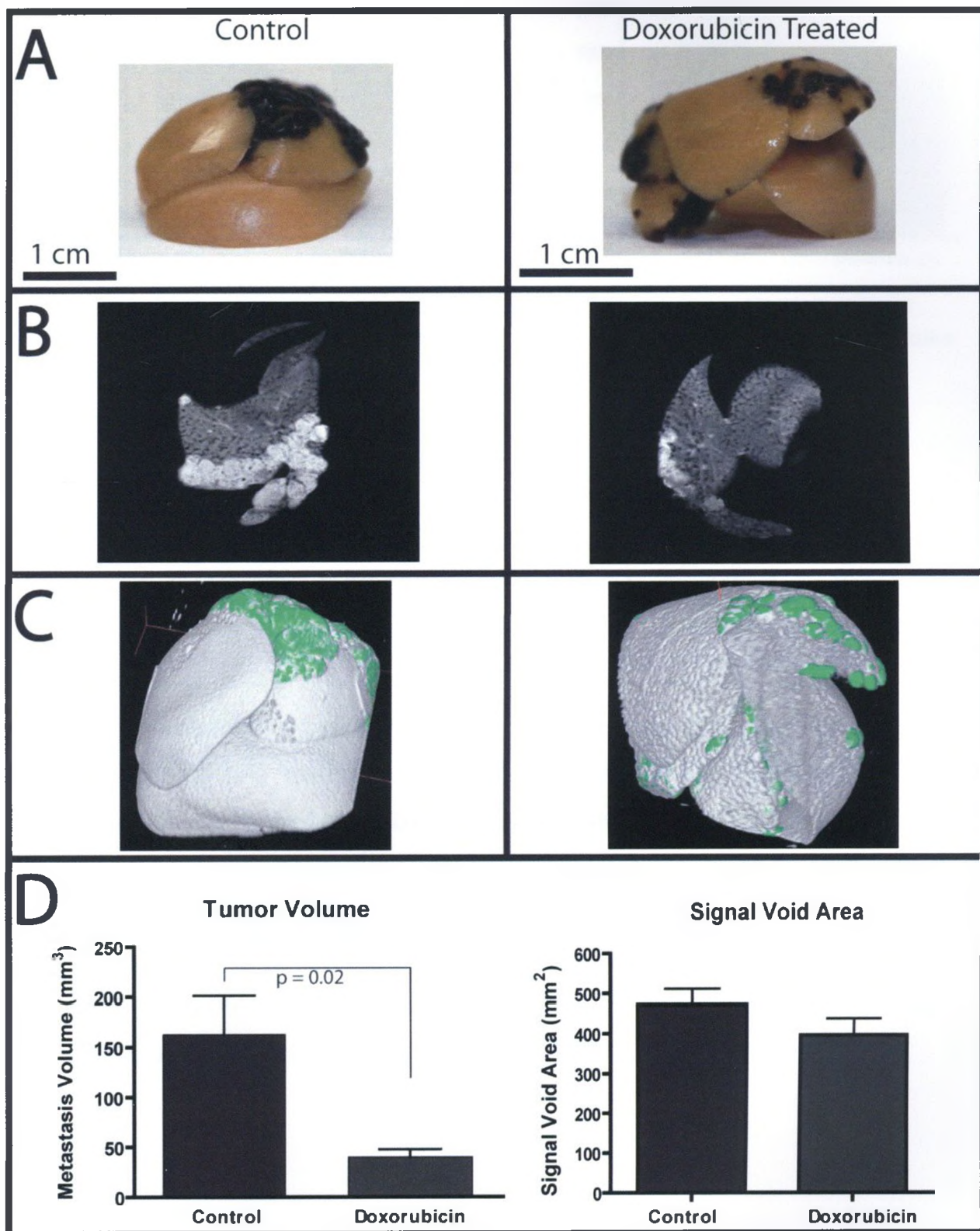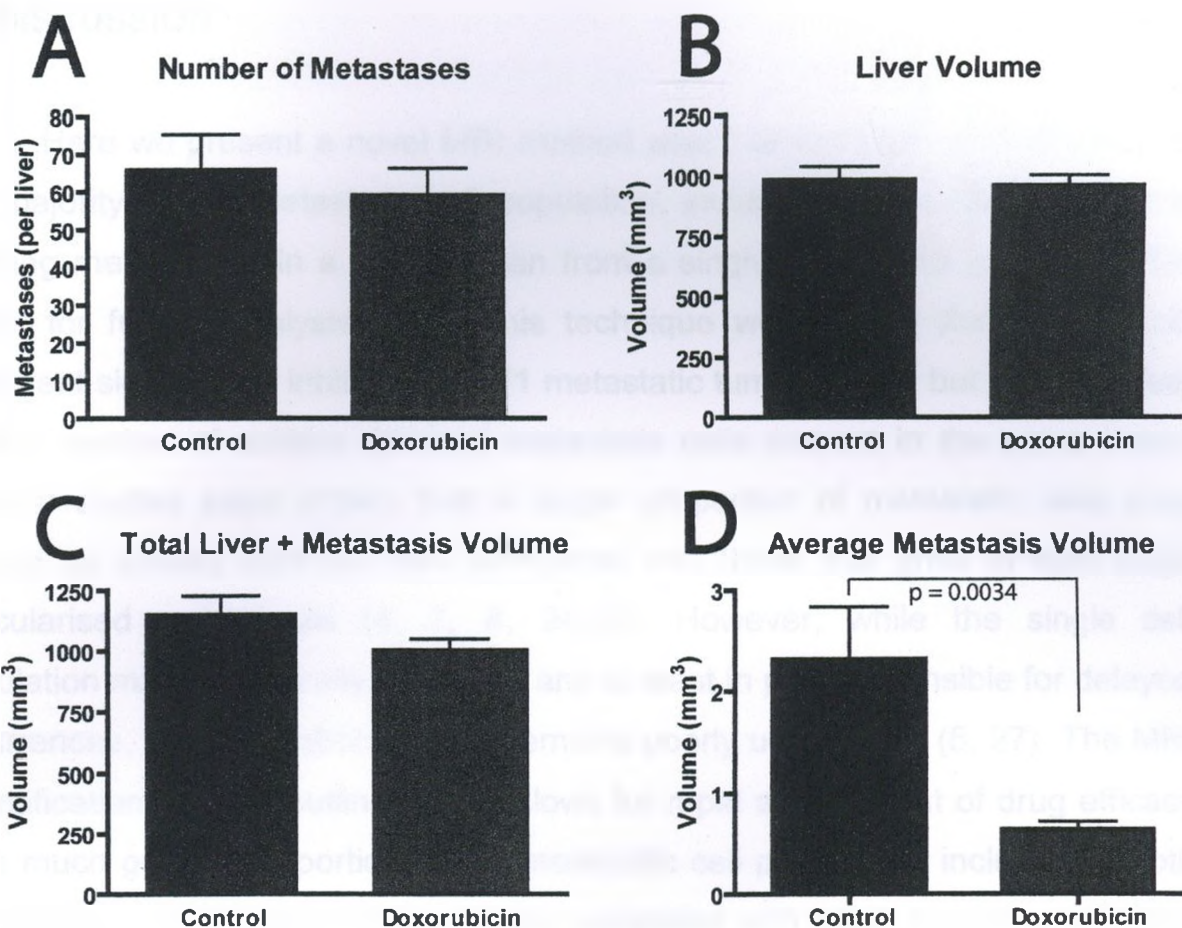
Figure 2.5 – Number of metastases (A), liver volume (B), total metastasis and liver volume (C) and average metastasis volume (D) as calculated from MR images of vehicle control and doxorubicin treated mice. A statistically significant decrease was observed in the average metastasis volume (t-test, n = 22, p = 0.0034). No significant difference between treated and control value were observed for number of metases (A), liver volume (B) or total metastasis and liver volume (P > 0.05). All data were acquired from the same images used to generate signal void area and tumor volume.

2.4 DISCUSSION

Here we present a novel MRI method which allows rapid quantification of the majority of the metastatic cell population, including both solitary cells and growing metastases, in a whole organ from a single scan while preserving the tissue for further analysis. Using this technique we showed that doxorubicin treatment significantly inhibited B16F1 metastatic tumor growth but had no effect on the number of solitary dormant metastatic cells present in the same livers. Several studies have shown that a larger proportion of metastatic cells may remain as solitary dormant cells compared with those that grow to form large vascularised metastases (4, 7, 8, 24-26). However, while the single cell population may be clinically important and at least in part responsible for delayed recurrences, this population of cells remains poorly understood (5, 27). The MRI quantification method outlined here allows for rapid assessment of drug efficacy on a much greater proportion of the metastatic cell population, inclusive of both metastases and solitary dormant cells, compared with other currently available methods of quantification.

Multiple MRI based techniques are currently used to detect and quantify iron oxide labelled cells (19). These include detection of iron labelled hepatocytes, macrophages, dendritic, cancer and stem cells using T1, T2 and T2* weighted imaging techniques, and quantification using multiple MRI parameters including T2, R2 and R2* (20, 28-35). It has been established qualitatively that the number of MPIO labelled human breast cancer cells delivered to the brain is associated with the number MRI signal voids (18). In addition, it has been shown that the spatial arrangement of signal voids found in MR images of the brain and liver corresponded with cellular fluorescence from MPIO labelled cells in these tissues (17, 18). Due to signal void "blooming" (MRI signal void appearing much larger than the actual MPIO labelled cell) and the proximity of cells to one another, a single MRI signal void is not always due to a single cell (16, 36). This appears to be observable in Fig. 2.1 where the size and number of signal voids increases with cell number. However, here we show there

is a strong correlation (R^2 values of 0.83-0.96) between signal void area in MR images and the number of metastatic cells present in the liver, indicating that signal void area is proportional to numbers of single cells present. This correlation is especially high ($R^2 = 0.96$) in the range between 3.75 x 10^4 and 1.5 x 10^5 cells (12.5-50% of cells initially injected). This is important as results from experimental metastasis models in which solitary cell fate has been quantified have shown this is the range within which the number of solitary dormant metastatic cells would most commonly be expected to fall (5, 7, 8). Consistent with this, we found that total signal void area from MPIO labelled B16F1 cells at day 9 accounted for a much smaller (6.5 x 10^4 +/- 5.8 x 10^3), however still significant, proportion of the 3 x 10^5 cells initially injected.

Our finding that doxorubicin treatment inhibited metastasis growth but did not decrease the number of solitary MPIO labelled B16F1 cells (Fig. 2.4) is in agreement with results of a previous experiment in which mouse mammary carcinoma cells were quantified by fluorescent optical imaging (5). That study also showed that doxorubicin inhibited metastatic burden, while not affecting the numbers of single cells present. And while the full significance of the dormant metastatic cell population remains to be understood, it is likely that exclusion of this population of metastatic cells from analysis of treatment efficacy plays a role in treatment failure leading to recurrence (5, 15, 27, 37-40). A growing number of metastasis models have demonstrated that solitary dormant metastatic cells retain their capacity to proliferate, forming late growing metastases or primary tumors following isolation and re-injection (4, 7, 8, 16, 24-26). The quantification method we present here advances the study of treatment effect on metastatic cells as it is currently the only method we are aware of that possesses the capability to detect, localize and quantify the majority of the metastatic cell population in whole organs without destroying the tissue and while preserving a 3D digital record. Currently, only a small proportion of the metastatic cell population is sampled in order to determine the effect of treatment in most studies. Taking into consideration the heterogeneous nature of the metastatic cell population it may not be possible to develop treatments capable of fully

eliminating metastatic disease until the effect of any compound on the entire population is understood. The method that we present here represents an opportunity to assess the effect of treatment on a significant population of metastatic cells that may be responsible for often significant failure rates in treatment of metastatic disease.

2.5 REFERENCES

1. Goldie JH, Coldman AJ. The genetic origin of drug resistance in neoplasms: implications for systemic therapy. Cancer Res. 1984;44:3643-53.

2. Agarwal R, Kaye SB. Ovarian cancer: strategies for overcoming resistance to chemotherapy. Nat. Rev. Cancer 2003;3:502-16.

3. Van den Broeck A, Sergeant G, Ectors N, Van Steenbergen W, Aerts R, Topal B. Patterns of recurrence after curative resection of pancreatic ductal adenocarcinoma. Eur J Surg Oncol 2009; doi:10.1016/j.ejso.2008.12.006.

4. Goodison S, Kawai K, Hihara J, Jiang P, Yang M, Urquidi V et al.. Prolonged dormancy and site-specific growth potential of cancer cells spontaneously disseminated from nonmetastatic breast tumors as revealed by labeling with green fluorescent protein. Clin. Cancer Res. 2003;9:3808-14.

5. Naumov GN, Townson JL, MacDonald IC, Wilson SM, Bramwell VHC, Groom AC et al.. Ineffectiveness of doxorubicin treatment on solitary dormant mammary carcinoma cells or late-developing metastases. Breast Cancer Res. Treat. 2003;82:199-206.

6. Chambers AF, Groom AC, MacDonald IC. Dissemination and growth of cancer cells in metastatic sites. Nat. Rev. Cancer 2002;2:563-72.

7. Cameron MD, Schmidt EE, Kerkvliet N, Nadkarni KV, Morris VL, Groom AC et al.. Temporal progression of metastasis in lung: cell survival, dormancy, and location dependence of metastatic inefficiency. Cancer Res. 2000;60:2541-6.

8. Luzzi KJ, MacDonald IC, Schmidt EE, Kerkvliet N, Morris VL, Chambers AF et al.. Multistep nature of metastatic inefficiency: dormancy of solitary cells after successful extravasation and limited survival of early micrometastases. Am. J. Pathol. 1998;153:865-73.

9. Weissleder R, Pittet MJ. Imaging in the era of molecular oncology. Nature 2008;452:580-9.

10. Hoffman RM. In vivo real-time imaging of nuclear-cytoplasmic dynamics of dormancy, proliferation and death of cancer cells. APMIS 2008;116:716-29.

11. Graham KC, Ford NL, MacKenzie LT, Postenka CO, Groom AC, MacDonald IC et al.. Noninvasive quantification of tumor volume in preclinical liver metastasis models using contrast-enhanced x-ray computed tomography. Invest Radiol 2008;43:92-9.

12. Sahai E. Illuminating the metastatic process. Nat. Rev. Cancer 2007;7:737-49.

13. Graham KC, Wirtzfeld LA, MacKenzie LT, Postenka CO, Groom AC, MacDonald IC et al.. Three-dimensional high-frequency ultrasound imaging for longitudinal evaluation of liver metastases in preclinical models. Cancer Res. 2005;65:5231-7.

14. Wirtzfeld LA, Graham KC, Groom AC, Macdonald IC, Chambers AF, Fenster A et al.. Volume measurement variability in three-dimensional high-frequency ultrasound images of murine liver metastases. Phys Med Biol 2006;51:2367-81.

15. Naumov GN, MacDonald IC, Chambers AF, Groom AC. Solitary cancer cells as a possible source of tumour dormancy?. Semin. Cancer Biol. 2001;11:271-6.

16. Heyn C, Ronald JA, Mackenzie LT, MacDonald IC, Chambers AF, Rutt BK et al.. In vivo magnetic resonance imaging of single cells in mouse brain with optical validation. Magn Reson Med 2006;55:23-9.

17. Shapiro EM, Sharer K, Skrtic S, Koretsky AP. In vivo detection of single cells by MRI. Magn Reson Med 2006;55:242-9.

18. Heyn C, Ronald JA, Ramadan SS, Snir JA, Barry AM, MacKenzie LT et al.. In vivo MRI of cancer cell fate at the single-cell level in a mouse model of breast cancer metastasis to the brain. Magn Reson Med 2006;56:1001-10.

19. Liu W, Frank J. Detection and quantification of magnetically labeled cells by cellular MRI. Eur J Radiol 2008; doi:10.1016/j.ejrad.2008.09.021.

20. Foster-Gareau P, Heyn C, Alejski A, Rutt BK. Imaging single mammalian cells with a 1.5 T clinical MRI scanner. Magn Reson Med 2003;49:968-71.

21. Qin Y, Van Cauteren M, Osteaux M, Willems G. Quantitative study of the growth of experimental hepatic tumors in rats by using magnetic resonance imaging. Int. J. Cancer 1992;51:665-70.

22. Qin Y, Van Cauteren M, Osteaux M, Schally AV, Willems G. Inhibitory effect of somatostatin analogue RC-160 on the growth of hepatic metastases of colon cancer in rats: a study with magnetic resonance imaging. Cancer Res. 1992;52:6025-30.

23. Namasivayam S, Martin DR, Saini S. Imaging of liver metastases: MRI. Cancer Imaging 2007;7:2-9.

24. Naumov GN, MacDonald IC, Weinmeister PM, Kerkvliet N, Nadkarni KV, Wilson SM et al.. Persistence of solitary mammary carcinoma cells in a secondary site: a possible contributor to dormancy. Cancer Res. 2002;62:2162-8.

25. Logan PT, Fernandes BF, Di Cesare S, Marshall JA, Maloney SC, Burnier MNJ. Single-cell tumor dormancy model of uveal melanoma. Clin. Exp. Metastasis 2008;25:509-16.

26. Suzuki M, Mose ES, Montel V, Tarin D. Dormant cancer cells retrieved from metastasis-free organs regain tumorigenic and metastatic potency. Am. J. Pathol. 2006;169:673-81.

27. Goss P, Allan AL, Rodenhiser DI, Foster PJ, Chambers AF. New clinical and experimental approaches for studying tumor dormancy: does tumor dormancy offer a therapeutic target?. APMIS 2008;116:552-68.

28. Rad AM, Arbab AS, Iskander ASM, Jiang Q, Soltanian-Zadeh H. Quantification of superparamagnetic iron oxide (SPIO)-labeled cells using MRI. J Magn Reson Imaging 2007;26:366-74.

29. de Vries IJM, Lesterhuis WJ, Barentsz JO, Verdijk P, van Krieken JH, Boerman OC et al.. Magnetic resonance tracking of dendritic cells in melanoma patients for monitoring of cellular therapy. Nat. Biotechnol. 2005;23:1407-13.

30. Bos C, Delmas Y, Desmoulière A, Solanilla A, Hauger O, Grosset C et al.. In vivo MR imaging of intravascularly injected magnetically labeled mesenchymal stem cells in rat kidney and liver. Radiology 2004;233:781-9.

31. Hauger O, Frost EE, van Heeswijk R, Deminière C, Xue R, Delmas Y et al.. MR evaluation of the glomerular homing of magnetically labeled mesenchymal stem cells in a rat model of nephropathy. Radiology 2006;238:200-10.

32.   Liu W, Dahnke H, Rahmer J, Jordan EK, Frank JA. Ultrashort T(2) (*) relaxometry for quantitation of highly concentrated superparamagnetic iron oxide (SPIO) nanoparticle labeled cells. Magn Reson Med 2009;61(4):761-6.

33.   Arbab AS, Janic B, Knight RA, Anderson SA, Pawelczyk E, Rad AM et al.. Detection of migration of locally implanted AC133+ stem cells by cellular magnetic resonance imaging with histological findings. FASEB J. 2008;22:3234-46.

34.   Dekaban GA, Snir J, Shrum B, de Chickera S, Willert C, Merrill M et al.. Semiquantitation of Mouse Dendritic Cell Migration In Vivo Using Cellular MRI. J. Immunother. 2009;32:240–251.

35.   Foster PJ, Dunn EA, Karl KE, Snir JA, Nycz CM, Harvey AJ et al.. Cellular magnetic resonance imaging: in vivo imaging of melanoma cells in lymph nodes of mice. Neoplasia 2008;10:207-16.

36.   Dodd SJ, Williams M, Suhan JP, Williams DS, Koretsky AP, Ho C. Detection of single mammalian cells by high-resolution magnetic resonance imaging. Biophys. J. 1999;76:103-9.

37.   Demicheli R, Biganzoli E, Boracchi P, Greco M, Retsky MW. Recurrence dynamics does not depend on the recurrence site. Breast Cancer Res. 2008;10:R83.

38.   Schewe DM, Aguirre-Ghiso JA. ATF6alpha-Rheb-mTOR signaling promotes survival of dormant tumor cells in vivo. Proc. Natl. Acad. Sci. U.S.A. 2008;105:10519-24.

39.   Aguirre-Ghiso JA. Models, mechanisms and clinical evidence for cancer dormancy. Nat. Rev. Cancer 2007;7:834-46.

40.   Townson JL, Chambers AF. Dormancy of solitary metastatic cells. Cell Cycle 2006;5:1744-50.

3. THE SYNTHETIC TRITERPENOID CDDO-IMIDAZOLIDE SUPPRESSES EXPERIMENTAL LIVER METASTASIS

The content of this chapter has been adapted from "The synthetic triterpenoid CDDO-Imidazolide suppresses experimental liver metastasis", submitted for review, by J. L. Townson, K. Liby, L.M. Mackenzie, C. Simedrea, P. J. Foster, I. C. MacDonald, M. B. Sporn and A. F. Chambers.

3.1 INTRODUCTION

Liver is a common site of metastatic disease from a number of cancers, including colon and melanoma, and is associated with poor survival (1-3). Improvements in surgical techniques and chemotherapy treatment have increased mean survival times, however 5 year survival rates remain low even after all clinically detectable metastases are surgically removed and adjuvant therapy administered (4-6). Thus, new approaches to treat liver metastases are needed.

The synthetic triterpenoid 1-[2-cyano-3-,12-dioxooleana-1,9(11)-dien-28-oyl]imidazole (CDDO-Im) is one of a number of synthetic oleanane triterpenoids that have been shown to elicit multifunctional effects dependent on both cell type and drug concentration (7). These effects include the potential to induce cell differentiation, cell cycle arrest (8) and apoptosis (independent of multidrug resistance status) (9, 10) in a number of difference cancer cell lines (7, 11). Pharmacodynamic characterization of CDDO-Im following oral dosing has revealed that CDDO-Im is stable in the digestive system, readily absorbed and pharmacologically active in a number of organs including the liver (12), suggesting a potential role for CDDO-Im in treatment of liver metastases. Yet while synthetic triterpenoids have been shown to successfully inhibit orthotopic and ectopic tumors, lung metastasis and carcinogen induced tumor growth in multiple experimental models (8, 10, 13-16), their effect on metastatic liver disease is unknown.

Although liver metastasis is often fatal, experimental models have revealed that metastasis is an inefficient process whereby the majority of metastatic cells that arrive in the liver do not form large vascularized metastases (17-21). Instead, many cells arriving in a secondary site will undergo apoptosis, and some may remain, often for extended periods of time, as solitary dormant cells alone or amidst proliferating metastases (17, 18, 22-29). The heterogeneous nature of the metastatic cell population makes it unlikely that all cells will respond uniformly to treatment. This situation has been demonstrated in experimental metastasis model in which doxorubicin significantly inhibited the growth of large actively growing metastases, but had no effect on the number and viability of solitary cells or their ability to form late occurring metastases following treatment (30, Chapter 2). Thus, new therapies should be tested for their effects on both sub-populations of metastatic cells, those that are actively proliferating and those that are dormant, in order to better understand and use new treatments.

Here we assessed the effect of the synthetic triterpenoid CDDO-Im on the metastatic cell lines B16F1 (murine melanoma) and HT-29 (human colon carcinoma) in 2D culture and in experimental liver metastasis models in vivo. We found that CDDO-Im inhibited proliferation and induces apoptosis of HT-29 and B16F1 cells in culture, in a concentration dependent manner, similar to findings reported for other cell lines (7, 11, 14, 31-35). We used standard histology to assess the effect on metastatic burden, and found that CDDO-Im inhibited growth of metastasis from both cell lines. We also used a novel MRI technique to simultaneously quantify the effect of CDDO-Im on both actively proliferating B16F1 metastases as well as solitary, dormant cells in whole livers. This approach confirmed the results from standard histology, showing that CDDO-Im treatment significantly decreased metastatic tumor burden, size and volume, and further showed that treatment had no effect on the numbers of dormant cells present in the livers. These results suggest that CDDO-Im may have a role to play in the treatment of actively proliferating liver metastases from multiple tumor types.

3.2 MATERIALS AND METHODS

3.2.1 *Cell culture and MPIO labeling*

Cell culture and MPIO labeling were performed as described previously (19, 24, 36). Briefly, B16F1 murine melanoma and HT-29 human colon carcinoma cells (both from the American Type Culture Collection, Manassas, VA) were maintained in alpha-minimal essential media (α-MEM) (Invitrogen, Burlington, Canada) containing 10% fetal bovine serum (FBS) (Sigma, Mississauga, Canada) at 37°C and 5% CO_2. B16F1 cells were labeled with micrometer-sized iron oxide nanoparticles (MPIO) in a T75 tissue culture flask using media with FBS when 70-90% confluent. MPIO beads (312.5 µl, 0.9 µm diameter, 63% magnetite, labeled with Dragon Green, catalog #MC05F; Bangs Laboratories Inc, Fishers, IN, USA) were then added to 10 ml of media with FBS/flask and incubated for 24 hrs, as described (26 and Chapter 2). Cells were washed thoroughly with serum free α-MEM then centrifuged and re-suspended in serum free α-MEM at the appropriate concentration for injection.

3.2.2 *CDDO-IM Treatment and imaging of 2D culture*

Details regarding the synthesis of a number of synthetic triterpenoids, including CDDO-Im (1-[2-cyano-3-,12-dioxooleana-1,9(11)-dien-28-oyl]imidazole), has been published previously (13, 37, 38). CDDO-Im used in these experiments was provided by Dr. Michael Sporn (Dartmouth College, Hanover, NH). Stock vials of CDDO-Im were kept frozen in DMSO and diluted to the appropriate concentration in cell culture media as required. To determine the effect of CDDO-Im on HT-29 and B16F1 cells in 2D cell culture, cells were seeded in a 6 or 24 well tissue culture plates. 48 hours following seeding of cells, CDDO-Im in DMSO (or DMSO alone) was diluted with alpha-MEM plus 10% FBS to the appropriate concentration and added to each well. Images were then acquired from each well, using a Zeiss Axiovert 200 inverted microscope with

incubation system, every 24-48 hours following treatment until day 9. Three images per well (3-4 wells per concentration) were analyzed in order to determine the number of cells per field of view (10x, Ph1).

3.2.3 *Experimental Metastasis assay and CDDO-Im treatment in vivo*

Female 6-10 weeks old C57BL/6 (for the B16F1 cells) (Harlan, Indianapolis, IN) or NIH III mice (for the HT-29 cells) (Charles River, Wilmington, MA) were cared for in accordance with the Canadian Council on Animal Care, under a protocol approved by the University of Western Ontario Council on Animal Care. For experimental liver metastasis assays, mice were anesthetised with an i.p. injection of xylazine/ketamine (2.6 mg ketamine and 0.13 mg xylazine per 20 g body mass). Anesthetised mice received mesenteric injections of 100 μL of B16F1 (3×10^5 cells) or 200 μL of HT-29 (2×10^6 cells) cells suspended in alpha-MEM to target cells directly to liver as described previously (19). Mice were then treated with CDDO-Im (800 mg/kg diet) mixed in a powdered diet (NIH-31 modified mouse diet, Harlan). NIH III mice were treated with CDDO-Im 5 days a week while C57BL/6 mice were treated continuously for the duration of the experiment. Diet with CDDO-Im or vehicle control (ethanol and neobee oil) was replaced every 48 hours for NIH III mice and every 72 hours for C57Bl/6 mice. At endpoint (56 days for HT-29 and 7-11 days for B16F1) mice were sacrificed, livers were removed and fixed in formalin for at least 48 hours prior to sectioning for histology or imaging by MRI.

3.2.4 *Tumor burden, volume and solitary cell quantification and statistics*

Metastatic tumor burden was determined by quantifying the area of tumor and normal tissue from at least 5 random histological hematoxylin and eosin (H&E) stained sections of the liver as described previously (30). Liver tumor volume (apparent as signal hyperintensity; i.e. white regions) and MPIO labeled cells/signal void area (signal hypointensity; i.e. dark regions) were also quantified

in some experiments using a novel MRI technique we recently developed (See Chapter 2). Briefly, at endpoint livers were removed and fixed in 10% neutral buffered formalin for at least 48 hours. Intact livers were then scanned using a clinical 3T GE EXCITE whole body MR system with customized animal gradient insert coil and radiofrequency (RF) coil. Tumor volume and signal void area were quantified using a semi-automated procedure in which a fixed pixel intensity was manually defined and subsequent volume and area measurements were automated using VgStudio (Dresden, Germany) or Image J (NIH, Bethesda, MD) software respectively.

All statistics were performed with GraphPad Prism software (La Jolla, CA). T-tests were performed to determine if significant differences existed in observed means of tumor burden, tumor volume and solitary cell signal void area. All statistics are reported as mean value +/- standard error.

3.3 RESULTS

3.3.1 CDDO-Im inhibited growth, altered morphology and induced apoptosis in B16F1 and HT-29 cells in vitro

To determine the effects of CDDO-Im on B16F1 (Fig. 1A,B) and HT-29 (Fig. 3.1C and D) cells in 2D cell culture, cells were treated with CDDO-Im or vehicle control as described in Materials and Methods. Dose dependent and multifunctional effects of CDDO-Im were observed in the response of both B16F1 and HT-29 cells to treatment (Fig. 3.1A-D), consistent with results described previously in other cancer cell lines (7, 11, 14, 31-35). Longitudinal observation of cells following exposure to CDDO-Im revealed readily apparent changes in morphology as well as growth arrest at concentrations between 100-200 nM. As seen in Fig. 1A and C, cell morphology and growth arrest were evident by 48 hours following CDDO-Im treatment. At higher concentrations (greater than 300-400 nM), CDDO-Im induced apoptosis (cell shrinkage, rounding, detachment and

apoptotic bodies observed) in both B16F1 and HT-29 cells (Fig. 3.1A and C). Cell death was verified by trypan blue staining (data not shown).
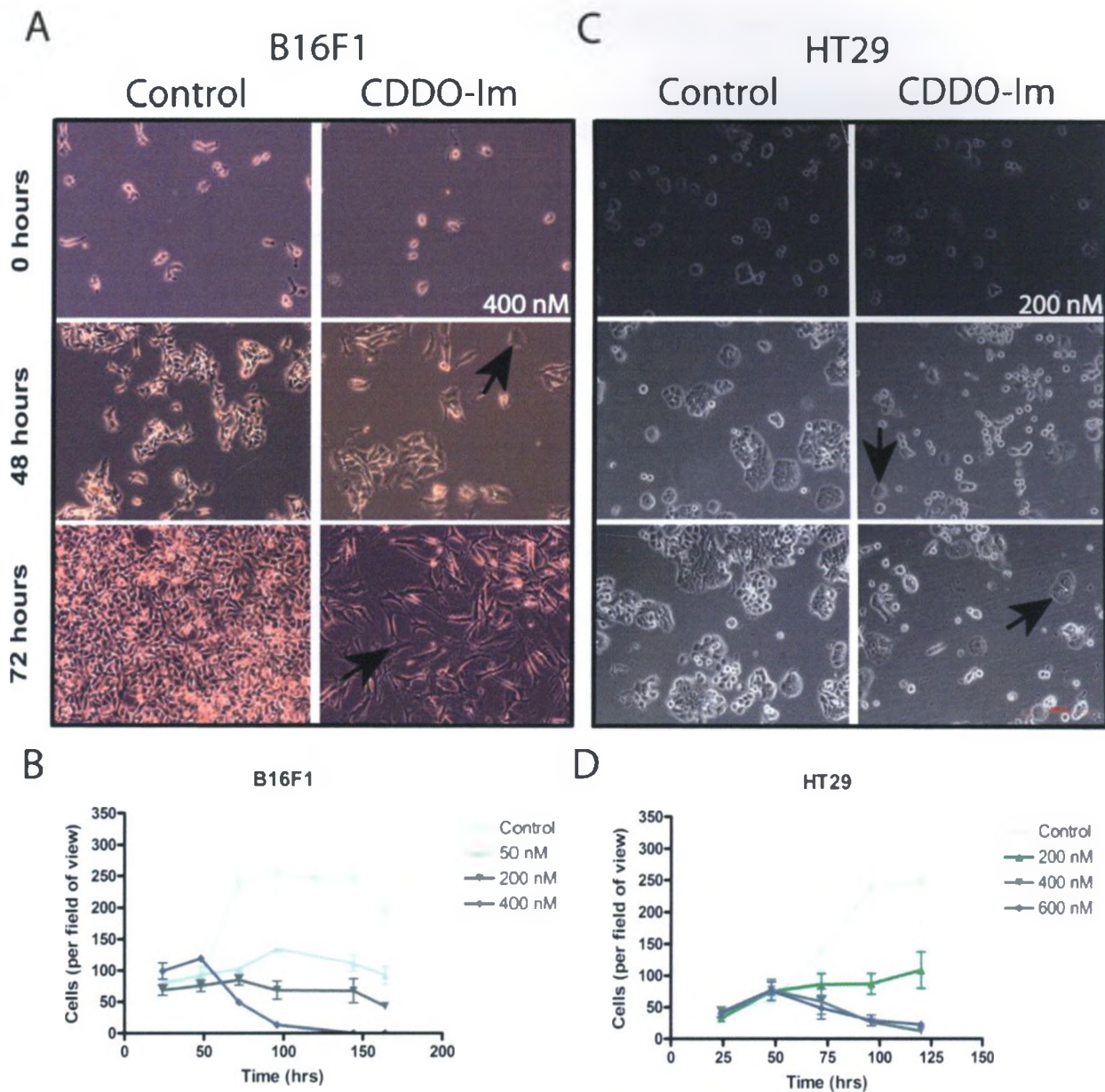
Figure 3.1 – CDDO-Im inhibited growth and induces apoptosis in B16F1 and HT-29 cells in vitro. Nanomolar concentrations of CDDO-Im arrested growth or induced apoptosis in both B16F1 (A) and HT-29 cells (C). 200 nM CDDO-Im was sufficient to inhibit proliferation and alter cell morphology (arrows) while at 300-400 nM apoptosis was induced (A- D).

3.3.2 CDDO-Im inhibited in vivo growth of HT-29 liver metastases

To determine the effect of CDDO-Im treatment on liver metastases from HT-29 human colon carcinoma cells, we used an experimental liver metastasis model. NIH III mice were first injected with 2×10^6 HT-29 cells via the mesenteric vein to target liver and then treated with CDDO-Im (800 mg/kg diet) or vehicle control commencing immediately following cell injections. Treatment was continued for 56 days as described in Materials and Methods. At endpoint livers were removed, weighed and fixed for histological analysis. CDDO-Im treatment resulted in a decrease in the size of metastases (white areas on liver surface) that were apparent in surface images of whole intact livers (Fig. 3.2A and B - arrows). Subsequent quantification of tumor burden from random histological samples (Fig. 3.2 A and B − right panels) showed that CDDO-Im treatment significantly decreased metastatic burden more than 70% (t-test, $p < 0.05$, Control n = 10, 31.9 ± 9.4%, Treated n = 8, 8.5 ± 3.5%) HT-29 tumor burden (Fig. 3.2C).
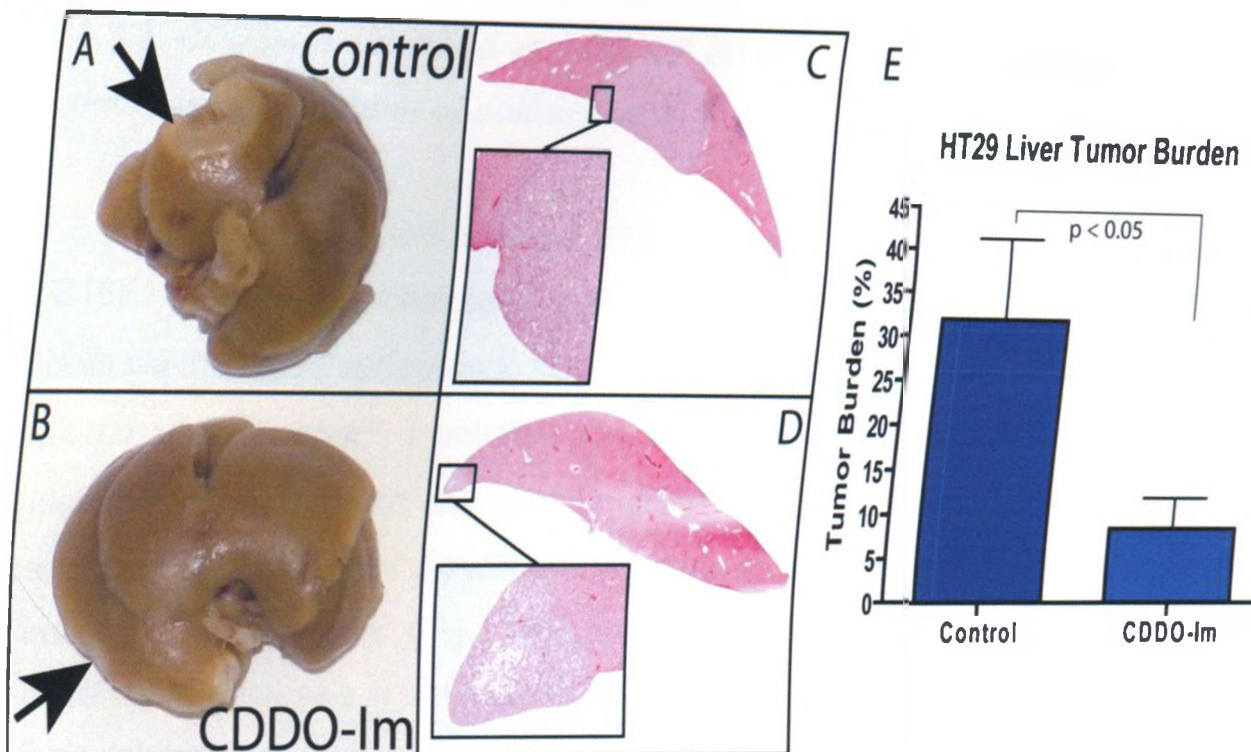
Figure 3.2 – CDDO-Im inhibited HT-29 liver metastasis growth in vivo. 2×10^6 HT-29 cells were delivered to the liver via mesenteric vein injection. CDDO-Im treatment, or vehicle control, via diet (800 mg/kg diet) immediately following cell injection and continued 5 days a week until endpoint. Metastatic burden was determined histologically. Livers were removed at day 56, fixed, sectioned and stained by H&E. At least 5 liver sections per mouse were used to determine liver metastasis burden. CDDO-Im treatment significantly decreased (t-test, $p < 0.05$, Control n = 10, 31.9 ± 9.4%, Treated n = 8, 8.5 ± 3.5%).

3.3.3 *CDDO-Im inhibited growth of B16F1 liver metastases but did not decrease the number of solitary cells*

To determine the effect of CDDO-Im treatment on liver metastases from B16F1 mouse melanoma cells, C57BL/6 mice were injected with 3×10^5 B16F1 cells via the mesenteric vein to target liver and treated with CDDO-Im (800 mg/kg diet) or vehicle control. Treatment commenced immediately following surgery and lasted for the duration of the experiment. At endpoint livers were removed, fixed and scanned using a 3T clinical MR scanner as described above. As apparent in images of whole livers (Fig. 3.3A and B), CDDO-Im treatment resulted in an observable decrease in the size of metastases apparent on the surface of the liver. Inhibition of metastasis growth was quantified by analysis of MR images in order to determine tumor burden (tumor volume/total volume). Liver tumor burden in CDDO-Im treated mice was found to be decreased by 50% compared to vehicle control treated mice (t-test, $p < 0.05$, control n = 10, 30.5 ± 3.9%, CDDO-Im treated, n = 10, 14.7 ± 3.0%) (Fig. 3.3C).

In order to assess the effect of CDDO-Im treatment on the majority of the metastatic cell population, including both macroscopic metastases as well as solitary cells, we used a recently developed MRI technique capable of quantifying both tumor volume and the number of MPIO labeled solitary (signal void area) in the same liver. 3×10^5 B16F1 cells labeled with MPIO and injected via the mesenteric vein. Livers were recovered at day 11 and MR images were subsequently acquired by a single 6 minute scan of whole livers described above. Images were then analyzed to determine tumor volume (image hyperintensity volume) and signal void area from MPIO labeled cells (image hypointensity) as recently described (See Chapter 2). A reduction in size of B16F1 metastases was once again apparent in examination of the surface of whole livers (Fig. 3.4A). This decrease in metastasis size was also apparent in 2D MR images as the areas of hyperintensity, due to B16F1 metastases, were decreased in images of CDDO-Im treated mice (Fig. 3.4B - arrows). 3D images of whole intact livers, in which metastases are pseudocolored green, were

rendered from 2D images (Fig. 3.4C). MR images of the entire liver were used in order to quantify total metastatic tumor volume and signal void area (i.e. number of MPIO labeled cells). CDDO-Im treatment resulted in a more than 60% reduction in tumor volume quantified from the MR images of the entire liver (t-test, $p < 0.05$, CDDO-Im treated, n =5, 1640 ± 498 mm^3, control = 4577 ± 1001 mm^3) (Fig. 3.5A). Despite the significant reduction in metastatic tumor volume, no significant change in the number of solitary dormant cells (signal void area) was observed (t-test, $p = 0.9$, CDDO-Im treated = 770 ± 105 mm^2, control, n = 6, 747 $\pm$ 122 mm^2) (Fig. 3.5B).
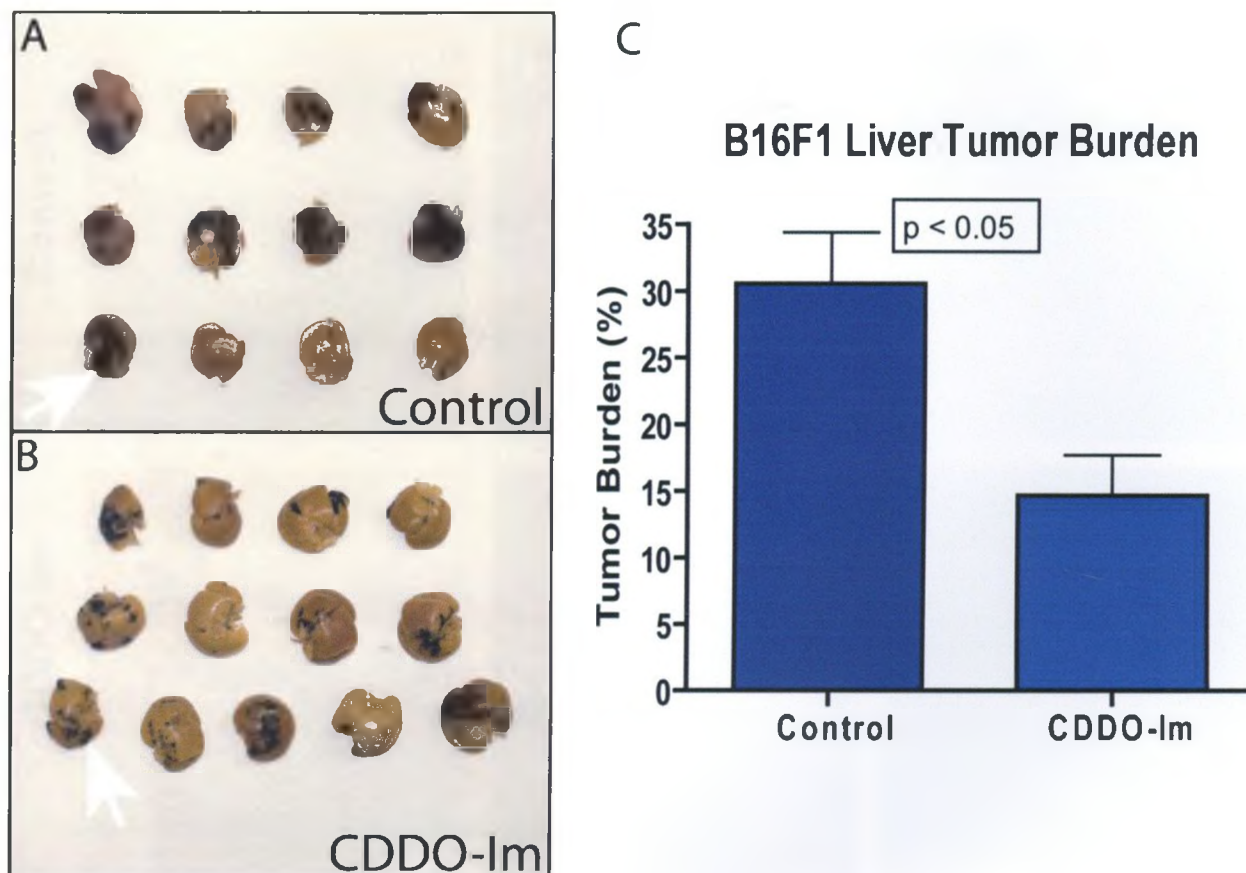
Figure 3.3 – CDDO-Im inhibited B16F1 liver metastasis growth in vivo. B16F1 metastases are apparent on the surface of whole livers as black areas (A and B). Metastases on the surface (white arrows) of whole livers appear to be smaller in CDDO-Im treated (B) than vehicle control (A) groups. Metastasis burden was determined by MRI. Analysis of MR images of whole livers (100 x 100 x 200 μm) revealed that CDDO-Im treatment significantly reduced B16F1 liver metastases burden (B) (p < 0.05, Control n = 10, 30.5 ± 3.9%, Treated, n = 10, 14.7 ± 3.0%).
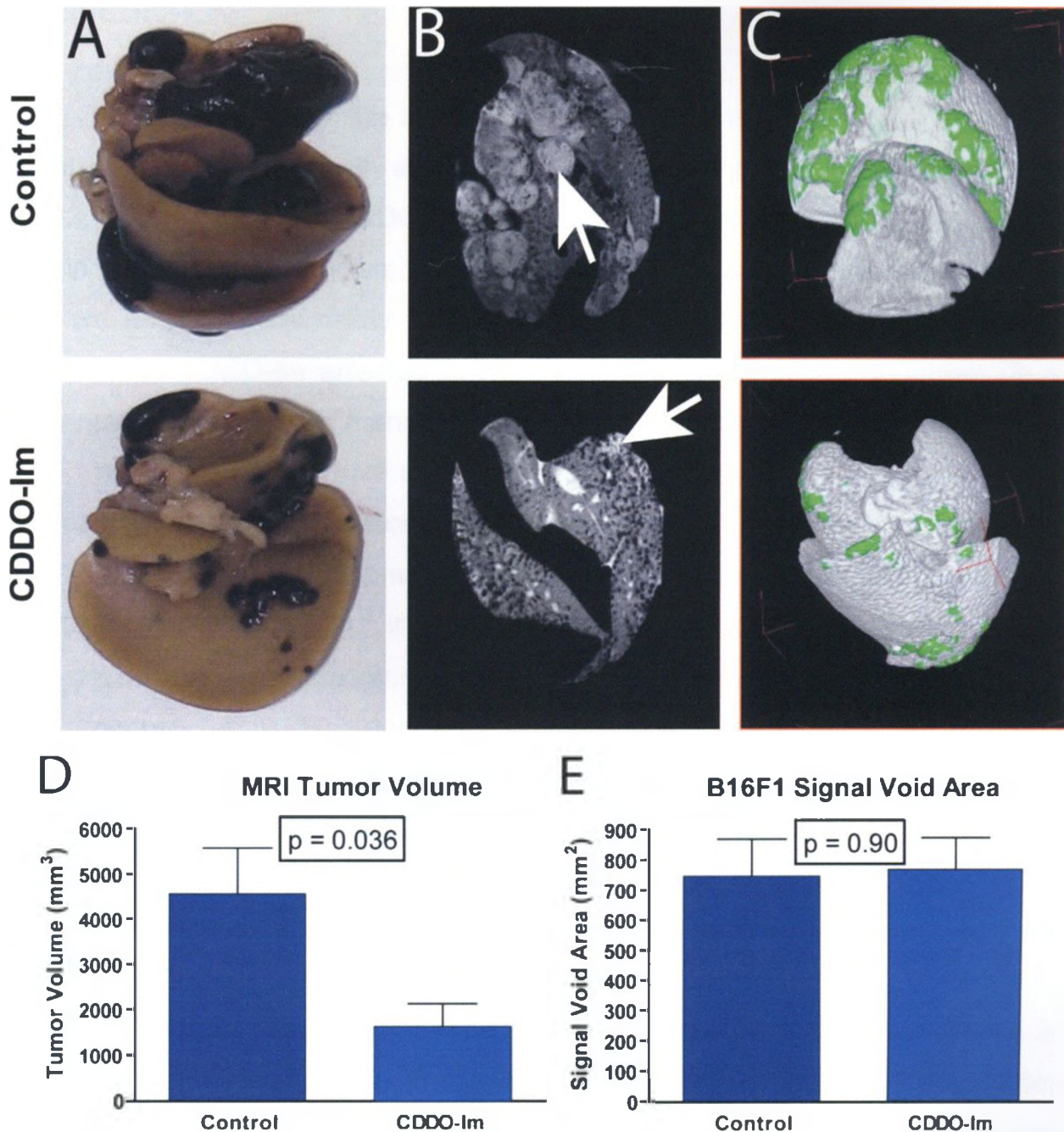
Figure 3.4 –CDDO-Im inhibited B16F1 liver metastasis growth. The reduction in metastasis size is readily apparent from surface image of whole livers (A), in 2D MR images (smaller hyperintense areas - arrows) (B) and in green pseudocolored tumor on the surface of rendered 3D images of whole livers (C). CDDO-Im inhibited B16F1 liver metastasis growth as measured by signal hyperintensity volume at endpoint (D) (t-test, total n = 11, p < 0.05), but did not affect the number of solitary dormant cells (signal void area) (t-test, p = 0.9).

3.4 DISCUSSION

While members of the synthetic triterpenoid family have been shown to inhibit primary tumor growth and subsequent spontaneous lung metastasis (8, 10, 13, 16), the effect of CDDO-Im on metastasis growth following the arrival of cells in the liver was unknown. Because CDDO-Im can accumulate in liver tissue, here we assessed the ability of this compound to inhibit liver metastasis. We showed that CDDO-Im arrested proliferation of and/or induced apoptosis (in a concentration dependent manner) in metastatic cell lines of two tumor types, B16F1 melanoma and HT-29 colon carcinoma. Oral treatment of mice, injected with cancer cells via the mesenteric vein (experimental metastasis assays), with CDDO-Im (800 mg/kg diet) was found to significantly inhibit liver metastasis growth from both cell lines in vivo by 50-70%, as detected both as surface metastases and by histology. We then used a novel MRI procedure, able to simultaneously quantify total whole-liver metastatic burden from growing metastases, as well as the population of non-dividing cancer cells that persist in the liver. This approach confirmed the results from histology that CDDO-Im significantly reduced metastatic burden by greater than 50%, and further showed that the population of solitary B16F1 cells present in the same livers was not reduced.

Liver is the second most common organ in which metastatic disease is found to occur and is significant cause of cancer related deaths (1). Even after initial treatment that leaves no clinically apparent metastases, recurrence and limited 5 year survival remain significant problems (4-6). As such, new treatment strategies are needed in order to more successfully treat metastatic liver disease. The ability to be dosed orally, to induce apoptosis or arrest growth in a variety of cancer cell lines, and the relatively high concentration that can accumulate in liver make CDDO-Im a logical candidate for study as a treatment of liver metastasis. Additionally, as CDDO-Im is capable of both inhibiting proliferation and inducing apoptosis in cancer cells (depending on concentration) it has a useful therapeutic property in that even at doses that are not lethal to cancer

cells, CDDO-Im may inhibit tumor growth by causing growth arrest or differentiation.

The mechanisms by which synthetic triterpenoids exert their diverse effects remain incompletely understood (7). This complexity is amplified by the cellular responses that differ based on concentration (not simply increasing the same effect) and on cell type. Synthetic triterpenoids may have an inhibitory affect on the growth of tumors via a number of mechanisms that include, inhibition of angiogenesis (39), pro-apoptotic signaling via both intrinsic and extrinsic (increase DR4 and DR5 expression/decrease cFLIP activity) pathways (9, 15) and inhibition of HER2 tyrosine kinase activity (16). In addition to the ability to inhibit tumor growth, synthetic triterpenoids have been shown to have a cytoprotective effect on non-cancer cells in experiments in which orally administered treatment reduced aflatoxin induced liver metastases (40) and vinyl carbamate induced lung tumors (41). Thus, synthetic triterpenoids have multifunctional treatment potential as they reduce carcinogenesis (40), inhibit growth (8, 16) and induce apoptosis in cancer cells (7, 9, 11, 15). Such multi-functional treatment strategies will likely be necessary to target the entire metastatic cells population.

It has been established previously that treatment with the cytotoxic chemotherapy doxorubicin is capable of reducing liver tumor burden and volume, but does not affect the number of dormant metastatic cells or their ability to proliferate and form late developing metastases (30 and Chapter 2). Here we show that CDDO-Im significantly inhibits metastatic tumor burden (HT-29 and B16F1) and volume (B16F1) by 50-80%, but does not decrease the number of solitary cells. However, as evident in the 2D culture treatment of HT-29 and B16F1 cells, at concentrations insufficient to induce apoptosis, cellular proliferation is inhibited. Thus, while the number of solitary dormant metastatic cells was not affected by CDDO-Im treatment, it is possible that continued treatment would maintain some of these cells in a dormant state. Indeed, the synthetic triterpenoid CDDO-Me has been shown to inhibit growth and induce apoptosis via Akt and mTOR (10), the later having recently been shown to

promote survival of dormant cells in vivo (42). It is worth noting that while the size of metastases appear smaller in surface images of livers from CDDO-Im treated mice, a significant number of metastases are still visible (Fig. 3.2 and 3.3), suggesting the slowing of growth, not the elimination of metastatic cells. Further studies with models of metastatic dormancy are required to more precisely address any effect of CDDO-Im treatment on individual solitary cells.

Here we have shown that the synthetic triterpenoid CDDO-Im significantly inhibits growth of metastases, with no effect on the number of solitary cells, in experimental metastasis models in which cells are injected directly to target them to the liver. It may be that in order to further reduce the number of macroscopic metastases and/or solitary dormant metastatic cells, other synthetic triterpenoids or combination treatment may be required. Indeed, prevention and treatment effects of a synthetic triterpenoids have both been found to be synergistic with the rexinoid LG100268 (43, 44). Our work presented here with CDDO-Im suggests that synthetic triterpenoids are able to inhibit liver metastasis growth and that they deserve further evaluation and development as a treatment for metastatic disease.

3.5 REFERENCES

1. Pickren J, Tsukada Y, Lane W. Liver Metastasis (ed. eds. Weiss, L. & Gilbert, L.) (G.K. Hall Medical Publishers, 1982).

2. Lee SM, Betticher DC, Thatcher N. Melanoma: chemotherapy. Br. Med. Bull. 1995;51:609-30.

3. Fong Y, Kemeny N, Paty P, Blumgart LH, Cohen AM. Treatment of colorectal cancer: hepatic metastasis. Semin Surg Oncol 1996;12:219-52.

4. Lochan R, White SA, Manas DM. Liver resection for colorectal liver metastasis. Surg Oncol 2007;16:33-45.

5. Rivoire M, Kodjikian L, Baldo S, Kaemmerlen P, Négrier S, Grange J. Treatment of liver metastases from uveal melanoma. Ann. Surg. Oncol. 2005;12:422-8.

6. Sharma S, Camci C, Jabbour N. Management of hepatic metastasis from colorectal cancers: an update. J Hepatobiliary Pancreat Surg 2008;15:570-80.

7. Liby KT, Yore MM, Sporn MB. Triterpenoids and rexinoids as multifunctional agents for the prevention and treatment of cancer. Nat. Rev. Cancer 2007;7:357-69.

8. Ling X, Konopleva M, Zeng Z, Ruvolo V, Stephens LC, Schober W et al.. The novel triterpenoid C-28 methyl ester of 2-cyano-3, 12-dioxoolen-1, 9-dien-28-oic acid inhibits metastatic murine breast tumor growth through inactivation of STAT3 signaling. Cancer Res. 2007;67:4210-8.

9. Hyer ML, Shi R, Krajewska M, Meyer C, Lebedeva IV, Fisher PB et al.. Apoptotic activity and mechanism of 2-cyano-3,12-dioxoolean-1,9-dien-28-oic-acid and related synthetic triterpenoids in prostate cancer. Cancer Res. 2008;68:2927-33.

10. Deeb D, Gao X, Jiang H, Dulchavsky SA, Gautam SC. Oleanane triterpenoid CDDO-Me inhibits growth and induces apoptosis in prostate cancer cells by independently targeting pro-survival Akt and mTOR. Prostate 2009;69:851-60.

11. Suh N, Wang Y, Honda T, Gribble GW, Dmitrovsky E, Hickey WF et al.. A novel synthetic oleanane triterpenoid, 2-cyano-3,12-dioxoolean-1,9-dien-28-oic

acid, with potent differentiating, antiproliferative, and anti-inflammatory activity. Cancer Res. 1999;59:336-41.

12. Yates MS, Tauchi M, Katsuoka F, Flanders KC, Liby KT, Honda T et al.. Pharmacodynamic characterization of chemopreventive triterpenoids as exceptionally potent inducers of Nrf2-regulated genes. Mol. Cancer Ther. 2007;6:154-62.

13. Place AE, Suh N, Williams CR, Risingsong R, Honda T, Honda Y et al.. The novel synthetic triterpenoid, CDDO-imidazolide, inhibits inflammatory response and tumor growth in vivo. Clin. Cancer Res. 2003;9:2798-806.

14. Lapillonne H, Konopleva M, Tsao T, Gold D, McQueen T, Sutherland RL et al.. Activation of peroxisome proliferator-activated receptor gamma by a novel synthetic triterpenoid 2-cyano-3,12-dioxooleana-1,9-dien-28-oic acid induces growth arrest and apoptosis in breast cancer cells. Cancer Res. 2003;63:5926-39.

15. Hyer ML, Croxton R, Krajewska M, Krajewski S, Kress CL, Lu M et al.. Synthetic triterpenoids cooperate with tumor necrosis factor-related apoptosis-inducing ligand to induce apoptosis of breast cancer cells. Cancer Res. 2005;65:4799-808.

16. Konopleva M, Zhang W, Shi Y, McQueen T, Tsao T, Abdelrahim M et al.. Synthetic triterpenoid 2-cyano-3,12-dioxooleana-1,9-dien-28-oic acid induces growth arrest in HER2-overexpressing breast cancer cells. Mol. Cancer Ther. 2006;5:317-28.

17. Logan PT, Fernandes BF, Di Cesare S, Marshall JA, Maloney SC, Burnier MNJ. Single-cell tumor dormancy model of uveal melanoma. Clin. Exp. Metastasis 2008;25:509-16.

18. Naumov GN, MacDonald IC, Weinmeister PM, Kerkvliet N, Nadkarni KV, Wilson SM et al.. Persistence of solitary mammary carcinoma cells in a secondary site: a possible contributor to dormancy. Cancer Res. 2002;62:2162-8.

19. Luzzi KJ, Varghese HJ, MacDonald IC, Schmidt EE, Kohn EC, Morris VL et al.. Inhibition of angiogenesis in liver metastases by carboxyamidotriazole (CAI). Angiogenesis 1998;2:373-9.

20. Chambers AF, MacDonald IC, Schmidt EE, Morris VL, Groom AC. Clinical targets for anti-metastasis therapy. Adv. Cancer Res. 2000;79:91-121.

21. Chambers AF, Groom AC, MacDonald IC. Dissemination and growth of cancer cells in metastatic sites. Nat. Rev. Cancer 2002;2:563-72.

22. Aguirre-Ghiso JA. Models, mechanisms and clinical evidence for cancer dormancy. Nat. Rev. Cancer 2007;7:834-46.

23. Suzuki M, Mose ES, Montel V, Tarin D. Dormant cancer cells retrieved from metastasis-free organs regain tumorigenic and metastatic potency. Am. J. Pathol. 2006;169:673-81.

24. Heyn C, Ronald JA, Mackenzie LT, MacDonald IC, Chambers AF, Rutt BK et al.. In vivo magnetic resonance imaging of single cells in mouse brain with optical validation. Magn Reson Med 2006;55:23-9.

25. Shapiro EM, Sharer K, Skrtic S, Koretsky AP. In vivo detection of single cells by MRI. Magn Reson Med 2006;55:242-9.

26. Heyn C, Ronald JA, Ramadan SS, Snir JA, Barry AM, MacKenzie LT et al.. In vivo MRI of cancer cell fate at the single-cell level in a mouse model of breast cancer metastasis to the brain. Magn Reson Med 2006;56:1001-10.

27. Goodison S, Kawai K, Hihara J, Jiang P, Yang M, Urquidi V et al.. Prolonged dormancy and site-specific growth potential of cancer cells spontaneously disseminated from nonmetastatic breast tumors as revealed by labeling with green fluorescent protein. Clin. Cancer Res. 2003;9:3808-14.

28. Cameron MD, Schmidt EE, Kerkvliet N, Nadkarni KV, Morris VL, Groom AC et al.. Temporal progression of metastasis in lung: cell survival, dormancy, and location dependence of metastatic inefficiency. Cancer Res. 2000;60:2541-6.

29. Luzzi KJ, MacDonald IC, Schmidt EE, Kerkvliet N, Morris VL, Chambers AF et al.. Multistep nature of metastatic inefficiency: dormancy of solitary cells after successful extravasation and limited survival of early micrometastases. Am. J. Pathol. 1998;153:865-73.

30. Naumov GN, Townson JL, MacDonald IC, Wilson SM, Bramwell VHC, Groom AC et al.. Ineffectiveness of doxorubicin treatment on solitary dormant

mammary carcinoma cells or late-developing metastases. Breast Cancer Res. Treat. 2003;82:199-206.

31. Chintharlapalli S, Papineni S, Konopleva M, Andreef M, Samudio I, Safe S. 2-Cyano-3,12-dioxoolean-1,9-dien-28-oic acid and related compounds inhibit growth of colon cancer cells through peroxisome proliferator-activated receptor gamma-dependent and -independent pathways. Mol. Pharmacol. 2005;68:119-28.

32. Ikeda T, Sporn M, Honda T, Gribble GW, Kufe D. The novel triterpenoid CDDO and its derivatives induce apoptosis by disruption of intracellular redox balance. Cancer Res. 2003;63:5551-8.

33. Kim KB, Lotan R, Yue P, Sporn MB, Suh N, Gribble GW et al.. Identification of a novel synthetic triterpenoid, methyl-2-cyano-3,12-dioxooleana-1,9-dien-28-oate, that potently induces caspase-mediated apoptosis in human lung cancer cells. Mol. Cancer Ther. 2002;1:177-84.

34. Stadheim TA, Suh N, Ganju N, Sporn MB, Eastman A. The novel triterpenoid 2-cyano-3,12-dioxooleana-1,9-dien-28-oic acid (CDDO) potently enhances apoptosis induced by tumor necrosis factor in human leukemia cells. J. Biol. Chem. 2002;277:16448-55.

35. Konopleva M, Tsao T, Ruvolo P, Stiouf I, Estrov Z, Leysath CE et al.. Novel triterpenoid CDDO-Me is a potent inducer of apoptosis and differentiation in acute myelogenous leukemia. Blood 2002;99:326-35.

36. Graham KC, Wirtzfeld LA, MacKenzie LT, Postenka CO, Groom AC, MacDonald IC et al.. Three-dimensional high-frequency ultrasound imaging for longitudinal evaluation of liver metastases in preclinical models. Cancer Res. 2005;65:5231-7.

37. Honda T, Rounds BV, Bore L, Finlay HJ, Favaloro FGJ, Suh N et al.. Synthetic oleanane and ursane triterpenoids with modified rings A and C: a series of highly active inhibitors of nitric oxide production in mouse macrophages. J. Med. Chem. 2000;43:4233-46.

38. Honda T, Rounds BV, Gribble GW, Suh N, Wang Y, Sporn MB. Design and synthesis of 2-cyano-3,12-dioxoolean-1,9-dien-28-oic acid, a novel and highly

active inhibitor of nitric oxide production in mouse macrophages. Bioorg. Med. Chem. Lett. 1998;8:2711-4.

39. Vannini N, Lorusso G, Cammarota R, Barberis M, Noonan DM, Sporn MB et al.. The synthetic oleanane triterpenoid, CDDO-methyl ester, is a potent antiangiogenic agent. Mol. Cancer Ther. 2007;6:3139-46.

40. Yates MS, Kwak M, Egner PA, Groopman JD, Bodreddigari S, Sutter TR et al.. Potent protection against aflatoxin-induced tumorigenesis through induction of Nrf2-regulated pathways by the triterpenoid 1-[2-cyano-3-,12-dioxooleana-1,9(11)-dien-28-oyl]imidazole. Cancer Res. 2006;66:2488-94.

41. Liby K, Royce DB, Williams CR, Risingsong R, Yore MM, Honda T et al.. The synthetic triterpenoids CDDO-methyl ester and CDDO-ethyl amide prevent lung cancer induced by vinyl carbamate in A/J mice. Cancer Res. 2007;67:2414-9.

42. Schewe DM, Aguirre-Ghiso JA. ATF6alpha-Rheb-mTOR signaling promotes survival of dormant tumor cells in vivo. Proc. Natl. Acad. Sci. U.S.A. 2008;105:10519-24.

43. Liby K, Risingsong R, Royce DB, Williams CR, Yore MM, Honda T et al.. Prevention and treatment of experimental estrogen receptor-negative mammary carcinogenesis by the synthetic triterpenoid CDDO-methyl Ester and the rexinoid LG100268. Clin. Cancer Res. 2008;14:4556-63.

44. Liby K, Black CC, Royce DB, Williams CR, Risingsong R, Yore MM et al.. The rexinoid LG100268 and the synthetic triterpenoid CDDO-methyl amide are more potent than erlotinib for prevention of mouse lung carcinogenesis. Mol. Cancer Ther. 2008;7:1251-7.

4. MONITORING METASTATIC CELL GROWTH AND CELL CYCLE PROGRESSION IN 2D AND 3D CELL CULTURE

4.1 INTRODUCTION

Multiple metastatic models have demonstrated that metastatic cell fate in a secondary site is heterogeneous, with cells undergoing apoptosis, remaining as solitary cells or progressing to form micrometastases or large vascularized metastases (1-9). In some metastatic models, solitary metastatic cells are observed alone for extended periods of time (1-39, 10). The solitary dormant metastatic cell population, in addition to dormant micrometastases, are believed to be at least partially responsible for cancer recurrence months to years following initial treatment (10-14). In addition, solitary dormant metastatic cells in mice have been shown to maintain their ability to proliferate in 2D culture or form subsequent metastases in vivo following treatment that effectively inhibits growth of large metastases (1-3). While the mechanisms responsible for maintaining solitary cell dormancy are beginning to be understood, monitoring cellular events such as cell cycle progression and the response to treatment in this dormant cell population remains a significant challenge (11-13,15).

Though a significant proportion of metastatic cells die shortly after arrival in the secondary site, a variable but often considerable proportion of metastatic cells persist in that tissue as solitary dormant cells for prolonged periods of time (2, 4-6,10, 16-18). These prolonged periods of dormancy observed in metastatic cells in vivo have not been reported in 2D cell culture (2, 4, 10, 19). However, Barkan et al., recently demonstrated that a number of cell lines, including the murine mammary carcinoma cell line D2.0R and the human mammary carcinoma MDA-MB-231, exhibit growth dynamics similar to those observed in vivo when grown in a 3D basement membrane matrix cell culture system (19). This included the observation of extended periods of solitary cell dormancy (19). They, and subsequent studies, found dormancy in 3D cell culture was partially controlled by integrin-β1 binding, downstream kinase activation and eventually changes in

expression of a number of cyclin dependent kinases (CDK) and cyclin dependent kinase inhibitors (CDKI) (19, 20).

While a number of imaging modalities are capable of imaging metastatic cell populations longitudinally, currently only magnetic resonance imaging (MRI) and optical imaging are capable of detecting solitary cells in vivo (2, 6, 8, 10, 16, 21). Further, MRI is not is not currently able to resolve subcellular events, and there are a number of technical challenges which limit the use of optical imaging for longitudinal studies of individual or small groups of cells. Thus, in order to monitor a defined metastatic population at the subcellular level, and within a microenvironment in which metastatic cell dormancy has been observed, we used bright field and fluorescent imaging techniques in a 3D cell culture model. In addition, in order to better monitor progression of the metastatic cell population, and assess the effect of CDDO-Im treatment on these cells, we used a newly developed reporter system of cell cycle progression, fluorescent ubiquination cell cycle indicator (fucci) (22, 23). While cell cycle progression can be assessed by staining cells and nuclei, these techniques are often toxic to the cells, require removal from the microenvironment or can be used only once (19, 20). As the fate of, response to treatment, and indeed phase of the cell cycle in which metastatic cells are arrested are not yet precisely known, longitudinal observation of the progression of cell cycle in both individual and groups of cells is required in order to more accurately address these questions.

Here we used a fluorescent cell cycle reporter system to monitor cell cycle progression of cells 2D and 3D cell culture. In 3D culture we show that cell area (from multiple bright field images) is an accurate surrogate measure of the number of cells and that initial cell density in 3D culture alters the subsequent growth dynamics and morphology of these cells. The synthetic triterpenoid CDDO-Im was demonstrated to have growth inhibiting effects on D2.0R and 231LN-fucci cells. Nuclear fluorescence from 231LN-fucci cells showed that the CDDO-Im arrested cell cycle at multiple stages resulting in increased number and intensity of fluorescence, with few non-fluorescent (recently divided) cells present in both 2D and 3D culture.

4.2 MATERIALS AND METHODS

4.2.1 *2D and 3D cell culture*

D2.0R and MDA-MB-231-luc-D3H2LN-fucci (hereafter 231LN-fucci) cells were grown in 2D culture in DMEM plus 10% FBS as described previously (2, 8, 10). CDDO-Im treatment and imaging is detailed in Chapter 3 Materials and Methods. For 3D cell culture experiments cells were grown in Matrigel (BD Biosciences) in 8 well chamber slides. An initial layer of Matrigel (125 μl) was dispersed in each well and placed in a cell culture incubator for 30 min to solidify. Cells were then counted and re-suspended at the appropriate cell concentration indicated in individual experiments using a 50:50 ratio of Matrigel and serum free media (125 μl of each in 8 well chamber slides). The first two layers were then placed the incubator for 45-60 minutes prior to be topped with 150 μl of DMEM + 10% FBS. Fresh DMEM + 10% FBS was then added every 2-3 days. Phenol red free media and Matrigel were used for 231LN-fucci experiments. For CDDO-Im treatment, all media was removed from above the Matrigel plug and 250 μL of CDDO-Im diluted or DMSO (vehicle control) in DMEM + 10% FBS was added at twice the final indicated concentration (i.e. 250 μL Matrigel/cells + 250 μL media + CDDO-Im).

4.2.2 *MDA-MB-231LN-fucci cells*

A lymphotrophic cell line, MDA-MB-231-luc-D3H2LN (hereafter 231LN), was purchased from Caliper Life Sciences (Hopkinton, MA). To facilitate detection of cell-cycle dynamics in breast cancer cells *in vitro* and *in vivo*, a two-plasmid fluorescent reporter system called fluorescent ubiquitination cell cycle indicator (*fucci*) (a kind gift from Atsushi Miyawaki) were serially transfected into 231LN cells. As described by Sakaue-Sawano and colleagues (23), expression of the mKO2-hCdt1 causes the nuclei of cells in G_1/S phase of the cell cycle to fluoresce red, whereas expression of the mAG-hGem causes nuclei of cells in

S/G$_2$/M phase to fluoresce green. In early S phase, cell nuclei fluoresce yellow. With respect to construction of the 231LN-fucci cell line, the procedure is outlined as follows. Briefly, 2μg mKO$_2$-hCdt1in a pcDNA-3.1-*neo* backbone was nucleofected into cells using the Nucleofector device as specified by manufacturer (Lonza, Burlington ON, Canada). Cells were grown in complete media containing geneticin (500μg/ml) (GIBCO, Grand Island, NY) which was changed every 3 days. High mKO$_2$-hCdt1 expressing clones were isolated by fluorescence activated cell sorting using a BD FACSVantage DiVa cell sorter equipped with a 633nm laser. mKO$_2$-hCdt1 expressing cells were subsequently nucleofected with 2μg mAG-hGem in a pcDNA-3.1-*hygro* backbone. Cells were grown in complete media containing Hygromycin B (700μg/ml) (Invitrogen, Carlsbad, CA) and changed every 3 days. High mKO$_2$-hCdt1 expressing clones were isolated by fluorescence activated cell sorting using a 488nm laser. To ensure that double-nucleofected cell line contained both mKO$_2$-hCdt1 and mAG-hGem constructs, cultured cells were enriched for G1/S phase nuclei with 100 μM mimosine and sorted for yellow fluorescence.

4.2.3 *Imaging, analysis and statistics*

Images were acquired using a Zeiss Axiovert 200 inverted microscope with incubator (CO2, humidity and temperature control). Bright field images were acquired at the time points indicated in each figure (every 24-48 hours) using multiple objective lenses and either DIC (3D) or Ph1 (2D) as shown on individual images. Two z-stacks consisting of 20-40 images (50-200 μm spacing) each were acquired per well. Cell area was quantified by a blinded observer using ImageJ software (NIH, Bethesda, MD) software. Each image (70-160 per well) was quantified by first thresholding the image and then segmenting cells or cell clusters using the magic wand tool.

4.3 RESULTS

4.3.1 *Cell pixel area correlates with the number of cells in 3D culture*

Quantification of cells in 3D, including dormant cells, has most recently been assessed by colorimetric assays or flow cytometry (19, 20). Here we attempted to determine if pixel area as quantified from multiple z-stack images of the cells in this 3D cell culture system correlated with the number of cells in the well. Increasing numbers of cells were suspended in Matrigel and multiple z-stacks (70-80 total images) were acquired per well. As described in Materials and Methods, images were quantified using Image J software to determine the total cell pixel area. 24 hours after suspending cells in Matrigel, cells were present as individual isolated cells regardless of the number of cells initially seeded (from 650 – 5000) (Fig. 4.1 B-E). The number of cells per well was found to strongly correlate with cell pixel area 24 hours following suspension of cells in the 3D growth matrix (r^2 = 0.99, p < 0.001).
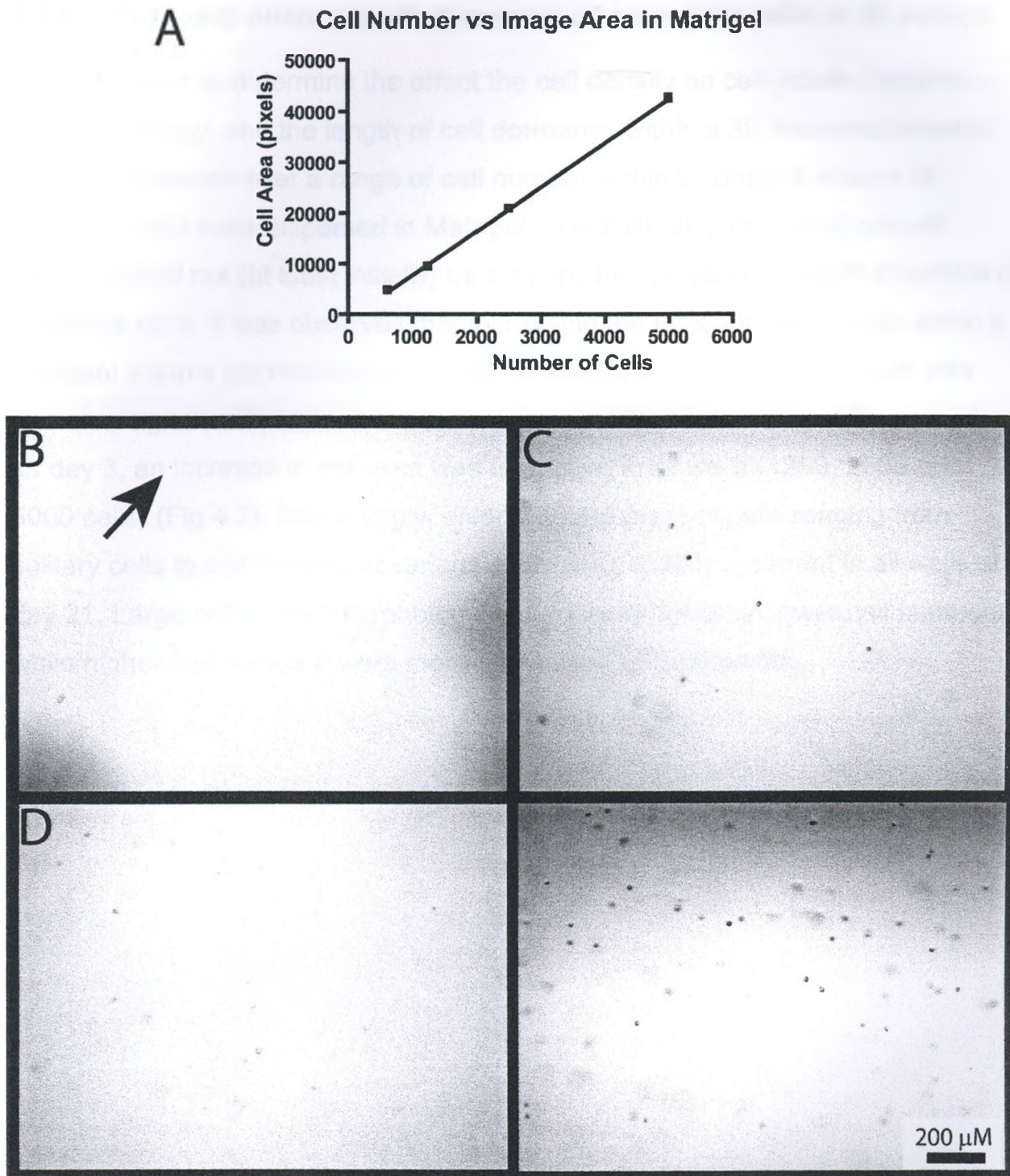
Figure 4.1 – The number of D2.0R cells initially suspended in Matrigel is highly correlated with the cell pixel area quantified from Matrigel wells at 24 hours. 140-160 images (4 z-stacks per cell density) from duplicate wells containing D2.0R cells (darker spots – arrow in B) were quantified in order to determine the relationship between cell number and pixel area. It was found that cell number and total cell pixel area were highly correlated (A) (r^2 = 0.99, p < 0.001).

4.3.2 *Cell density alters growth dynamics of metastatic cells in 3D culture*

In order to determine the effect the cell density on cell growth dynamics, cell morphology, and the length of cell dormancy within a 3D microenvironment, cells were seeded over a range of cell number within a constant volume of Matrigel. Cells were dispersed in Matrigel as individual cells so that cell-cell contact would not (at least initially) be responsible for altering growth dynamics of individual cells. It was observed that increasing the total number of cells within a constant volume (increasing cell density) resulted in an increased growth rate and also significantly altered cell morphology of D2.0R cells (Fig. 4.2). As early as day 3, an increase in cell area was quantified in all wells (1250, 2500 and 5000 cells) (Fig 4.2). Interestingly, diverse populations of cells ranging from solitary cells to cell clusters of various sizes were readily apparent in all wells at day 21. Large cell cluster morphology was more spherical at lower cell numbers while higher cell numbers were more invasive at all time points.
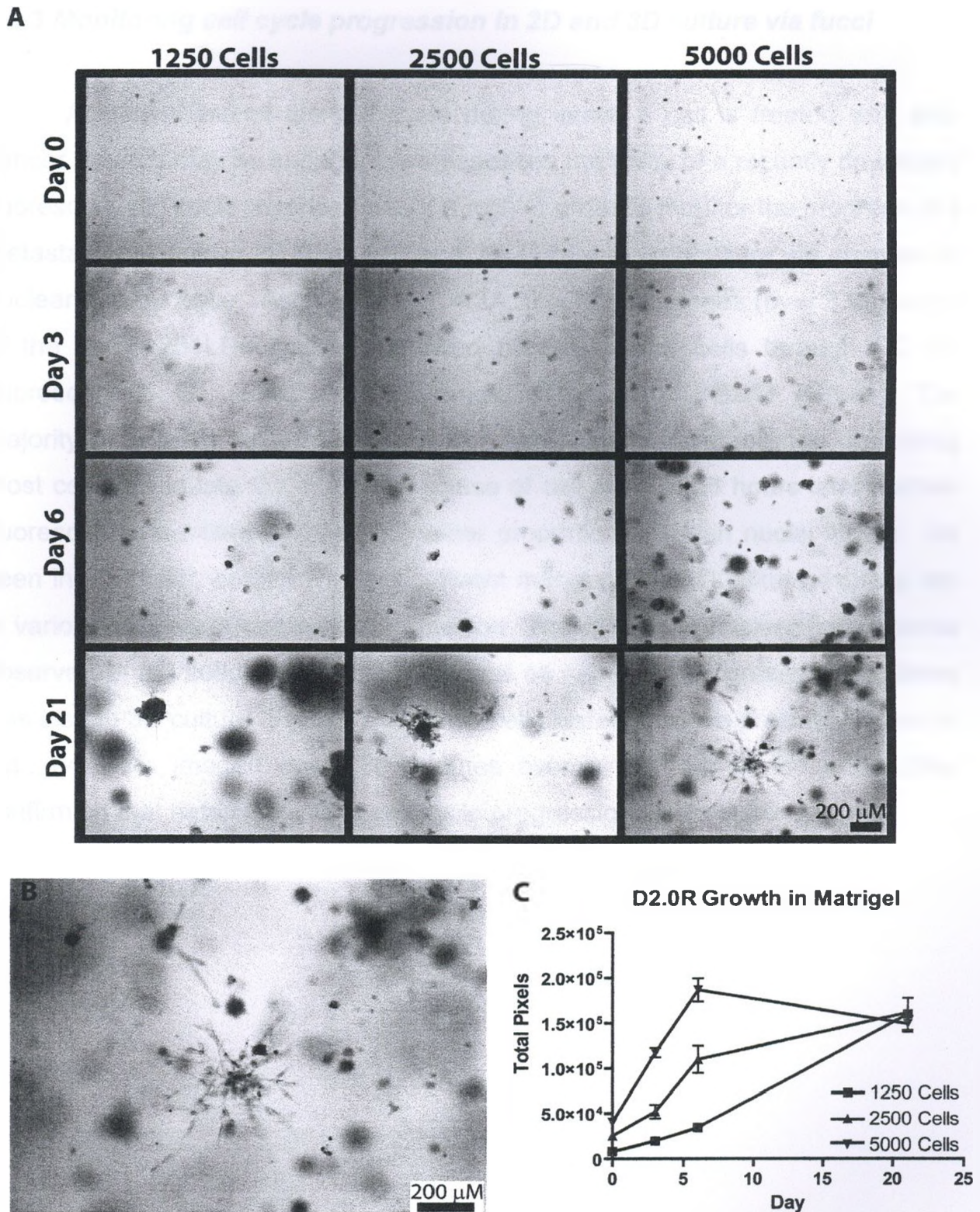
Figure 4.2 –Initial cell density alters cell growth dynamics (C) and morphology (A and B) of D2.0R cells in Matrigel. The rate of growth of cell area increased with the number of cells initially suspended in Matrigel (C). Solitary and clusters of cells were observed were observed in all wells at all time points (A and B).

4.3.3 *Monitoring cell cycle progression in 2D and 3D culture via fucci*

As the phase of the cell cycle during which a cell is treated with anti-cancer therapy may be important, we assessed the utility of a recently developed fluorescent cell cycle reporter system (fucci) in order to monitor the progress of a metastatic cell line in 2D (Fig. 4.3) and 3D (Fig. 4.4) cell culture via changes in nuclear fluorescence. As seen in Fig. 4.3A, time lapse images (over 33.5 hours) of the same 231LN-fucci cells showed progression of cells through G0 (no fluorescence), G1 (Red), G1/S (Orange/Yellow) and S/G2/M (Green). The majority of cells at time 0 (in Fig. 4.3A) are expressing red/orange, indicating most cells are in late G1 or early S phase of cell cycle. 33.5 hours later nuclear fluorescence is mixed with much greater proportion of green nuclei visible. As seen in Fig. 4.3C, cells in a near confluent monolayer in 2D culture express are in various phases of cell cycle progression. The change in nuclear fluorescence observed in 2D culture was also observed as cell cycle progressed over times was also in 3D culture (Fig. 4.4). The two cell clusters in close proximity shown in Fig. 4.4 were imaged every 30 minutes over a 25 hour period and further confirming that heterogeneity of cell cycle progression exists in 3D culture.

Figure 4.3 – Observing 231LN-fucci cell cycle progression via nuclear fluorescence in 2D cell culture. Time lapse images of the same field of view (10x, Ph1) shows the change in nuclear fluorescence of a population of cells over 33.5 hours (Fig. 4.3A). Progression of a single cell (arrow in Fig. 4.3A) throughout the cell cycle until mitosis (Fig. 4.3B). Fluorescent images (10X) were acquired from a near confluent monolayer and shown in Fig. 4.3C. Fluorescent channels are shown split into red fluorescent nuclei due to G1 cells (C1), green fluorescent nuclei due to S/G2/M cells (C2), and composite fluorescent image showing all nuclei including orange/yellow (dual red and green expressing) cells in G1/S (C3).

FIGURE 4.3

200 μM
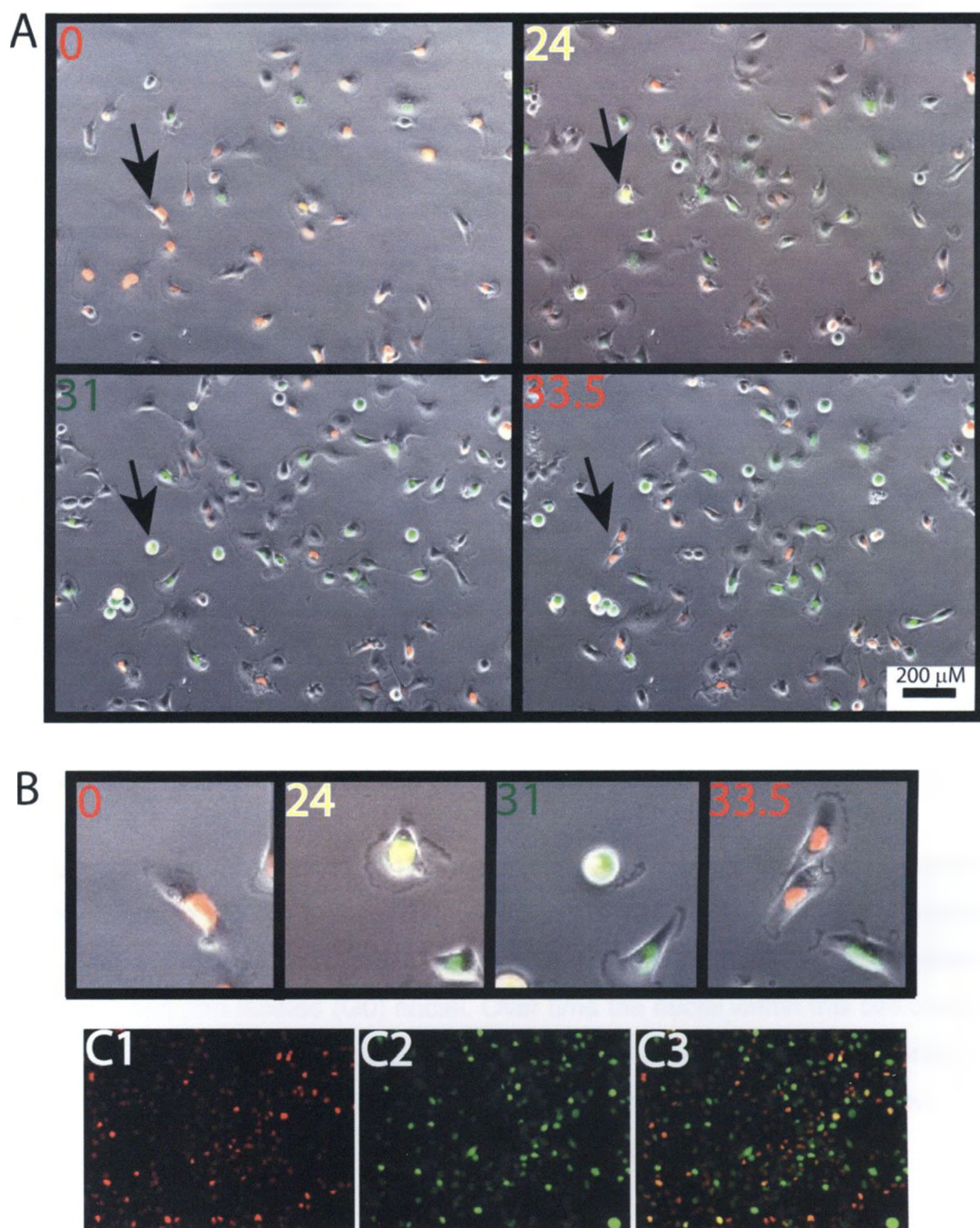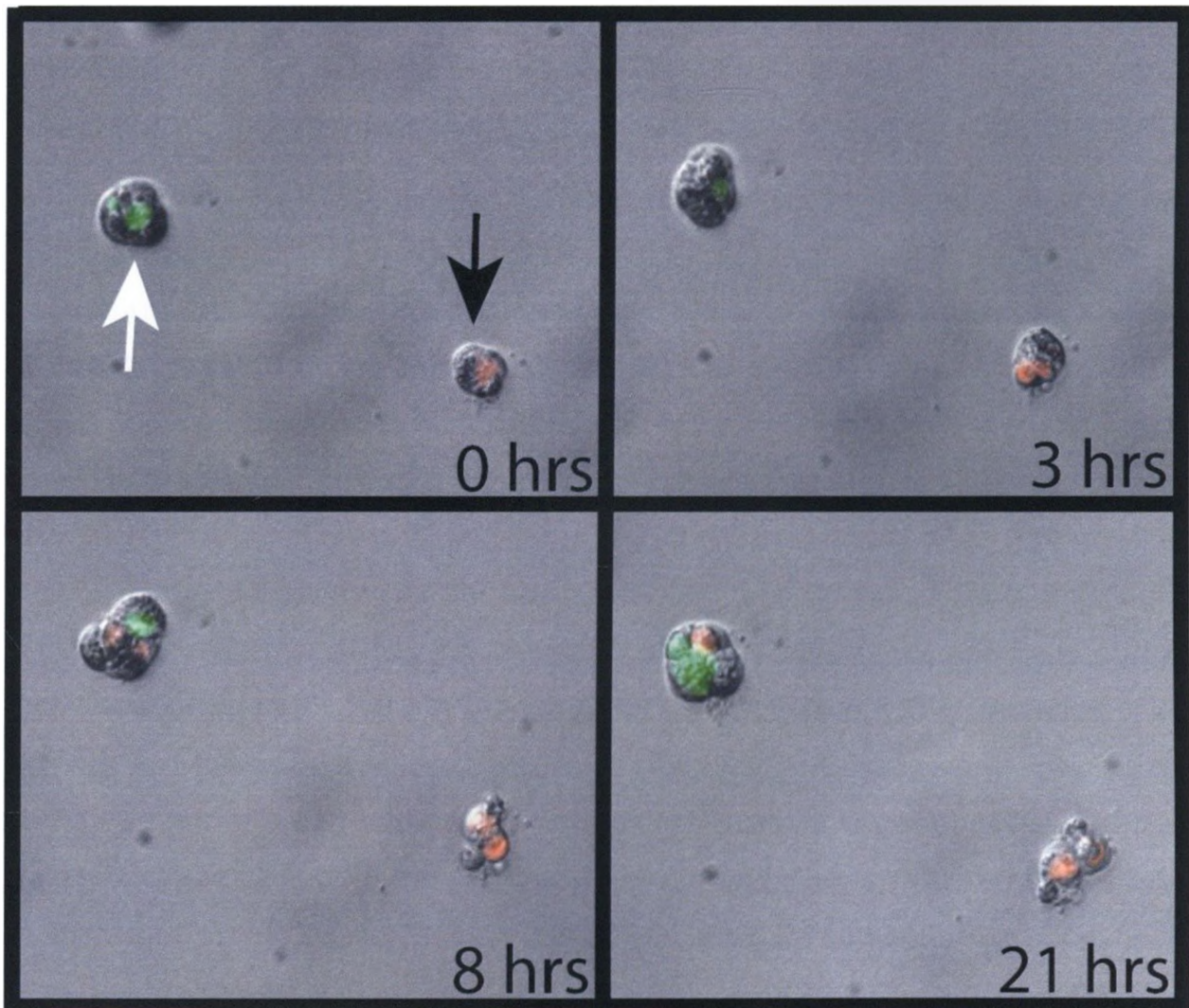
Figure 4.4 – Observing 231LN-fucci cell cycle progression via nuclear fluorescence in 3D cell culture. Two cell clusters can be seen at time 0 (upper left). The cell cluster indicated by the white arrow initially displays only green (S/G2/M) and non-labeled (G0) nuclei. Over time the nuclei within this cell cluster lose fluorescence (mitosis), become red (G1) and then yellow (G1/S). In contrast, nuclei in the second cell cluster are unlabelled and light red throughout the course of observation indicating cell cycle arrest (black arrow).

4.3.4 *CDDO-IM Inhibits growth of D2.0R and 231LN-Fucci cells in 2D culture*

Treatment with synthetic triterpenoids has previously been shown to inhibit proliferation by depleting cells in S phase while arresting cell cycle in G1/S and G2/M (24-26). Here we treated D2.0R and 231LN-fucci cells with the synthetic triterpenoid CDDO-Im in order to determine the effect of this treatment, capable of arresting cell cycle, on cells in 2D and 3D cell culture. As reported previously by us and others, CDDO-Im treatment induces both dose and cell type dependent effect on cells (27, Chapter 3). Here we show that CDDO-Im inhibits growth in both D2.0R and 231LN-fucci at 200 nM and kills cells at 400 nM (Fig. 4.5). Further, CDDO-Im was shown to alter cell morphology of cells at 200 and 400 nM as apparent in Fig 4.5. Analysis of nuclear fluorescence from 231LN-fucci cells treated with 500 nM CDDO-Im for 18 hours revealed an increase in the number and intensity of fluorescent nuclei (Fig. 4.6). The increase in intense red and green nuclei is consistent with previous publications showing cell cycle arrest by flow cytometry at both the G1/S and G2 (24-26). Fewer unlabelled or weakly labeled (corresponding to recently divided or early M phase cells) nuclei were apparent in the CDDO-Im treated cells (Fig. 4.6B2) than control cells (Fig. 4.6A2).
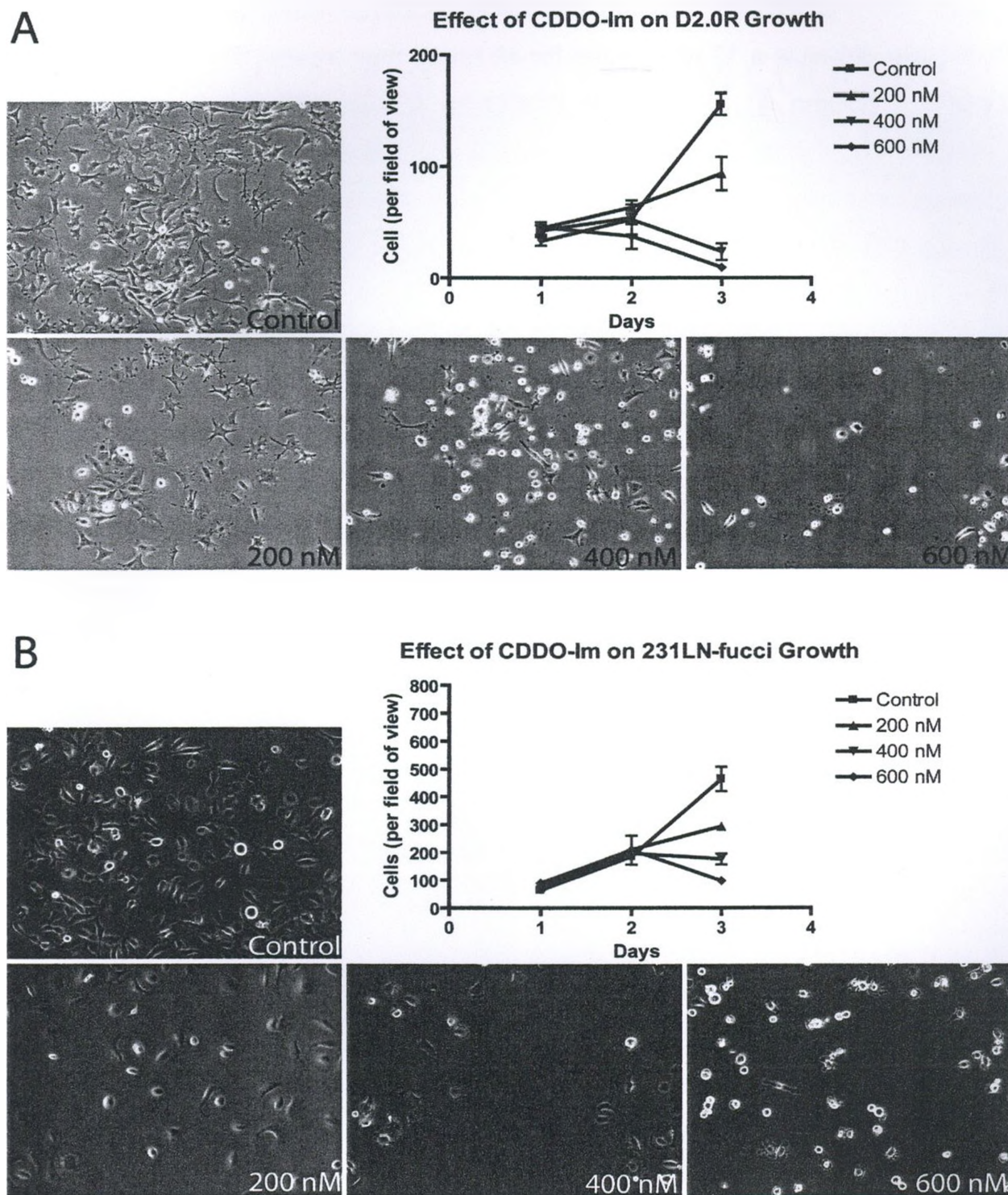
Figure 4.5 – CDDO-Im inhibits proliferation and induces apoptosis in D2.0R (A) and LN-fucci (B) cells in 2D cell culture. As apparent in the inset images, 24 hours following treatment, 200 nM CDDO-Im arrests growth while inducing little apoptosis. At 400 and 600 nM, significant apoptosis is observed (rounded cells – white halo).

Figure 4.6 – CDDO-Im arrested cell cycle in 231LN-fucci cells in 2D culture. Cells were grown in a 12 well plates for 48 hours then treated with vehicle control (DMSO - column A) or 500 nM CDDO-Im (column B). 18 hours following treatment bright field images (A1 and B1) and dual channel (red and green) fluorescent images (A2 and B2) were acquired. Merged images are also shown (A3 and B3). Arrest of cell cycle is indicated by the increase in the number and intensity of fluorescent nuclei. The limited number of non-fluorescent nuclei indicates no recent mitosis, while intensity is indicative of arrest in late G1 (red), G1/S (yellow) or late G2/M (dark green).

FIGURE 4.6

Vehicle Control | 500 nM CDDO-Im
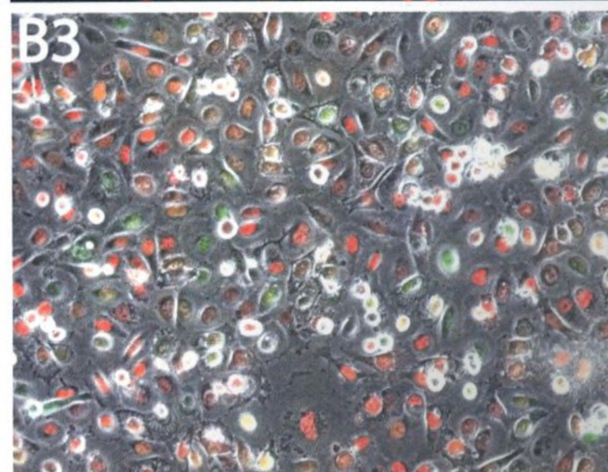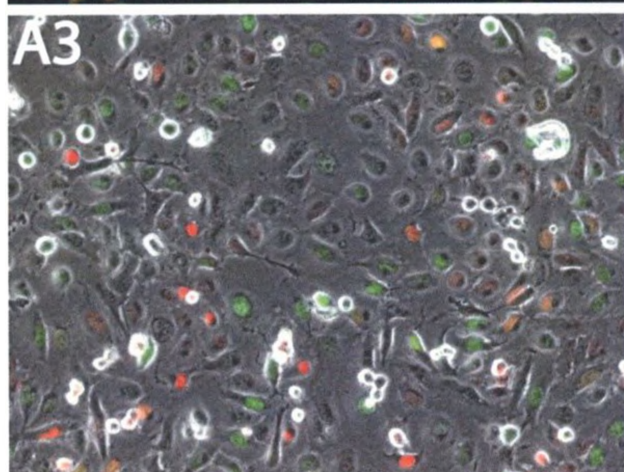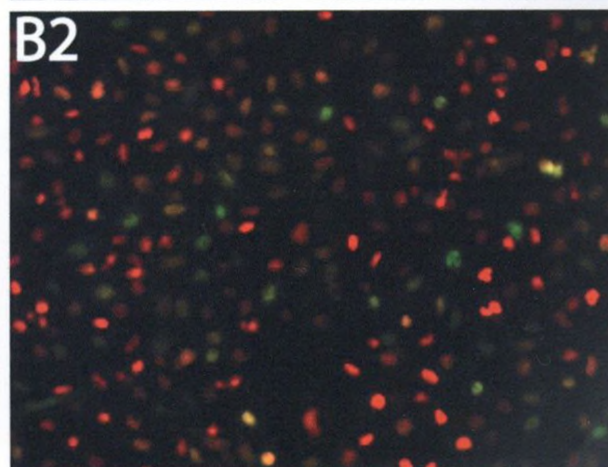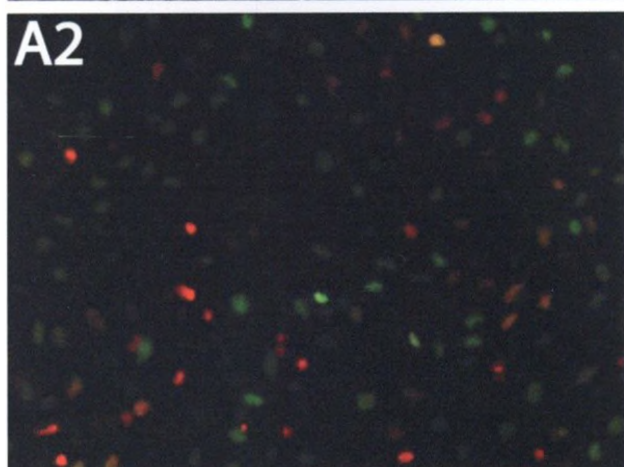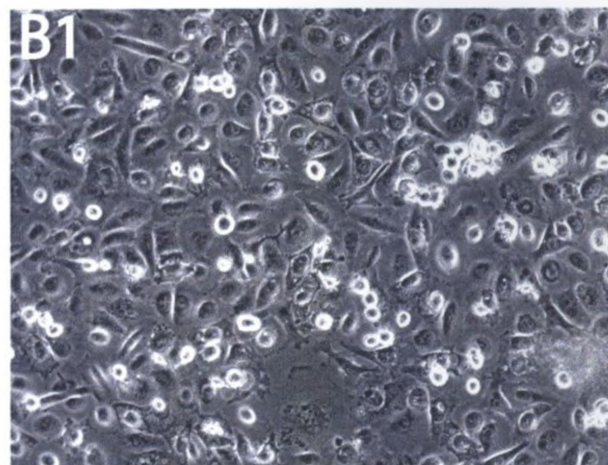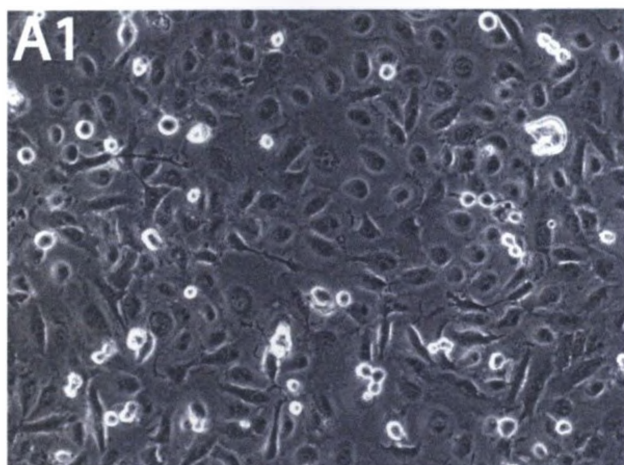
4.3.5 *CDDO-IM Inhibits growth of MDA-MB-231LN-Fucci cells in 3D Culture*

In order to determine the effect of CDDO-Im on 231LN-Fucci cells in 3D culture, cells were treated immediately or 9 days following suspension in Matrigel. Cells were treated with 400 nM CDDO-Im or vehicle control and imaged 48-72 hours post treatment. Longitudinal observation of cell clusters showed that a cell cluster treated with CDDO-Im did not actively progress through the cell cycle as indicated by the lack of change in nuclear fluorescence over the 28 hours (Fig 4.7A). However, cell nuclei were still observed to move within the cell cluster, with one cell migrating (as observed by red nuclear fluorescence) the entire length of the cell cluster, an event that was unnoticeable in bright field images. In contrast, nuclear fluorescence from cell clusters in control wells continued to change in number and intensity, indicating cell cycle progression (Fig. 4.7B).

Figure 4.7 - CDDO-Im arrests cell cycle of MDA-MB-231LN-fucci cells in 3D cell culture. MDA-MB-231LN-fucci cells were treated with 400 nM CDDO-Im (A) or vehicle control (B) 9 days after suspension in Matrigel to allow cells to form cell clusters. 72 hours following treatment bright field images and fluorescent images were acquired. Cell clusters were randomly chosen and followed for 28 hours, with images shown for treated (A) and control (B) cells. As represented in images of Fig 4.7A and B, cell clusters treated with CDDO-Im showed little change in fluorescent intensity or number of nuclei (Fig. 4.7A), whereas the number and intensity of fluorescent nuclei increased substantially in control clusters (Fig 4.7B) during the same time frame.

FIGURE 4.7

A   400 nM CDDO-Im

| Green (G2/M) | Red (G1) | Merged |

0 hrs

28 hrs

200 μM

B   Control

| Green (G2/M) | Red (G1) | Merged |

0 hrs

28 hrs

200 μM
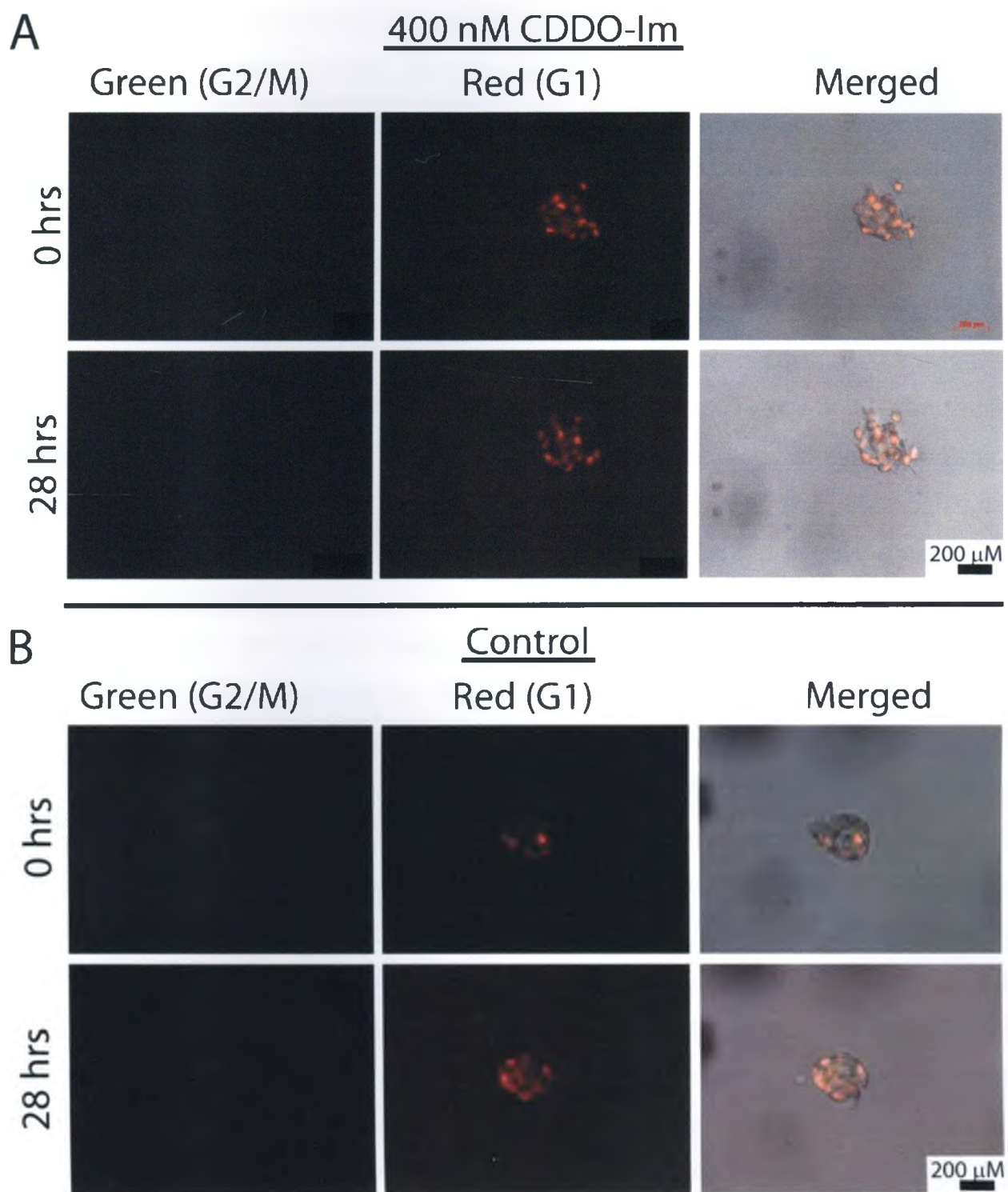
4.4 DISCUSSION

Here we demonstrate that a 3D cell culture system and fluorescent cell cycle reporter system (fucci) can be used to longitudinally image cell cycle progression and response to treatment by the heterogeneous metastatic cell population present within each well. We show that the number of cells in 3D culture strongly correlates with cell pixel area quantified from z-stacks and that increasing initial seeding density alters subsequent proliferation and cell morphology. 231LN-fucci cells were used to monitor cell cycle progression of individual cells or clusters of cells in both 2D and 3D cell culture. Treatment with the synthetic triterpenoid CDDO-Im, known to arrest cell growth at nanomolar concentrations in vitro, was shown to change cell morphology, arrest growth and induce cell death in both D2.0R and 231LN-fucci cell lines. In addition, cell cycle arrest of 231LN-fucci cells in both G1 and G2 was observed following treatment in 2D and 3D culture.

Metastatic dormancy is believed to contribute to the often significant rates of treatment failure for metastatic disease (2, 10, 11, 28, 29). In fact, it has been demonstrated that treatment that successfully decreases the size of large proliferating metastases has no effect on the number or viability of solitary dormant metastatic cells (2, Chapter 2 and 3). However, imaging cell cycle progression and the effect of treatment on the entire population of metastatic cells longitudinally remains a significant technical challenge in vivo. While less complex than the actual human (or mouse) microenvironment in which cancer cells are actually targeted, 3D basement membrane matrix cell culture systems such as the one used here provide a more complex microenvironment than traditional 2D culture. It has been repeatedly demonstrated that cells grown in such 3D microenvironments are able to mimic morphology observed in vivo (30, 31).

Most recently, 3D cell culture models have been used to mimic solitary metastatic cell dormancy observed in vivo in a number of metastatic cell lines including D2.0R and MDA-MB-231 (19, 20). In particular, the D2.0R cell line

which remains dormant for extended periods of time following mesenteric injection to target mouse liver (10, 19), has been shown to grow normally in 2D culture but remain dormant for almost two weeks in 3D culture (19, 20). Interestingly, while D2.0R cells grew slowly in our 3D experiments, not all cells were observed to exhibit the extended period of dormancy reported previously. This may be due to several factors including differences in the sensitivity of the quantification technique, variance in the composition of the growth factors and protein concentration in the Matrigel and number of cells used (31). Indeed, our results suggest that the number of cells originally suspended in the fixed Matrigel volume greatly influences subsequent cell morphology and proliferation, similar to other results published recently (20). As reported by Barkan et al., we did observe migration of individual cells to form small clusters prior to proliferation (19). Increasing density may thus increase the rate of proliferation as the size of cell clusters in vivo has been shown to alter the metastatic efficiency of cells injected in the lung (32). In addition, it has been proposed that a critical number of cells are required for metastatic cells to commence proliferation, analogous to bacterial quorum sensing (33).

Here we used a 3D culture system in which a heterogeneous population of metastatic cells, as is common in in vivo models of metastasis, is observed to exist. We were able to longitudinally imaging cell progression (including cell cycle) and the effect of treatment on these distinct cell populations. As the primary goal of anti-cancer therapies is to eradicate all cancer cells, the presence of this heterogeneous population is advantageous as differential treatment effects on these populations of cells can be observed. Combined with the fluorescent cell cycle system used here, it will be possible to longitudinally monitor the effect of treatment on cells at various stages of cell cycle progression. Metastatic cell dormancy has previously been defined by the absence of markers indicating apoptosis or proliferation, as well as retention of markers that are diluted and no longer visible following cell division (5, 6, 10, 16). In addition, cells can be stained for cell cycle markers to determine the phase of the cell cycle in which they currently exist. However, most cell cycle staining

procedures kill the cell in the process and are only suitable for time point experiments. Thus, the 3D cell culture systems of metastasis growth we describe and utilize here will be useful for future longitudinal studies to elucidate the differential effect of treatment on the entire population of metastatic cells present within a confined microenvironment.

4.5 REFERENCES

1. Goodison S, Kawai K, Hihara J, Jiang P, Yang M, Urquidi V et al.. Prolonged dormancy and site-specific growth potential of cancer cells spontaneously disseminated from nonmetastatic breast tumors as revealed by labeling with green fluorescent protein. Clin. Cancer Res. 2003;9:3808-14.

2. Naumov GN, Townson JL, MacDonald IC, Wilson SM, Bramwell VHC, Groom AC et al.. Ineffectiveness of doxorubicin treatment on solitary dormant mammary carcinoma cells or late-developing metastases. Breast Cancer Res. Treat. 2003;82:199-206.

3. Guba M, Cernaianu G, Koehl G, Geissler EK, Jauch KW, Anthuber M et al.. A primary tumor promotes dormancy of solitary tumor cells before inhibiting angiogenesis. Cancer Res. 2001;61:5575-9.

4. Naumov GN, MacDonald IC, Chambers AF, Groom AC. Solitary cancer cells as a possible source of tumour dormancy?. Semin. Cancer Biol. 2001;11:271-6.

5. Cameron MD, Schmidt EE, Kerkvliet N, Nadkarni KV, Morris VL, Groom AC et al.. Temporal progression of metastasis in lung: cell survival, dormancy, and location dependence of metastatic inefficiency. Cancer Res. 2000;60:2541-6.

6. Luzzi KJ, MacDonald IC, Schmidt EE, Kerkvliet N, Morris VL, Chambers AF et al.. Multistep nature of metastatic inefficiency: dormancy of solitary cells after successful extravasation and limited survival of early micrometastases. Am. J. Pathol. 1998;153:865-73.

7. Morris VL, MacDonald IC, Koop S, Schmidt EE, Chambers AF, Groom AC. Early interactions of cancer cells with the microvasculature in mouse liver and muscle during hematogenous metastasis: videomicroscopic analysis. Clin. Exp. Metastasis 1993;11:377-90.

8. Heyn C, Ronald JA, Mackenzie LT, MacDonald IC, Chambers AF, Rutt BK et al.. In vivo magnetic resonance imaging of single cells in mouse brain with optical validation. Magn Reson Med 2006;55:23-9.

9. Logan PT, Fernandes BF, Di Cesare S, Marshall JA, Maloney SC, Burnier MNJ. Single-cell tumor dormancy model of uveal melanoma. Clin. Exp. Metastasis 2008;25:509-16.

10. Naumov GN, MacDonald IC, Weinmeister PM, Kerkvliet N, Nadkarni KV, Wilson SM et al.. Persistence of solitary mammary carcinoma cells in a secondary site: a possible contributor to dormancy. Cancer Res. 2002;62:2162-8.

11. Aguirre-Ghiso JA. Models, mechanisms and clinical evidence for cancer dormancy. Nat. Rev. Cancer 2007;7:834-46.

12. Brackstone M, Townson JL, Chambers AF. Tumour dormancy in breast cancer: an update. Breast Cancer Res. 2007;9:208.

13. Townson JL, Chambers AF. Dormancy of solitary metastatic cells. Cell Cycle 2006;5:1744-50.

14. Demicheli R, Terenziani M, Valagussa P, Moliterni A, Zambetti M, Bonadonna G. Local recurrences following mastectomy: support for the concept of tumor dormancy. J. Natl. Cancer Inst. 1994;86:45-8.

15. Goss P, Allan AL, Rodenhiser DI, Foster PJ, Chambers AF. New clinical and experimental approaches for studying tumor dormancy: does tumor dormancy offer a therapeutic target?. APMIS 2008;116:552-68.

16. Heyn C, Ronald JA, Ramadan SS, Snir JA, Barry AM, MacKenzie LT et al.. In vivo MRI of cancer cell fate at the single-cell level in a mouse model of breast cancer metastasis to the brain. Magn Reson Med 2006;56:1001-10.

17. Morris VL, Koop S, MacDonald IC, Schmidt EE, Grattan M, Percy D et al.. Mammary carcinoma cell lines of high and low metastatic potential differ not in extravasation but in subsequent migration and growth. Clin. Exp. Metastasis 1994;12:357-67.

18. Morris VL, Tuck AB, Wilson SM, Percy D, Chambers AF. Tumor progression and metastasis in murine D2 hyperplastic alveolar nodule mammary tumor cell lines. Clin. Exp. Metastasis 1993;11:103-12.

19. Barkan D, Kleinman H, Simmons JL, Asmussen H, Kamaraju AK, Hoenorhoff MJ et al.. Inhibition of metastatic outgrowth from single dormant tumor cells by targeting the cytoskeleton. Cancer Res. 2008;68:6241-50.

20. Shibue T, Weinberg RA. Integrin beta1-focal adhesion kinase signaling directs the proliferation of metastatic cancer cells disseminated in the lungs. Proc. Natl. Acad. Sci. U.S.A. 2009;106:10290-5.

21. Shapiro EM, Sharer K, Skrtic S, Koretsky AP. In vivo detection of single cells by MRI. Magn Reson Med 2006;55:242-9.

22. Sakaue-Sawano A, Ohtawa K, Hama H, Kawano M, Ogawa M, Miyawaki A. Tracing the silhouette of individual cells in S/G2/M phases with fluorescence. Chem. Biol. 2008;15:1243-8.

23. Sakaue-Sawano A, Kurokawa H, Morimura T, Hanyu A, Hama H, Osawa H et al.. Visualizing spatiotemporal dynamics of multicellular cell-cycle progression. Cell 2008;132:487-98.

24. Alabran JL, Cheuk A, Liby K, Sporn M, Khan J, Letterio J et al.. Human neuroblastoma cells rapidly enter cell cycle arrest and apoptosis following exposure to C-28 derivatives of the synthetic triterpenoid CDDO. Cancer Biol. Ther. 2008;7:709-17.

25. Han S, Peng L, Chung S, DuBois W, Maeng S, Shaffer AL et al.. CDDO-Imidazolide inhibits growth and survival of c-Myc-induced mouse B cell and plasma cell neoplasms. Mol. Cancer 2006;5:22.

26. Lapillonne H, Konopleva M, Tsao T, Gold D, McQueen T, Sutherland RL et al.. Activation of peroxisome proliferator-activated receptor gamma by a novel synthetic triterpenoid 2-cyano-3,12-dioxooleana-1,9-dien-28-oic acid induces growth arrest and apoptosis in breast cancer cells. Cancer Res. 2003;63:5926-39.

27. Liby KT, Yore MM, Sporn MB. Triterpenoids and rexinoids as multifunctional agents for the prevention and treatment of cancer. Nat. Rev. Cancer 2007;7:357-69.

28. Demicheli R. Tumour dormancy: findings and hypotheses from clinical research on breast cancer. Semin. Cancer Biol. 2001;11:297-306.

29. Retsky MW, Demicheli R, Hrushesky WJM, Baum M, Gukas ID. Dormancy and surgery-driven escape from dormancy help explain some clinical features of breast cancer. APMIS 2008;116:730-41.

30. Lee GY, Kenny PA, Lee EH, Bissell MJ. Three-dimensional culture models of normal and malignant breast epithelial cells. Nat. Methods 2007;4:359-65.

31. Benton G, George J, Kleinman HK, Arnaoutova IP. Advancing science and technology via 3D culture on basement membrane matrix. J. Cell. Physiol. 2009;221:18-25.

32. Liotta LA, Saidel MG, Kleinerman J. The significance of hematogenous tumor cell clumps in the metastatic process. Cancer Res. 1976;36:889-94.

33. Hickson J, Diane Yamada S, Berger J, Alverdy J, O'Keefe J, Bassler B et al.. Societal interactions in ovarian cancer metastasis: a quorum-sensing hypothesis. Clin. Exp. Metastasis 2009;26:67-76.

5. GENERAL DISCUSSION

This chapter contains concepts and parts of a previously published review "Dormancy of solitary metastatic cells", by J. L. Townson and A. F. Chambers in Cell Cycle. 2006 Aug;5:1744-50.

5.1 THESIS SUMMARY

Within a given population of cancer cells, and metastatic cells in particular, it has been established that significant variance exists in expression of cell surface markers, the period of dormancy, treatment resistance mechanisms, the rate of proliferation and growth and indeed the eventual fate of each cell. Perhaps most clinically relevant, a differential response to treatment by cells within a metastatic cell population has also been found to exist (1, Chapters 2 and 3). It is likely that this heterogeneity observed within the metastatic population contributes to the often significant rates of treatment failure and cancer recurrence (2, 3). As such, the primary goal of this thesis was to develop and utilize methods for imaging and quantification of the majority of the metastatic cell population in order to assess the effect of anti-cancer treatments on this heterogeneous cell population. Studies completed in order to attain this goal are described in Chapters 2-4.

By adapting an MR imaging technique initially used to detect the presence of solitary iron labelled cells in the liver and brain (4-6), quantification of solitary MPIO labelled cancer cells and metastases larger than 200 μm in the same whole liver was possible. It was found that the number of MPIO labelled B16F1 cells injected into the liver (via mesenteric vein) was highly correlated with the total signal void area in MR images of the same livers. This technique was then used to assess the effect of doxorubicin treatment on both growing metastases and solitary dormant metastatic cells within the same organ. In agreement with previously published results using different cell lines (1), it was found that doxorubicin successfully inhibited the growth of large B16F1 metastases but had

no effect on the number of solitary dormant cells. As it was hypothesized that doxorubicin would have no effect on the number of solitary cells due to their cell cycle dormancy, the whole liver MRI quantification technique developed in Chapter 2 was again utilized to quantify the effect of a novel cancer treatment hypothesized to be able to induce apoptosis in dormant metastatic cells.

Synthetic triterpenoids, including CDDO-Im, have multifunction effects including inducing growth arrest and apoptosis of cancer cells in vivo (7-10). Further, they have been shown to inhibit formation of drug induced lung and liver cancer, as well as growth of primary tumors and subsequent lung metastases in mice (7, 9, 11-14). In order to determine the effect of CDDO-Im on liver metastases in mice, we quantified the effect of CDDO-Im treatment on HT-29 and B16F1 cells in vitro and in experimental liver metastases models. We demonstrated that the synthetic triterpenoid CDDO-Im is capable of inhibiting cell proliferation and inducing cell death in HT-29 and B16F1 cells in 2D culture. Further, it was shown that orally dosed CDDO-Im is capable of significantly (50-70%) inhibiting liver metastasis growth in mice. Yet despite the significant reduction in tumor burden and tumor volume as assessed by histology and MRI, CDDO-Im was found to have no effect on the number of solitary metastatic cells in the same livers. However, as CDDO-Im is known to inhibit proliferation at doses insufficient to induce apoptosis, it remains to be determined if CDDO-Im could have an effect on cell cycle progression of these metastatic cells in vivo.

While the MRI technique developed and used in Chapters 2 and 3 is capable of assessing the effect of treatment on the fate of metastatic cells, it reveals little regarding individual cellular information. Thus, in order to better understand the effect of treatment on individual cells within the metastatic cell population, we used 2D and 3D cell culture. As outlined in Chapter 4, a 3D cell culture system and fluorescent reporters of cell cycle were utilized together in order to develop and test a method for assessment of the effect of anti-cancer treatments on the whole metastatic cell population at the cellular level. We found that initial seeding density in Matrigel, as well as CDDO-Im treatment, influenced

subsequent growth dynamics and cell morphology. Notably, at all densities a mix of solitary cells and cell clusters of various sizes were observed.

5.2 DISCUSSION

5.2.1 *Metastatic cell heterogeneity*

In a population of metastatic cells within the same tissue, many cells undergo apoptosis, some begin proliferating and others remain dormant. This is noteworthy if it is assumed that a tumor arises from a single cell and all metastatic cells are thus clonally derived. However, the reasons for the variability in the fate of these cells in not fully understood (2, 15-17). Furthermore, the choice of proliferation, apoptosis or dormancy occurs not only after initial arrest of the cells, but constantly as many initially dormant cells undergo apoptosis or start proliferating over time (18-22). It is unknown if solitary dormant metastatic cells are a specialized subpopulation of cells that are programmed to stay in a dormant state, an unspecialized subpopulation of cells that are not well suited for growth in the new microenvironment, or a combination of both (23). Experiments in which metastatic breast cancer cell lines were sorted by cancer stem cell markers (cells with high aldehyde dehydrogenase activity and CD44 high/CD24 low expression) show cells and cell lines with this CSC phenotype are more malignant and metastatic in mouse models (24). In any case, all solitary dormant metastatic cells are worthy of note in that while they have likely originated from a primary tumor that has acquired all six hallmark of cancer capabilities described by Hanahan and Weinberg (25), they have either lost or are able to control some of these capabilities while other cells from the same source have or do not. The balance between ability to provide self-sufficiency in growth signals and insensitivity to anti-growth signals appears to be reversed in dormant cancer cells in secondary sites. As the majority of metastatic cells that arrive in a secondary site undergo apoptosis, dormancy may be an active method of evading apoptosis for those cells that remain dormant or subsequently begin proliferating.

Dormancy could be viewed as a selective advantage for cells that have not yet acquired the capability of growing in a specific ectopic microenvironment. Indeed, studies addressing the role of the microenvironment in dormancy of metastatic cell lines have found that interactions with the microenvironment and subsequent cell signalling is an important regulator of dormancy (2, 16, 17). It was noted that that in the 3D cell culture system used here, which is relatively homogenous microenvironment, a heterogeneous population of cells (based number of cell per cluster and invasive phenotype) existed. This allows for future studies in which to address differential response to treatment by a metastatic cell population.

5.2.2 *Imaging metastatic cell response to treatment*

Metastatic cell fate is influenced by the microenvironment, however, as the complexity of the microenvironment approaches that of the human host in which metastatic disease is treated, the difficulty assessing cellular events and the response to treatment increases dramatically. Even in the mouse where the presence of solitary dormant metastatic cells has been verified after injection of a number of different cell lines, it is difficult to determine if these cells are truly dormant or to observe them in vivo over a period of time due to destruction of tissue caused by growing metastases and by traditional histological analysis (1, 20, 21). A solitary dormant metastatic cell has been defined, after the fact and by histology, as a cell undergoing neither proliferation nor apoptosis and therefore negative for Ki67 or TUNEL staining, and/or one which has retained an exogenously provided fluorescent or other marker that is no longer visible after a few cell divisions (18, 19). As this definition relies on histological assessment, it is an indication of the state of the cell only at that particular moment. Use of endogenous fluorescence has also been used to identify dormant metastatic cells, however once gain the expression of whole cell fluorescence alone is not indicative of the cells past or future cell cycle progression (26, 27). In addition, this definition of a solitary dormant metastatic cell as one that is neither proliferating nor undergoing apoptosis is accurate but does not give any

indication of the mechanism of dormancy and therefore does not provide a basis for distinguishing between cells that will continue to remain dormant, undergo apoptosis or eventually start proliferating.

The use of MRI to quantify the effect of treatment as outlined in this thesis has a number of advantages. These include rapid image acquisition (6 minutes), sampling of the entire organ of interest, preservation of a digital images of the entire organ (2D and 3D), and very important in this context, the ability to quantify nearly the entire population of metastatic cells (solitary MPIO labelled cells and metastases larger than 200 μm). In addition, as demonstrated by Shapiro et al., solitary iron labelled hepatocytes could be detected in vivo in mouse liver by MRI following migration from the spleen (5). While longitudinal imaging was not performed for the studies presented in this thesis, it is routine to do such in experimental brain metastasis models and these techniques could be modified for longitudinal liver imaging. As with most imaging modalities, the MR based technique for the quantification of solitary cells used here is not without limitations. While retention of the iron label by non-dividing cancer cells is responsible for the signal voids apparent in MR images, the possible accumulation of iron label in the liver (and other cells) following death of the originally labelled cell would lead to artificially high signal void area and an overestimation of the number of cells within the liver. It would thus be difficult to assess small changes in cell number due to treatment. However, multiple lines of evidence suggest this is not a significant problem in the method used here. First, previous publications have shown a significant loss of signal hypointensity over time when cells that are expected to die or begin proliferation are monitored longitudinally in the brain (4, 6). In addition, while injection of dead cells into the spleen or free iron label into the liver did result in signal hypointensity in the liver, the pattern and intensity of this signal loss were different and less intense than signal loss due to live labelled cells (5). With respect to the B16F1 cell line used here, a decrease in signal void area accounting for more than two thirds of the originally injected cells was observed at endpoint (day 9). This is similar to the decrease in the number of solitary B16F1 cells observed previously by optical

quantification methods (21). As mentioned in Chapters 2 and 3, the MRI quantification method used here was intended to measure the effect of treatment on the majority of the metastatic cell populations. However, the inability of this MRI technique to determine the fate of a specific cell (i.e. did it die or divide?) or subcellular response to treatment, necessitates the use of a separate technique. In order to address this, optical imaging of cells in a 3D cell culture model in which both solitary cells and growing metastases were observed was pursued.

Treatment of B16F1, HT-29, D2.0R and 231LN-fucci cells with 200-400 nM CDDO-Im caused cell death, a change in morphology and growth arrest all within the same treatment group (i.e. same well) in 2D culture experiments. In vivo, such a differential effect is primarily only observed as smaller or fewer tumors without a complete understanding of the intrinsic differences accounting for the differential response to treatment from cell to cell. 3D culture models combined with the fluorescent nuclear cell cycle reporters used here allow for more detailed analysis of the cellular response to treatment. The presence of a heterogeneous population of cells (based on number of cells per cluster and differences in cell cycle status) allows for future studies examining the relationship between "tumor" size, cell cycle status and timing of treatment. Indeed, even the ability to longitudinally image cell cycle progression in 2D culture is interesting. As the majority of cell quantification techniques rely on single time point measurements of duplicate populations (i.e. hemacytometer and flow cytometry) or surrogates of cell viability (i.e. colorimetric assays), individual differences in cell cycle progression of cells within the same microenvironment may be obscured. Direct assessment of this will be possible using fucci expressing cells. While growth of the majority of 231LN-fucci cells was inhibited by 400 nM CDDO-Im in 3D models, 48 hours following treatment a small proportion of cells were still found to have divided. This is analogous to growth observed in vivo following treatments that inhibit the size of metastases without decreasing the number of solitary cells. The ability to monitor these cells longitudinally, and assess cell cycle dynamics, will assist in differentiating the response of different cell populations to anti-cancer treatments.

5.3 *FUTURE DIRECTIONS*

5.3.1 *Use of MRI for quantification of the effect of treatment on the metastatic cell population*

The MRI quantification technique here has a number of advantages (discussed previously), however a number of questions exist particularly with respect to the fate of the iron label over time. In order to address this question more the following experiments should be performed:

- Inject stable fluorescent (or other stable cell marker) MPIO labelled cells into liver, remove and scan a single liver lobe by MRI in order to create a 3D reconstruction of location of individual signal voids. Thin section the same lobe for histology in order to generate an equivalent 3D reconstruction to determine the relationship between a population of signal voids and the location of cells and iron label.

- Determine the fate of iron following a cell death by injecting dying (but not dead) cells or by using an inducible apoptosis plasmid system.

- Recover MPIO labelled cells from liver at endpoint to verify cell viability and iron retention.

5.3.2 *CDDO-Im and other novel treatment strategies*

CDDO-Im is an interesting anti-cancer treatment in that it is neither a classic chemotherapy nor a molecular targeting agent with a single molecular target. Identifying the control pathways of dormancy will allow for tailored combinations, however synthetic triterpenoids exert a natural combinational therapy approach and are currently being evaluated in clinical trials for a number of metastatic cancers. Logical experiments stemming from the results presented here include:

- Combination treatment with rexinoids (10).

- Use of the more potent (and currently in clinical trials) synthetic triterpenoid CDDO-Me in experimental metastasis models.

- Controlled oral gavage dosing to determine how metastasis growth inhibition is related to the dose administered.

5.3.3 *Longitudinal assessment of treatment and cell cycle progression in 2D and 3D*

The ability to longitudinally and simultaneously image (optically) a heterogeneous metastatic cell population, their cell cycle progression via nuclear fluorescence and their response to treatment allows for a number of follow up studies to be performed and questions to be answered including:

- Comparison of multiple drugs with different mechanism of actions.

- Comparison of the same drug at different stages of cell cycle

- Do dormant (at least temporarily) cancer cells exist in 2D culture just in smaller numbers?

- Does treatment sensitivity change with the number of cells in a cluster?

- What stage(s) of cell cycle are solitary dormant cells arrested at in vivo?

5.4 CONCLUSION

Thirty eight years have passed since the "War on Cancer" was officially initiated in the United States. Since then significant time and financial resources have been dedicated to clinical and basic cancer research and treatment development. This research has led to exponential growth in our understanding of cancer risk factors and cancer cell biology. Yet while treatment success stories exist for some specific types of cancers, treatment of metastatic disease is often ineffective. This is likely in part due to the way in which treatments for cancer are developed. While the cancer cell population is known to be heterogeneous, anti-cancer therapies are often developed to treat the entire population by the same mechanism. Here we developed and utilized tools to better understand the effect of treatment on the majority of the metastatic cell population. Due to the fact that it is a relatively under-studied and likely under-treated population of cells, specific attention was paid here to solitary dormant cells. However, large clinically apparent metastatic tumors will continue to be the primary clinical target until therapies that can successfully eradicate cancer cells before they reach this stage can be developed. It is expected that the work presented here will enable the screening of therapeutic strategies for their efficacy against not just a subset of the metastatic cell population, but the population as a whole.

5.5 REFERENCES

1. Naumov GN, Townson JL, MacDonald IC, Wilson SM, Bramwell VHC, Groom AC et al.. Ineffectiveness of doxorubicin treatment on solitary dormant mammary carcinoma cells or late-developing metastases. Breast Cancer Res. Treat. 2003;82:199-206.

2. Aguirre-Ghiso JA. Models, mechanisms and clinical evidence for cancer dormancy. Nat. Rev. Cancer 2007;7:834-46.

3. Demicheli R. Tumour dormancy: findings and hypotheses from clinical research on breast cancer. Semin. Cancer Biol. 2001;11:297-306.

4. Heyn C, Ronald JA, Mackenzie LT, MacDonald IC, Chambers AF, Rutt BK et al.. In vivo magnetic resonance imaging of single cells in mouse brain with optical validation. Magn Reson Med 2006;55:23-9.

5. Shapiro EM, Sharer K, Skrtic S, Koretsky AP. In vivo detection of single cells by MRI. Magn Reson Med 2006;55:242-9.

6. Heyn C, Ronald JA, Ramadan SS, Snir JA, Barry AM, MacKenzie LT et al.. In vivo MRI of cancer cell fate at the single-cell level in a mouse model of breast cancer metastasis to the brain. Magn Reson Med 2006;56:1001-10.

7. Deeb D, Gao X, Jiang H, Dulchavsky SA, Gautam SC. Oleanane triterpenoid CDDO-Me inhibits growth and induces apoptosis in prostate cancer cells by independently targeting pro-survival Akt and mTOR. Prostate 2009;69:851-60.

8. Hyer ML, Shi R, Krajewska M, Meyer C, Lebedeva IV, Fisher PB et al.. Apoptotic activity and mechanism of 2-cyano-3,12-dioxoolean-1,9-dien-28-oic-acid and related synthetic triterpenoids in prostate cancer. Cancer Res. 2008;68:2927-33.

9. Ling X, Konopleva M, Zeng Z, Ruvolo V, Stephens LC, Schober W et al.. The novel triterpenoid C-28 methyl ester of 2-cyano-3, 12-dioxoolen-1, 9-dien-28-oic acid inhibits metastatic murine breast tumor growth through inactivation of STAT3 signaling. Cancer Res. 2007;67:4210-8.

10. Liby KT, Yore MM, Sporn MB. Triterpenoids and rexinoids as multifunctional agents for the prevention and treatment of cancer. Nat. Rev. Cancer 2007;7:357-69.

11. Konopleva M, Zhang W, Shi Y, McQueen T, Tsao T, Abdelrahim M et al.. Synthetic triterpenoid 2-cyano-3,12-dioxooleana-1,9-dien-28-oic acid induces growth arrest in HER2-overexpressing breast cancer cells. Mol. Cancer Ther. 2006;5:317-28.

12. Hyer ML, Croxton R, Krajewska M, Krajewski S, Kress CL, Lu M et al.. Synthetic triterpenoids cooperate with tumor necrosis factor-related apoptosis-inducing ligand to induce apoptosis of breast cancer cells. Cancer Res. 2005;65:4799-808.

13. Lapillonne H, Konopleva M, Tsao T, Gold D, McQueen T, Sutherland RL et al.. Activation of peroxisome proliferator-activated receptor gamma by a novel synthetic triterpenoid 2-cyano-3,12-dioxooleana-1,9-dien-28-oic acid induces growth arrest and apoptosis in breast cancer cells. Cancer Res. 2003;63:5926-39.

14. Place AE, Suh N, Williams CR, Risingsong R, Honda T, Honda Y et al.. The novel synthetic triterpenoid, CDDO-imidazolide, inhibits inflammatory response and tumor growth in vivo. Clin. Cancer Res. 2003;9:2798-806.

15. Townson JL, Chambers AF. Dormancy of solitary metastatic cells. Cell Cycle 2006;5:1744-50.

16. Shibue T, Weinberg RA. Integrin beta1-focal adhesion kinase signaling directs the proliferation of metastatic cancer cells disseminated in the lungs. Proc. Natl. Acad. Sci. U.S.A. 2009;106:10290-5.

17. Barkan D, Kleinman H, Simmons JL, Asmussen H, Kamaraju AK, Hoenorhoff MJ et al.. Inhibition of metastatic outgrowth from single dormant tumor cells by targeting the cytoskeleton. Cancer Res. 2008;68:6241-50.

18. Naumov GN, MacDonald IC, Weinmeister PM, Kerkvliet N, Nadkarni KV, Wilson SM et al.. Persistence of solitary mammary carcinoma cells in a secondary site: a possible contributor to dormancy. Cancer Res. 2002;62:2162-8.

19. Naumov GN, MacDonald IC, Chambers AF, Groom AC. Solitary cancer cells as a possible source of tumour dormancy?. Semin. Cancer Biol. 2001;11:271-6.

20. Cameron MD, Schmidt EE, Kerkvliet N, Nadkarni KV, Morris VL, Groom AC et al.. Temporal progression of metastasis in lung: cell survival, dormancy, and location dependence of metastatic inefficiency. Cancer Res. 2000;60:2541-6.

21. Luzzi KJ, MacDonald IC, Schmidt EE, Kerkvliet N, Morris VL, Chambers AF et al.. Multistep nature of metastatic inefficiency: dormancy of solitary cells after successful extravasation and limited survival of early micrometastases. Am. J. Pathol. 1998;153:865-73.

22. Holmgren L, O'Reilly MS, Folkman J. Dormancy of micrometastases: balanced proliferation and apoptosis in the presence of angiogenesis suppression. Nat. Med. 1995;1:149-53.

23. Croker A, Townson J, Allan A, Chambers A. Tumor Dormancy, Metastasis, and Cancer Stem Cells (ed. eds. Teicher, B. & Bagley, R.) (Humana Press, 2009).

24. Croker AK, Goodale D, Chu J, Postenka C, Hedley BD, Hess DA et al.. High aldehyde dehydrogenase and expression of cancer stem cell markers selects for breast cancer cells with enhanced malignant and metastatic ability. J. Cell. Mol. Med. 2008;:.

25. Hanahan D, Weinberg RA. The hallmarks of cancer. Cell 2000;100:57-70.

26. Logan PT, Fernandes BF, Di Cesare S, Marshall JA, Maloney SC, Burnier MNJ. Single-cell tumor dormancy model of uveal melanoma. Clin. Exp. Metastasis 2008;25:509-16.

27. Goodison S, Kawai K, Hihara J, Jiang P, Yang M, Urquidi V et al.. Prolonged dormancy and site-specific growth potential of cancer cells spontaneously disseminated from nonmetastatic breast tumors as revealed by labeling with green fluorescent protein. Clin. Cancer Res. 2003;9:3808-14.

APPENDIX 1 – Copyright agreements

This thesis contains material from a previously published manuscript in *Cell Cycle,* a book chapter in press by *Springer Publishing* and a manuscript submitted to Cancer *Research. Cell Cycle, Springer Publishing and Cancer Research* do not require that the author of a publication receive copyright permission for duplication of the published article, for the purpose of a thesis or dissertation, as long as the source of the material is properly referenced. In sections of this thesis where previously published work has been incorporated, the proper reference is given at the beginning of the section. The prior notification of such inclusion is also required by Springer Publishing and was sent 31 Aug 09.

APPENDIX 2 – Ethics approval for use of animal subjects

Western

10.01.08
*This is the 3rd Renewal of this protocol
*A Full Protocol submission will be required in 2009

Dear Dr. **MacDonald**

Your Animal Use Protocol form entitled:

In Vivo Video Microscopy: Identifying the steps in matastasis and therapeutic target

has had its yearly renewal approved by the Animal Use Subcommittee.

This approval is valid from **10.01.08 to 09.30.09**

The protocol number for this project remains as **2005-025**

1. This number must be indicated when ordering animals for this project.
2. Animals for other projects may not be ordered under this number.
3. If no number appears please contact this office when grant approval is received.
   If the application for funding is not successful and you wish to proceed with the project, request that an internal
   scientific peer review be performed by the Animal Use Subcommittee office.
4. Purchases of animals other than through this system must be cleared through the ACVS office. Health
   certificates will be required.

REQUIREMENTS/COMMENTS
Please ensure that individual(s) performing procedures on live animals, as described in this protocol, are familiar
with the contents of this document.

c.c. N Hague, W Lagerwerf

The University *of* Western Ontario
Animal Use Subcommittee / University Council on Animal Care
Health Sciences Centre, ● London, Ontario ● CANADA – N6A 5C1
PH: 519-661-2111 ext. 86770 ● FL 519-661-2028 ● www.uwo.ca / animal

Dear Dr. **Chambers**

Your Animal Use Protocol form entitled:

Non-Invasive Imaging of Metastasis: Detection, Monitoring and Intervention

has had its yearly renewal approved by the Animal Use Subcommittee.

This approval is valid from **10.01.08 to 09.30.09**

The protocol number for this project remains as **2005-052**

1. This number must be indicated when ordering animals for this project.
2. Animals for other projects may not be ordered under this number.
3. If no number appears please contact this office when grant approval is received.
   If the application for funding is not successful and you wish to proceed with the project, request that an internal scientific peer review be performed by the Animal Use Subcommittee office.
4. Purchases of animals other than through this system must be cleared through the ACVS office. Health certificates will be required.

REQUIREMENTS/COMMENTS
Please ensure that individual(s) performing procedures on live animals, as described in this protocol, are familiar with the contents of this document.

c.c. N Hague, W Lagerwerf

The **University** *of* **Western Ontario**
Animal Use Subcommittee / University Council on Animal Care
Health Sciences Centre, ● London, Ontario ● CANADA – N6A 5C1
PH: 519-661-2111 ext. 86770 ● FL 519-661-2028 ● www.uwo.ca / animal